FREQUENCY RESPONSE OF WEB SYSTEMS CONTAINING LOAD CELLS AND DANCERS, DIMENSIONAL ANALYSIS, AND MODEL REFERENCE ADAPTIVE SCHEMES FOR TENSION CONTROL

By

RAUL PRAMOD RAJARAM

BACHELOR OF ENGINEERING

GOVERNMENT COLLEGE OF ENGINEERING,

PUNE

MAHARASHTRA, INDIA

AUGUST, 2002

Submitted to the Faculty of the
Graduate College of
Oklahoma State University
in partial fulfillment of
the requirements for
the Degree of
MASTER OF SCIENCE
JULY, 2010

FREQUENCY RESPONSE OF WEB SYSTEMS CONTAINING LOAD CELLS AND DANCERS, DIMENSIONAL ANALYSIS, AND MODEL REFERENCE ADAPTIVE SCHEMES FOR TENSION CONTROL

Thesis Approved:

Dr. P. R. Pagilla

Thesis Advisor

Dr. L. L. Hoberock

Committee Member

Dr. J. J. Shelton

Committee Member

Dr. Mark Payton

Dean of the Graduate College

ACKNOWLEDGMENTS

I owe a debt of gratitude to many individuals who have helped the completion of thesis. First of all, I wish to express my sincerest appreciation to my advisor, Dr. P. R. Pagilla for his valuable guidance, intelligent supervision, and friendship during my graduate program. I am forever indebt to him for his motivation and technical insights, allowing me to broaden my horizons in advanced control system and web handling processes. It was a great honor and pleasure to have complete research projects with him and I can only hope to continue his guidance in my future advisor role.

I would like to extend my warmest thanks to my masters committee members: Dr. J. J. Shelton for his insights in web handling related problems and Dr. L. L. Hoberock for his unending support and guidance in completion of this research. Their suggestions and understanding made the development of this thesis a positive learning experience.

I would also like to thank my research colleagues at Oklahoma State University Mauro Cimino, Aravind Seshadri, Carlo Branca, Yu Diao, Jamie Lynch, Kadhim Jabbar, Ben Pacini, Muthappa Ponjanda-Madappa, Shyam Konduri, Yaowei Lu and Daman Bareiss for their timely support and suggestions.

I owe a special debt of gratitude to Nilesh Siraskar for his encouragement and assistance to develop interest in control systems. He is one of the great mentor and friend in my life.

Finally and most deeply, I would like to express my appreciation to my mother, my grandmother and other relatives for their love, dedication, support, patience and

inspiration throughout my life. Without their faith and blessings, I would have never reached this level in my life.

TABLE OF CONTENTS

LIST OF TABLES

LIST OF FIGURES

Figure Page

NOMENCLATURE

Chapter 1:

A	:	Area of cross-section of web
b	:	Coefficient of friction of pendulum dancer
d	:	Pendulum dancer roller diameter
E	:	Modulus of elasticity of web material
f_i	:	Coefficient of friction of i^{th} roller
F_p	:	Pneumatic cylinder pressure force
F_s	:	Pneumatic cylinder spring force
g	:	Gravitational constant
J_i	:	Inertia of i^{th} roller
J_p	:	Pendulum dancer inertia
k	:	Pneumatic cylinder spring constant
k_p	:	Proportional gain in a PI controller
k_{rf}	:	Reference proportional gain
l	:	Length of pendulum dancer
L_i	:	Length of i^{th} web span
m_i	:	Mass of i^{th} roller
M	:	Amplitude of the disturbance
M_p	:	Mass of pendulum dancer
n_i	:	Gear ratio of i^{th} motor
R_i	:	Radius of i^{th} roller
s	:	Laplace variable

t	:	Time parameter
t_i	:	Actual web tension in i^{th} web span
T_i	:	Web tension variation in i^{th} web span
u_i	:	Torque input to i^{th} roller
v_i	:	Velocity of i^{th} roller
V_i	:	Velocity variation of i^{th} roller
y	:	Pneumatic cylinder spring displacement
ρ	:	Density of web material
ν	:	Frequency (Hz)
ω_{ld}	:	Cut-off frequency in a PI controller
ζ	:	Damping ratio for a second order system
α	:	Web span angle
$\Delta\alpha$	:	Web span angle variation
θ	:	Pendulum dancer angle with respect to vertical axis
Θ	:	Pendulum dancer angle variation

Subscripts:

i	:	Span index, $i = 0, 1, 2, \ldots$
S	:	Related to S-wrap roller
r	:	Reference value
U	:	Related to unwind

Chapter 2:

F_d	:	Disturbance force
m_r	:	Number of repeating parameters
M_c	:	Mass of carriage
n_d	:	Number of parameters in system
N	:	Number of roller in accumulator
Q	:	Fundamental quantity
t_c	:	Average tension in accumulator
x_c	:	Carriage position
Π	:	Dimensionless parameter

Chapter 3:

e_i	:	Tracking error
n	:	Upper bound on degree of polynomial
n_m	:	Relative degree of model
n_p	:	Relative degree of plant
t_m	:	Tension output of model
V	:	Lyapunov function
x	:	State vector
γ	:	Adaptive gain
τ	:	Time constant
θ_c	:	Controller parameters
ω	:	Vector of filter parameters

CHAPTER 1

INTRODUCTION

Web handling is the study of transport of webs on rollers through processing machinery. Web materials are processed in a continuous, flexible strip form. Many types of materials and products found in day-to-day life are manufactured and processed in the form of a web. Examples include papers, textiles, plastic films, thin metals, and composites. In order to cope up with the growing market demand for inexpensive consumer products, manufacture of materials in rolled form has increased considerably.

Web tension control plays an important role in web processing and quality of finished web products. During web processing it is essential to maintain web tension within a specified tolerance band to ensure smooth process operations. Web materials pass through many consecutive processing sections during manufacturing of a product, for example coating, printing, drying, cleaning, etc. Different processing sections require different levels of tension specifications. Low web tension may create slackness in webs and may affect processes like printing and coating. High web tension may cause tears and wrinkles of web material. Severe tension variations may disrupt the quality of the final product and result in losses like decrease in production rate, machine hardware damage, etc. Therefore, it is essential to maintain web tension within a prescribed band when it is transported on rollers.

Figure 1.1 shows a large experimental web platform called the Euclid Web Line (EWL) which is available at the Web Handling Research Center (WHRC). This line mimics many typical features of an industrial process line and consists of four sections:

Figure 1.1: Euclid Web Processing Line (Unwind Section)

unwind, master speed, process, and rewind. Any web transport system consists of mechanical components like idle and driven rollers, unwind and rewind rolls, driving motors, tension sensing elements like dancers, load cells, etc. Web material properties and longitudinal dynamic characteristics influence the behavior of the web in the transport direction (machine direction). The web behavior in lateral direction (cross machine direction) is influenced by web material properties, web tension, and characteristics of various mechanical components. Therefore, in order to minimize web tension variations and transport the web, longitudinal and lateral behavior of webs must be studied. Longitudinal and lateral web dynamics play an important role in tension control and ultimately the quality of the finished product.

The focus of this research is on control of web tension in the longitudinal direction. Extensive literature related to longitudinal tensional control and mathematical models for longitudinal control can be found. Campbell [1], King [2], Brandenburg [3],

and Shelton [4] laid fundamental background for the study of longitudinal dynamics of a moving web. A span is defined as the web between two adjacent rollers. The model that considers entering web span tension was developed in [2]. Brandenburg [3] and Shelton [4] assumed strain in the web to be very small and derived the governing equation for web tension in a span. Non-ideal effects such as moisture change and temperature variation on tension variation was studied in [5]. An overview of longitudinal and lateral dynamic behavior and tension control can be found in [6]. Tension control in multi span web systems was presented by Wolfermann [7] and Schroder [8]. In their research, driven roller speed control was proposed for multi span system with optimal output feedback.

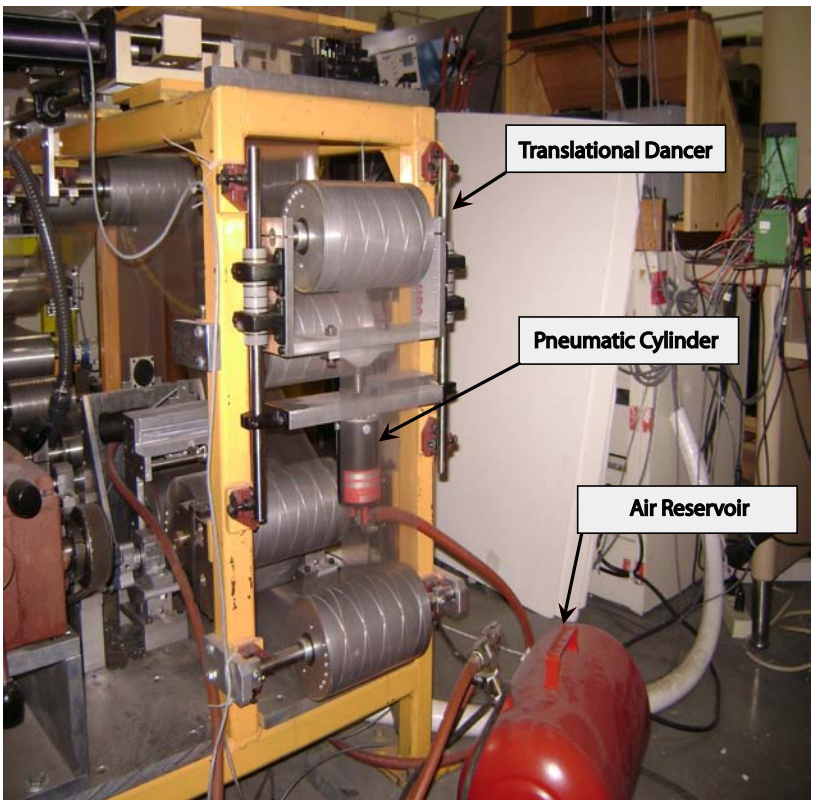

Figure 1.2: Translational Dancer

A dancer is a device consisting of a roller and a mechanical platform which facilitates motion of the axis of rotation of the roller. The platform for the translational dancer shown in Figure 1.2, consists of linear guides or raceways on which the axis

of rotation of the roller is allowed to move based on tension variations. The motion of the axis of the rotation is restrained by a force applied either by a pneumatic or hydraulic cylinder and this force is equal to twice the value of the reference web tension. Any change in web tension from the reference in adjacent spans of the dancer roller results in the motion of the axis of rotation of the roller. The platform for the rotational dancer (often called the pendulum dancer) shown in Figure 1.3, consists of the arm of a pivoted pendulum whose end is connected to the axis of rotation of the dancer roller. The arm of the pendulum is restrained by a force as in the case of the translational dancer. The axis of rotation oscillates about the pivot when the web tension deviates from its reference.

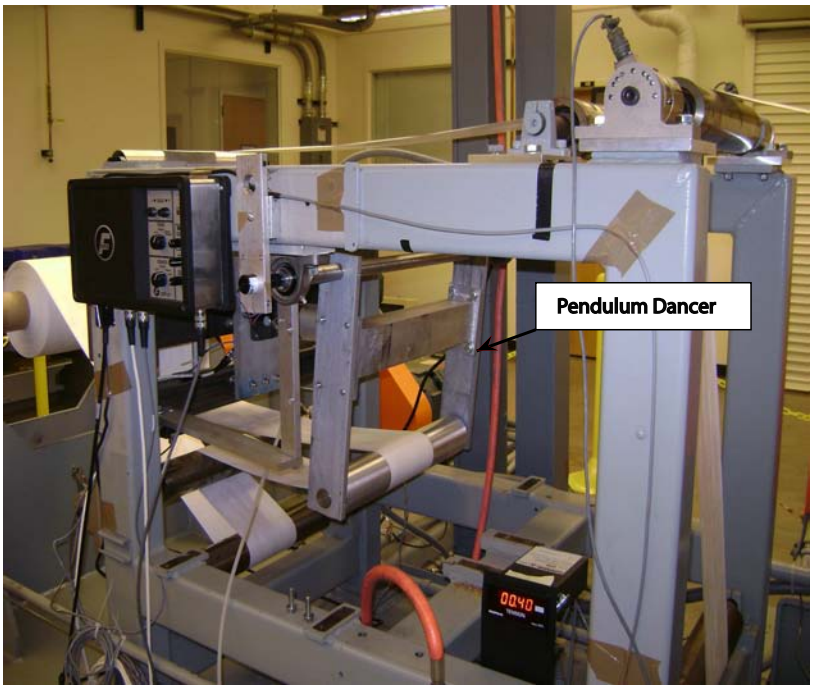

Figure 1.3: Pendulum Dancer

Two strategies are mainly used for tension control, load-cell-based and dancer based feedback control systems. In the load-cell-based scheme, web tension measured by load cells mounted on idle rollers shown in Figure 1.4, is used as the feedback for the tension control system. In the dancer based scheme, displacement of the dancer

(either linear or rotational) due to web tension variations is used as feedback for the tension control system.

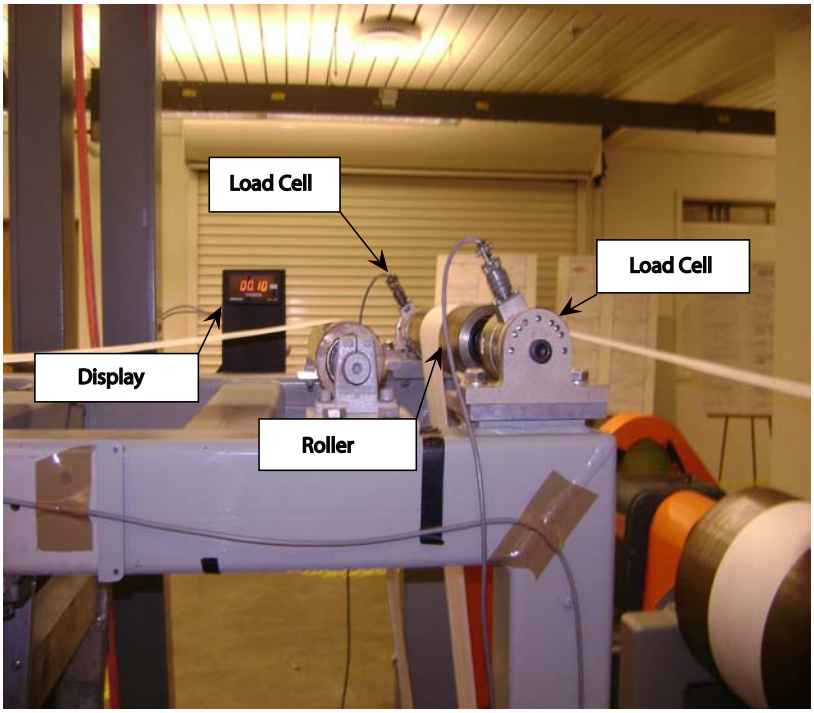

Figure 1.4: Load Cell

Initial research on the evaluation of control systems using dancer and load cell can be found in [9]-[10]. A model for unwind and translational dancer system based on linearized tension dynamics and calculation of minimum resonant frequencies was developed in [9]. The natural frequency of a subsystem consisting idle rollers was theoretically calculated in [9]. In [10], experimental verification of a model is performed by conducting a series of experiments and relevance is proved between theoretical frequency response data and experimental data. The dynamic behavior of an idler system is studied in [11]. Frequency response study is done for idler system to evaluate the natural frequencies of the system. Frequency response experiments conducted in [11], show agreement between model simulated natural frequencies and experimentally obtained natural frequencies.

The first part of this thesis is on investigation of frequency response of load cell and

dancer systems. A detailed frequency response study is conducted for the pendulum dancer which acts as an inferred tension sensing element. This frequency response study is conducted for the unwind section of a web line between unwind roll and a driven roller consisting of a number of idle rollers for web transport and a pendulum dancer. A mathematical model is developed for the pendulum dancer and included in generalized state space model. Computer simulations are performed based on the developed linearized state space model. Experiments are conducted for the dancer feedback system and compared with load cell feedback idler system. The ability of dancer and load cell feedback control systems to regulate tension during acceleration and deceleration of web line is studied. A controller normalization procedure is used to determine the gains for the dancer feedback system based on the load cell idler system, and this procedure is discussed. An electronic pressure regulator and air reservoir are installed on EWL for the pendulum dancer system which improve tension regulation. The procedure on controller normalization, which compares load cell and dancer feedback control systems, led us to the study of dimensional analysis. The goal of controller normalization is to match controller gains based on the relation between dancer position and load cell tension. The normalization study initiated a general question: Can we evaluate process parameters and controller gains for any general web line based on the existing experimental web platform with well tuned controller gains?

The second part of this thesis includes a study of scaling of process parameters and controller gains based on dimensional analysis. Dimensional analysis is extensively studied and developed in the science of fluid mechanics. Dimensional analysis technique can be applied to interconnected large scale systems such as robotics, web handling system, etc. The concept of dimensional analysis and Pi parameter evaluation techniques are discussed in [12]. The application of dimensional analysis to robotics system is discussed in [13]. Dimensional analysis technique simplifies the

design and analysis of complex systems.

The dimensionless model and dimensional analysis applications for web transport system are explored. The study of dimensional analysis discusses the basic concept of dimensions. The Buckingham Pi theorem and its application to interconnected systems are also discussed and presented in this thesis. The Buckingham Pi theorem is a technique used to evaluate dimensionless parameters in a system. The essential dynamic equivalence condition for dimensional analysis is explained and a method to scale process and controller parameters is presented. Numerical examples are provided to show the scaling of process parameters of a web system. Dimensional analysis is also applied to primitive web handling elements such as an accumulator in a continuous process line [14] and a pendulum dancer.

The existing PI control scheme for tension control needs extensive tuning to obtain the desired performance. In many web handling systems, some of the process parameters such as modulus of material and bearing friction are unknown. Also the existing PI control strategy once tuned does not perform well with change in web configuration, web flow path, and web materials. These changing parameters in a web system requires a controller that can adapt to the changes. These current issues with existing control systems motivates development of adaptive control techniques for tension control. The area of focus of this study is on Model Reference Adaptive Control (MRAC) schemes. Direct, indirect and simplified adaptive PI control schemes are designed for the unwind section of EWL.

A Web transport system is a large scale system consisting of a number of interconnected subsystems. Most large scale systems are complex in nature and can be simplified by decomposing into a number of interconnected subsystems. For large scale systems, two control schemes are used in general: centralized control and decentralized control. Centralized control is complex in design and needs to handle huge data from all the subsystems. Also failure to any subsystem may paralyze the cen-

tralized system and make the overall system unstable. In decentralized control, data related to neighboring subsystems is only required to control the subsystem. Failure of any subsystem may not affect the entire operation of the plant. Implementation of decentralized control is easy compared to centralized control. Different types of control schemes can be conceived for web transport systems. Adaptive control, H_∞ robust control, and LQG/LTR designs are some of the techniques available for control of tension.

Early development of decentralized controller and challenges were discussed in [15]-[16]. The concept of augmented error is introduced and used to develop stable MRAC schemes for plants with relative degree 1 and 2 in [17]. In [18], the theory is extended to design and analyze MRAC schemes for plants with known relative degree of arbitrary positive value. Decentralized model reference adaptive control (MRAC) was considered in [19]-[20]. In [21], the classical centralized adaptive control theory is extended to decentralized adaptive control. Direct decentralized adaptive controllers are developed for interconnected systems and drifting problem of process parameters is discussed in [21]. Indirect MRAC scheme is designed for relative degree 1 and 2 systems in [22]. Model reference adaptive system based on the gradient method is described in [23]. The linearized dynamic model for web velocity and web tension and decentralized control scheme were proposed in [24] and [25]. In [26] and [27], a state space reference model is developed for a large scale system and a special model reference adaptive control scheme was designed and applied to a web process line.

Model reference adaptive schemes for web tension control, in order to meet the desired performance specifications given in terms of reference model are studied in this thesis. Model reference schemes were originally known to have been introduced in flight control; a schematic of an adaptive system is shown in Figure 1.5.

Three types of model reference adaptive control schemes, direct, indirect and simple adaptive PI controller are considered for web tension control. The designed

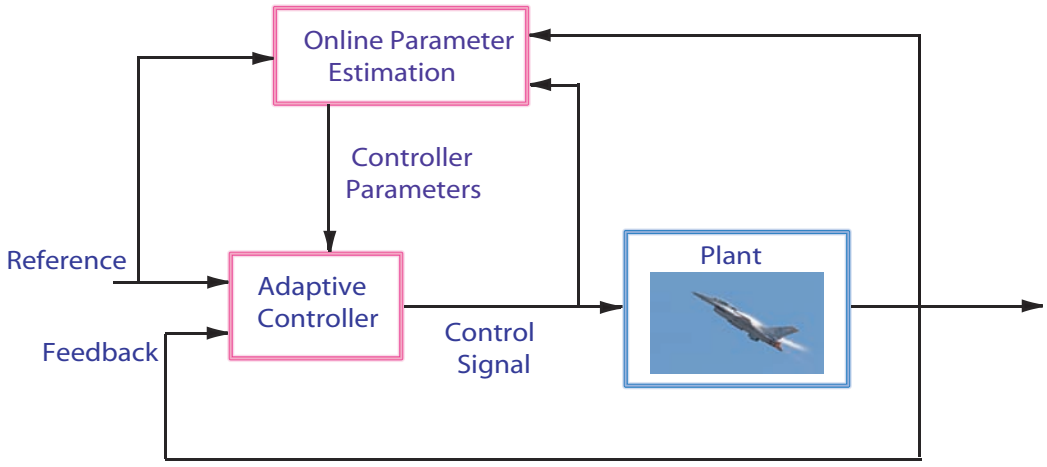

Figure 1.5: Schematic of Adaptive System

controllers are experimentally verified for tension regulation and compared with a well tuned PI controller. An adaptive PI controller is developed and implemented for load cell as well for dancer feedback systems. Sigma (σ) modification is used to avoid estimated parameter drift problem. Standard deviations of steady state measured tension signal are used as performance indices for comparison.

1.1 Contributions

The contributions of the research work involved in this thesis may be summarized as follows:

- A mathematical model for the pendulum dancer and adjacent spans was developed. The model consists of governing equations for the motion of the dancer roller and tension in web spans adjacent to the dancer roller. Frequency response experiments were conducted to obtain the minimum resonance frequency of dancer and load cell systems. The developed model was able to predict the minimum resonant frequency identified by frequency response experiments.

- Time domain experiments were performed to compare the performance of dancer and load cell tension feedback systems. A controller normalization procedure

was developed to determine the controller gains for the dancer based control scheme based on a given well tuned load cell based control scheme.

- The pneumatic system for the pendulum dancer was improved by installing an electronic pressure regulator and an air reservoir between the air supply and the pneumatic cylinder. This electronic pressure regulator is also integrated into the Rockwell Hardware Controller which facilitates precise setting of reference tension from the Rockwell control program used to control the motors of the Euclid Web Line. This enhancement in the pneumatic system improves tension regulation; experimental results verify this aspect.

- Dimensional analysis was performed for web tension and roller velocity dynamics. Dimensional analysis helps in simplifying the governing equations by reducing the number of variables. The dimensionless dynamics can be used to scale process parameters and reference variables of the web line. Several numerical examples were provided to investigate the dimensionless tension and velocity dynamics for scaling of process parameters. Dimensional analysis was also performed for two primitive elements, accumulator and dancer.

- Three types of model reference adaptive schemes, direct, indirect, and adaptive PI were designed and implemented on the EWL. Extensive experiments were performed to evaluate the performance of these adaptive schemes. One key benefit of the adaptive scheme for tension control over fixed gain controllers is that the adaptive controller can be used with different web materials, web line configuration, and sensing systems without much tuning. One limitation is simplifying the adaptive schemes for ease of implementation on industrial web lines.

CHAPTER 2

Modeling and Frequency Response of Web Tension with a Pendulum Dancer

In web processing lines, web tension is typically regulated using an outer loop that provides a trim to the velocity reference of the inner velocity loop. The feedback signal for the outer tension loop is either a position signal from a dancer or a tension signal from load cells mounted on a roller. The focus of this chapter is on modeling a pendulum dancer system, studying the frequency response of web tension with pendulum dancer position as feedback, and comparing dancer position feedback and load cell tension feedback in terms of web tension regulation. The frequency response study gives insights into the benefits and limitations of using dancer and load cell rollers for tension control and relates the limitations to the accuracy of tension control systems. The frequency response study also facilitates design and implementation of efficient filters using statistical methods for better tension regulation.

This chapter describes the derivation of a dynamic model of the pendulum dancer system which consists of the spans adjacent to the dancer roller, upstream and downstream idle rollers, dancer roller, and the pivoted pendulum dancer loaded by a pneumatic actuator. The dynamic model of the pendulum dancer differs from that of the load cell. Due to the motion of the dancer, the span lengths adjacent to the dancer are changing, and this should be incorporated into the modeling of web tensions in adjacent spans. First, a nonlinear dynamic model is derived followed by a linearization of the nonlinear model around operating values. A state space description of the pendulum dancer system that can be used to determine the resonant frequencies of a

web line section between two driven rollers containing the pendulum dancer is given. The state space model is also used to conduct model simulations.

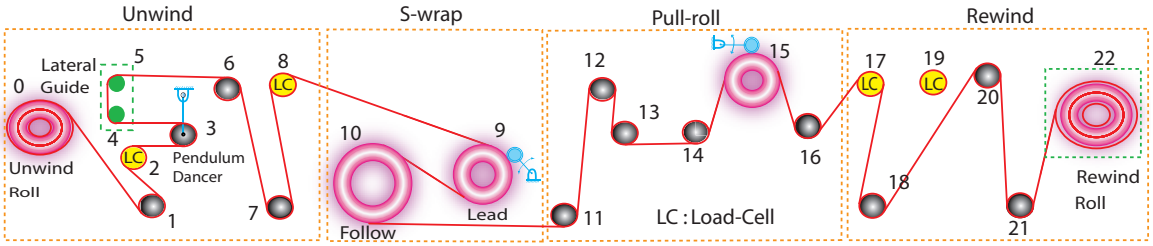

Figure 2.1: Euclid Web Line Sketch

The unwind section of the Euclid Web Line (EWL) shown in Figure 2.1, which contains a pendulum dancer and several load cell (LC) rollers, is used to conduct both time-domain and frequency-domain experiments. The time-domain study corresponds to evaluation of the dancer and load-cell based control systems to regulate tension in the presence of speed changes, i.e., acceleration and deceleration of the line. A controller normalization procedure that can be used to determine the gains of the dancer based controller from load cell based controller, and vice-versa, is discussed. This procedure is based on the assumption that the web is elastic. The dancer and load cell control strategies are compared based on frequency response experimental results.

Finally, we discuss enhancements made to the pendulum dancer system by replacing the mechanical pressure regulator with an Electromechanical Pressure Regulator (EPR) that allows for setting the pressure in the pneumatic cylinder precisely. The EPR is integrated into the Rockwell controller allowing for setting the pressure in the pneumatic cylinder remotely. Time domain and frequency response experiments with the EPR show that tension oscillations are reduced by precisely controlling the pneumatic cylinder pressure.

The rest of the chapter is organized as follows. The pendulum dancer system model including the linearization of the nonlinear model is discussed in Section 2.1.

In Section 2.2 dancer and load cell based control strategies are discussed, together with a procedure for normalization of the controllers. Pendulum dancer pneumatic system is discussed in Section 2.3. Experimental platform, procedure and results for both time-domain and frequency-domain experiments are given in Section 2.4. Evaluation of the new electromechanical pressure regulator is given in Section 2.5. A summary and some concluding remarks are given in Section 2.6.

2.1 Pendulum Dancer System Model

2.1.1 Web Span Tension Dynamics

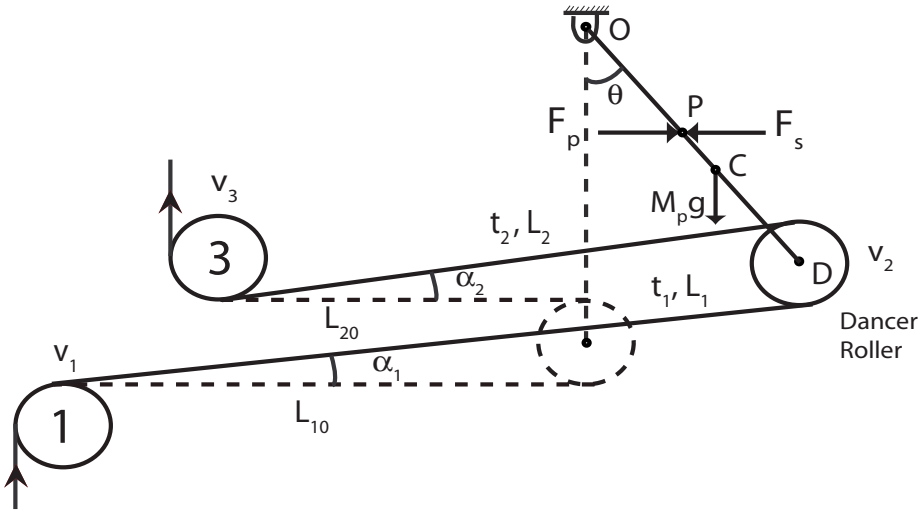

Figure 2.2: Pendulum Dancer

Modeling of web span tension dynamics with fixed length has been described in many studies. In this study, tension dynamics is derived in a pendulum dancer web span with time varying length as shown in Figure 2.2. The derivation of tension dynamic model is based on conservation of mass in a control volume: the change of the mass of web in span is equal to difference between the amount of mass of web span coming from previous span and the mass of web span leaving for next span. The

law of mass conservation can be expressed as:

$$\frac{d}{dt}\int_{x_i(t)}^{x_{i+1}(t)} \rho(x,t)A(x,t)dx = \rho_i A_i v_i - \rho_{i+1}A_{i+1}v_{i+1} \tag{2.1}$$

where $x_i(t)$ and $x_{i+1}(t)$ are the web positions on the i^{th} and $i+1^{th}$ rollers, v_i is the web velocity on the i^{th} roller, ρ is the density of web material, and A is the cross-section area of web .

Consider an infinite element of the web in the longitudinal direction. The length, width, and height of the element are given by

$$dx = (1+\epsilon_x)dx_u, \tag{2.2}$$

$$w = (1+\epsilon_w)w_u, \tag{2.3}$$

$$h = (1+\epsilon_h)h_u \tag{2.4}$$

where ϵ denotes strain in the web material, the subscript u denotes the unstretched state.

The mass of the infinitesimal element of the web can be expressed as

$$dm = \rho(x,t)A(x,t)dx = \rho_u(x,t)A_u(x,t)dx_u \tag{2.5}$$

Substituting the equation (2.2) into (2.5) results in:

$$\frac{\rho(x,t)A(x,t)}{\rho_u(x,t)A_u(x,t)} = \frac{dx_u}{dx} = \frac{1}{1+\epsilon_x(x,t)} \tag{2.6}$$

So, mass conservation equation can be expressed as

$$\frac{d}{dt}\int_{x_i}^{x_{i+1}} \frac{\rho_u(x,t)A_u(x,t)}{1+\epsilon_x(x,t)}dx = \frac{\rho_{u_i}(x_i,t)A_{u_i}(x_i,t)v_i(t)}{1+\epsilon_{x_i}(x_i,t)} - \frac{\rho_{u_{i+1}}(x_{i+1},t)A_{u_{i+1}}(x_{i+1},t)v_{i+1}(t)}{1+\epsilon_{x_{i+1}}(x_{i+1},t)} \tag{2.7}$$

Under the assumption that density of the web material and cross section area are constants for the unstretched material, that is $\rho_u = \rho_{u_i} = \rho_{u_{i+1}}$ and $A_u = A_{u_i} = A_{u_{i+1}}$, the equation (2.7) can be simplified to

$$\frac{d}{dt}\int_{x_i}^{x_{i+1}} \frac{1}{1+\epsilon_x(x,t)}dx = \frac{v_i(t)}{1+\epsilon_{x_i}(x_i,t)} - \frac{v_{i+1}(t)}{1+\epsilon_{x_{i+1}}(x_{i+1},t)} \tag{2.8}$$

Considering small strain, $\epsilon_x \ll 1$, one can write

$$\frac{1}{1+\epsilon_x} \approx 1 - \epsilon_x \tag{2.9}$$

So the equation (2.8) can be written as

$$\frac{d}{dt}\int_{x_i}^{x_{i+1}} (1-\epsilon_x(x,t))dx = v_i(t)(1-\epsilon_{x_i}(x_i,t)) - v_{i+1}(t)(1-\epsilon_{x_{i+1}}(x_{i+1},t)) \tag{2.10}$$

Assuming uniform strain along the length of the span, that is $\epsilon_x(x,t) = \epsilon_{x_i}(t)$, the equation (2.10) can be written as

$$\frac{d}{dt}\int_{x_i}^{x_{i+1}} (1-\epsilon_{x_i}(t))dx = v_i(t)(1-\epsilon_{x_i}(t)) - v_{i+1}(t)(1-\epsilon_{x_{i+1}}(t)) \tag{2.11}$$

Applying the Leibnitz rule for differentiation of integral terms

$$\frac{d}{dt}\left(\int_{\phi(t)}^{\psi(t)} f(x,t)dx\right) = \int_{\phi(t)}^{\psi(t)} \frac{\partial f(x,t)}{\partial t}dx - \frac{d\phi}{dt}f(\phi(t),t) + \frac{d\psi}{dt}f(\psi(t),t), \tag{2.12}$$

equation (2.11) can be expressed as

$$\int_{x_i}^{x_{i+1}} dx\frac{d}{dt}(1-\epsilon_{x_i}(t)) + (1-\epsilon_{x_i}(t))\frac{d}{dt}\left(\int_{x_i}^{x_{i+1}} dx\right) = v_i(t)(1-\epsilon_{x_i}(t)) - v_{i+1}(t)(1-\epsilon_{x_{i+1}}(t)) \tag{2.13}$$

Consider a pendulum dancer web span of time-varying length, $x_i = 0$ and $x_{i+1} = L_i(t)$. The strain dynamics (2.13) can be expressed as

$$\int_0^{L_i} dx\frac{d}{dt}(-\epsilon_{x_i}(t)) + (1-\epsilon_{x_i}(t))\frac{d}{dt}(L_i(t)) = v_i(t)(1-\epsilon_{x_i}(t)) - v_{i+1}(t)(1-\epsilon_{x_{i+1}}(t)) \tag{2.14}$$

Assume the web to be elastic. Hooke's law expresses the relation between web tension and strain as $t_{i-1} = \epsilon_i AE$ and $t_i = \epsilon_{i+1}AE$, where E is the modulus of elasticity of web material and t_i is the web tension in the i^{th} span (the $i+1^{th}$ span is between the i^{th} and the $i+1^{th}$ rollers). Substitute Hooke's law in equation (2.14) to get

$$L_i(t)\left(-\frac{\dot{t}_i}{AE}\right) + \left(1-\frac{t_i}{AE}\right)\dot{L}_i(t) = v_i(t)\left(1-\frac{t_{i-1}}{AE}\right) - v_{i+1}(t)\left(1-\frac{t_i}{AE}\right) \tag{2.15}$$

The web tension dynamics in the i^{th} web span are given by the following equations:

$$\dot{t}_i = \frac{AE}{L_i}(v_{i+1}-v_i) + \frac{1}{L_i}(v_i t_{i-1} - v_{i+1}t_i) + \frac{1}{L_i}(AE - t_i)\dot{L}_i \tag{2.16}$$

2.1.2 Velocity Dynamics

The web velocity dynamics on the i^{th} idle roller is

$$\dot{v}_i = \frac{R_i^2}{J_i}(t_i - t_{i-1}) - \frac{f_i}{J_i}v_i \tag{2.17}$$

where R_i is the radius of i^{th} roller, J_i is the inertia of i^{th} roller, and f_i is the coefficient of viscous friction for the i^{th} roller.

In the case of a dancer roller, the dynamics of the oscillatory motion of the dancer roller needs to be considered. The angular motion of the pivoted pendulum affects web tension in spans adjacent to the dancer roller. Consider the sketch of a pendulum dancer and its adjacent spans as shown in Figure 2.2.

The web tension dynamics for the upstream and downstream spans of the dancer roller, respectively, are given by the following equations based on application of equation (2.16):

$$L_1(t)\dot{t}_1 = AE(v_2 - v_1) + t_0v_1 - t_1v_2 + (AE - t_1)\dot{L}_1(t) \tag{2.18}$$

$$L_2(t)\dot{t}_2 = AE(v_3 - v_2) + t_1v_2 - t_2v_3 + (AE - t_2)\dot{L}_2(t) \tag{2.19}$$

where

$$L_1(t) = \frac{L_{10} + (l+d)\sin\theta}{\cos\alpha_1}, \quad L_2(t) = \frac{L_{20} + l\sin\theta}{\cos\alpha_2}$$

The additional term in the tension dynamics is due to the time varying span lengths adjacent to the dancer roller.

The equation that describes the dynamics of the angular motion of the pendulum dancer around the pivot point 'O' is given by

$$J_p\ddot{\theta} + b\dot{\theta} + M_pgz(\sin\theta) + F_sy - F_py + t_2l\cos(\theta - \alpha_2) + t_1(l+d)\cos(\theta - \alpha_1) = 0 \tag{2.20}$$

where J_p is the pendulum dancer inertia, b is the coefficient of friction of pendulum dancer, M_p is the mass of pendulum dancer, g is the gravitational constant, z is the

height of mass center, l is the length of the pendulum dancer, d is the diameter of the dancer roller, $F_p = pA_e$ is the pneumatic cylinder pressure force, $F_s = Ky$ is the pneumatic cylinder spring force, p is the pneumatic pressure, A_e is the cylinder cross section area, k is the spring constant, and y is the spring displacement.

2.1.3 Linearized Dynamics

Linearization of the nonlinear dynamic model is required to facilitate analysis of resonant frequencies in the system. Of particular importance is the minimum resonant frequency, and how it behaves as a function of the physical parameters of the web as well as those of the associated web handling elements. A comprehensive study on frequency response analysis of a system of idle rollers can be found in [11]. The focus in this chapter is on discussion related to inclusion of a pendulum dancer as a feedback device, whose angular position variations reflect changes in web tension. The linearized dynamics is used for this analysis. The nonlinear dynamics of the pendulum dancer can be linearized by defining the following perturbations:

$$\begin{aligned} T_i &= t_i - t_{ri}, \qquad V_i = v_i - v_{ri} \\ \Theta &= \theta - \theta_r, \qquad \Delta\alpha_i = \alpha_i - \alpha_{ri} \end{aligned} \tag{2.21}$$

where t_{ri}, v_{ri}, θ_r, and α_{ri} are tension reference, velocity reference, pendulum dancer reference angle with respect to vertical axis, and web span angle, respectively. T_i, V_i, Θ and $\Delta\alpha_i$ are variations of tension, velocity, pendulum angle and web span angle from their reference values.

Linearized Tension Dynamics:

The tension dynamics in the span upstream of the dancer roller can be rewritten by substituting equations (2.21) into the nonlinear pendulum dancer dynamics (2.18)

as

$$L_1(t)(\dot{T}_1 + \dot{t}_{r1}) = AE(V_2 + v_{r2} - V_1 - v_{r1}) + (T_0 + t_{r0})(V_1 + v_{r1}) \\ - (T_1 + t_{r1})(V_2 + v_{r2}) + (AE - T_1 - t_{r1})\dot{L}_1(t) \tag{2.22}$$

where the span length is given by

$$L_1(t) = \frac{L_{10} + (l + d)\sin(\Theta + \theta_r)}{\cos(\Delta\alpha_1 + \alpha_{r1})} \tag{2.23}$$

A prescribed reference web tension can be set by loading the arm of the pendulum dancer with a pneumatic actuator, then the pressure in the pneumatic cylinder is adjusted to obtain the required reference web tension. The pressure is adjusted such that the forced equilibrium position of the dancer is at zero degrees. Therefore, for this situation, the reference angle for the pendulum dancer is given by $\theta_r = \alpha_{r1} = 0$. Any deviations in web tension from its reference value result in oscillation of the pendulum and the corresponding angular position of the dancer is related to web tension variations. Since the perturbations are assumed to be small, under the assumption that the angles are small, i.e.,

$$\sin(\Theta) \approx \Theta,\ \cos(\Delta\alpha_i) \approx 1,$$

the equation for the span length (2.23) may be written as

$$L_1(t) = L_{10} + (l + d)\Theta \tag{2.24}$$

At the forced equilibrium position $\theta = \theta_r = 0$, $t_i = t_{ri}, v_i = v_{ri}$. Under the assumption that reference tension is constant, i.e., $\dot{t}_{ri} = 0$, the span tension dynamics is given by

$$(L_{10} + (l + d)\Theta)\dot{T}_1 = AE(V_2 - V_1) + v_{r1}T_0 + V_1 t_{r0} + V_1 T_0 - v_{r2}T_1 - V_2 t_{r1} - V_2 T_1$$

$$+(AE - T_1 - t_{r1})(l + d)\dot{\Theta} \tag{2.25}$$

The product of variations V_1T_0, $\Theta\dot{T}_1$, $T_1\dot{\Theta}$ and V_2T_1 are very small compared to the value of AE of the web material. Therefore, neglecting the products of variations,

the linearized web tension dynamics is

$$L_{10}\dot{T}_1 = AE(V_2 - V_1) + v_{r1}T_0 + V_1 t_{r0} - v_{r2}T_1 - V_2 t_{r1} + (AE - t_{r1})(l + d)\dot{\Theta} \quad (2.26)$$

Note that as in the nonlinear equations, the linearized dynamics also contain terms that are functions of length variations as a function of time.

Similarly one can derive the linearized dynamics in the web span downstream of the dancer roller, which is given by

$$L_{20}\dot{T}_2 = AE(V_3 - V_2) + v_{r2}T_1 + V_2 t_{r1} - v_{r3}T_2 - V_3 t_{r2} + (AE - t_{r2})l\dot{\Theta} \quad (2.27)$$

Linearized Velocity Dynamics:

The idle roller 1 velocity dynamics, neglecting bearing friction, is given by

$$\dot{v}_1 = \frac{R_1^2}{J_1}(t_1 - t_0) \quad (2.28)$$

Since the velocity dynamics is already linear, and since $t_1 - t_0 = T_1 - T_0$, assuming reference velocity is constant, i.e., $\dot{v}_r = 0$, the idle roller velocity dynamics is given by

$$\dot{V}_1 = \frac{R_1^2}{J_1}(T_1 - T_0) \quad (2.29)$$

Linearized Pendulum Dancer Dynamics:

The nonlinear dynamics of the pendulum dancer given in (2.20) is linearized in this subsection. In addition to the earlier defined variations (2.21), the perturbation in pressure from its reference value is defined as $P = p - p_r$ and at the forced equilibrium P=0. For small angular perturbations the following assumptions can be made:

$$\sin(\Theta) \approx \Theta, \quad \sin(\Delta\alpha) \approx \Delta\alpha, \quad \cos(\Theta) = \cos(\Delta\alpha) \approx 1$$

Therefore, in the variational variables, the pendulum dancer dynamics is given by

$$J_p\ddot{\Theta} + b\dot{\Theta} + M_p g z\Theta + Ky^2\Theta - PA_e y + T_2 l + T_2 l\Theta\Delta\alpha_2 + T_1(l + d) + T_1(l + d)\Theta\Delta\alpha_1 = 0 \quad (2.30)$$

Further, simplifications can be made to this equation by making assumptions such as the pressure variation in the pneumatic cylinder due to dancer motion is small and the product of variation, $\Theta\Delta\alpha_i$ is small. The effect of pressure variation is dampened by installing an air reservoir upstream of the supply to the pneumatic cylinder. Installation of this additional reservoir of adequate capacity results in maintaining approximately constant pressure inside the pneumatic cylinder. The dancer pneumatic system is discussed in detail in Section 2.3. Under these assumptions, the pendulum dancer dynamics is given by

$$J_p\ddot{\Theta} = -b\dot{\Theta} - M_p g z\Theta - ky^2\Theta - T_2 l - T_1(l+d) \tag{2.31}$$

2.1.4 Simplified State Equations for the EWL Unwind Section with the Pendulum Dancer

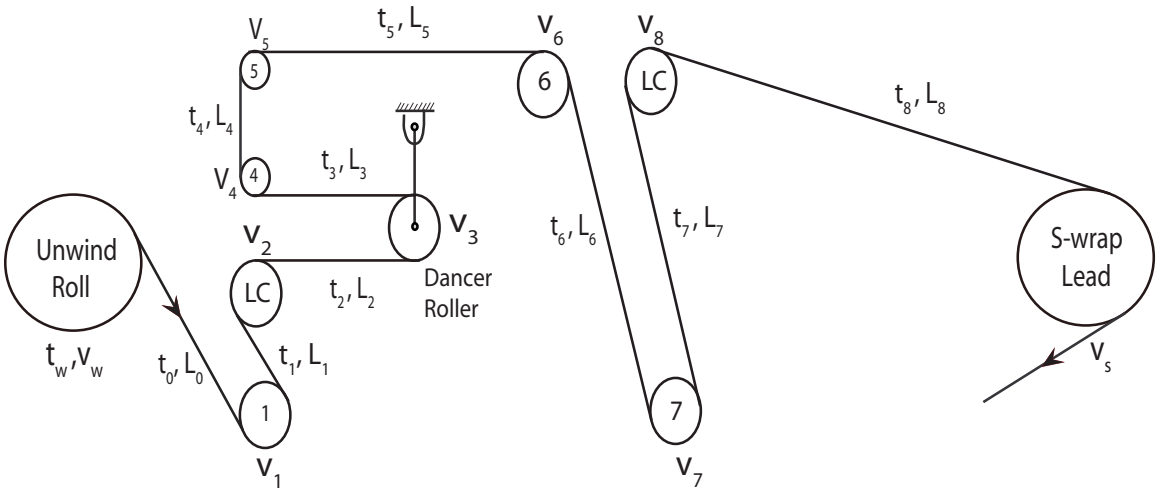

Figure 2.3: Euclid Web Line Unwind Section

Between the unwind roll and the S-wrap driven roller, the Euclid Web Line contains seven idle rollers including the dancer roller; see sketch of the EWL shown in Figure 2.3. Since there are many variables associated with the seven idle rollers, for presenting the state equations, we consider the simplified section as shown in Figure 2.4. The linearized equations given in the previous section can be expressed in

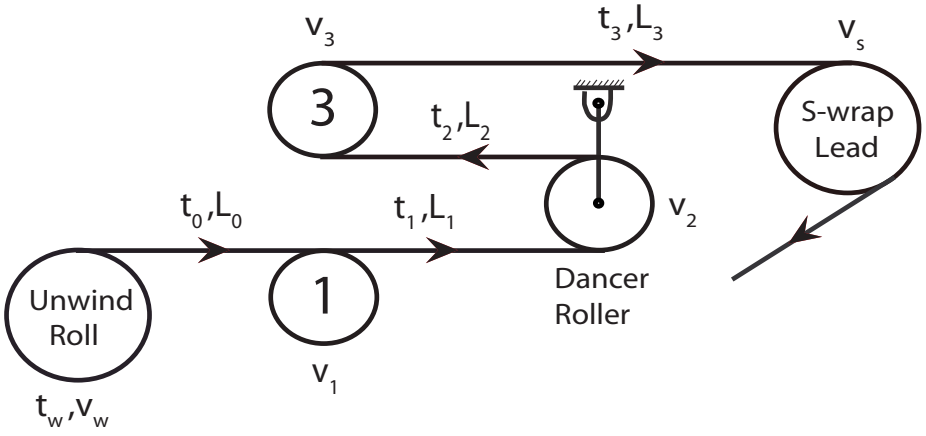

Figure 2.4: Simplified Unwind Section with Pendulum Dancer

state space form by defining the state and input vectors as

$$X = \begin{bmatrix} T_0 & V_1 & T_1 & V_2 & \Theta & \dot{\Theta} & T_2 & V_3 & T_3 \end{bmatrix}^T, \quad U = \begin{bmatrix} V_w & V_s \end{bmatrix}^T \tag{2.32}$$

The linearized state space equation representing the unwind section is given by

$$\dot{X} = \mathbb{A}X + \mathbb{B}U \tag{2.33}$$

where

$$\mathbb{A} = \begin{bmatrix} -P_0 & K_0 & 0 & 0 & 0 & 0 & 0 & 0 & 0 \\ -\frac{1}{m_1} & 0 & \frac{1}{m_1} & 0 & 0 & 0 & 0 & 0 & 0 \\ P_1 & -K_1 & -P_1 & K_1 & 0 & (l+d)K_1 & 0 & 0 & 0 \\ 0 & 0 & -\frac{1}{m_2} & 0 & 0 & 0 & \frac{1}{m_2} & 0 & 0 \\ 0 & 0 & 0 & 0 & 0 & 1 & 0 & 0 & 0 \\ 0 & 0 & \frac{l+d}{J_p} & 0 & -S_p & -B_p & -\frac{l}{J_p} & 0 & 0 \\ 0 & 0 & P_2 & -K_2 & 0 & lK_2 & -P_2 & K_2 & 0 \\ 0 & 0 & 0 & 0 & 0 & 0 & -\frac{1}{m_3} & 0 & \frac{1}{m_3} \\ 0 & 0 & 0 & 0 & 0 & 0 & P_3 & -K_3 & -P_3 \end{bmatrix} \tag{2.34}$$

$$\mathbb{B} = \begin{bmatrix} -K_0 & 0 \\ 0 & 0 \\ 0 & 0 \\ 0 & 0 \\ 0 & 0 \\ 0 & 0 \\ 0 & 0 \\ 0 & 0 \\ 0 & K_3 \end{bmatrix} \tag{2.35}$$

and

$$m_i = \frac{J_i}{R_i^2}; \quad P_i = \frac{V_r}{L_i}; \quad B_p = \frac{b}{J_p}; \quad K_i = \frac{AE - t_i}{L_i}; \quad S_p = \frac{ky^2 + M_p g z}{J_p}. \tag{2.36}$$

2.2 Dancer vs. Load Cell Feedback: Control Strategies and Normalization of Controllers

Web tension behavior in the unwind section of the EWL with dancer and load cell feedback control strategies are studied separately. The goal is to assess the ability of each strategy to regulate tension. Comparative experiments are conducted in both time and frequency domain. Time domain experiments are performed with step/ramp change in velocity while frequency domain experiments are performed by injecting sinusoidal velocity disturbances at the S-wrap roller. An approach to design equivalent PI tension controllers for both dancer and load-cell feedback control strategies is considered with normalizing gains. Controller normalization is required for a fair comparison of performance with the two strategies. In this section we discuss the control strategies and the controller normalization procedure.

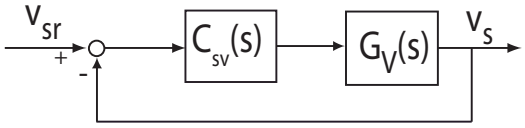

Figure 2.5: S-wrap Control Strategy

2.2.1 S-wrap Roller Control Strategy

Figure 2.5 represents the speed control scheme for the S-wrap roller which is under pure speed regulation. The transfer functions for the motor/load inertia J of the S-wrap roller and the PI controller in frequency domain are given by

$$G_v(s) = \frac{1}{Js},\ C_{sv}(s) = \frac{k_{ps}(s + \omega_{ld})}{s} \tag{2.37}$$

where k_{ps} is proportional gain, ω_{ld} is cut-off frequency.

The closed-loop dynamics for the S-wrap roller is given by

$$\frac{v_s(s)}{v_{sr}(s)} = \frac{k_{rf}(s + \omega_{ld})}{s^2 + k_{rf}s + k_{rf}\omega_{ld}} \tag{2.38}$$

where k_{rf} is reference proportional gain and ζ is damping ratio. Equation (2.38) is obtained by selecting $k_{ps} = Jk_{rf}$ with $k_{rf} = 15$ and $\omega_{ld} = \frac{k_{rf}}{4\zeta^2}$ with $\zeta = 1.1$.

2.2.2 Unwind Roll Control Strategy

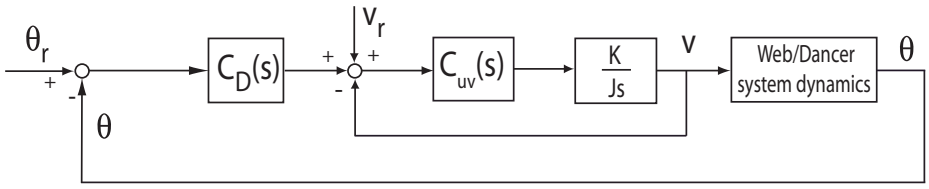

Figure 2.6: Dancer Control Strategy

The unwind roll is under a two-loop control strategy; the inner-loop provides speed regulation and the outer-loop provides a correction to the reference speed based on either tension feedback from a load-cell or dancer position feedback from a dancer. The unwind roll control strategy for the dancer and load-cell are shown in Figures 2.6

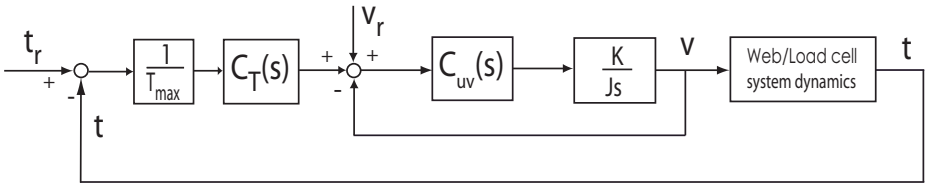

Figure 2.7: Load Cell Control Strategy

and 2.7, respectively. In the case of the dancer, the angular position of the dancer is sensed by a rotary variable differential transducer and the voltage signal is fed back to the outer-loop controller. The speed controller for the unwind roll is expressed as

$$C_{uv}(s) = \frac{Jk_{rf}(s + \omega_{ld})}{s} \tag{2.39}$$

where $k_{rf} = 15$, $\omega_{ld} = \frac{k_{rf}}{4\zeta^2}$ with $\zeta = 1.1$.

The transfer function for the outer-loop with load-cell tension feedback is given by

$$C_T(s) = \frac{k_p(s + \omega_{ld})}{s} \tag{2.40}$$

where k_p is the proportional gain and ω_{ld} is the zero crossover frequency. The dancer position feedback control strategy is selected based on the controller normalization procedure discussed in the following section.

2.2.3 Controller Normalization

A basis for comparison of the performance of control systems with dancer and load-cell feedback requires some form of normalization of controllers. This is done by a way of determining the dancer controller gains based on the development of a relationship between dancer angular position and web tension under the assumption that the web is elastic. Figure 2.8 shows a sketch of the dancer in equilibrium state with corresponding spring constants for the web spans. The relationship between the dancer position and web tension is given by

$$\Delta t_1 + \Delta t_2 = k_1(l + d)\Delta\theta + k_2 l\Delta\theta = \left(\frac{EA}{L_1}\frac{\pi(l + d)}{180}\right)\Delta\theta + \left(\frac{EA}{L_2}\frac{\pi l}{180}\right)\Delta\theta \tag{2.41}$$

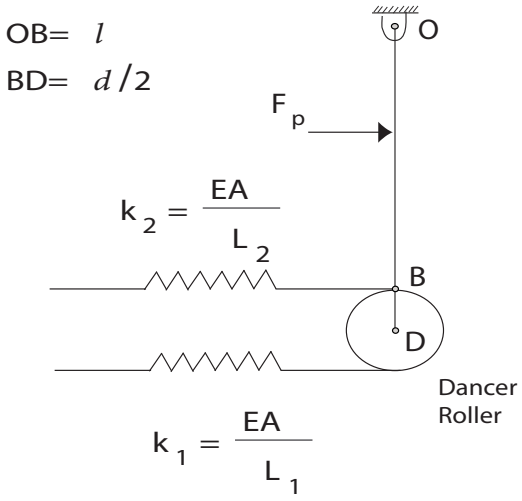

Figure 2.8: Pendulum Dancer in Equilibrium

where θ is in degrees. Assume that the downstream and upstream span lengths to the dancer roller are equal and the tension variation in each span is the same due to dancer motion, i.e., $L_1 = L_2 = L, \quad k_1 = k_2 = k, \quad \Delta t_1 = \Delta t_2 = \Delta t$. Also assume that $l \gg d$. With this the relationship between tension variation and dancer angular position variation is given by

$$\Delta t = k(\Delta\theta l) = \left(\frac{EA}{L}\right)\left(\frac{\pi l}{180}\right)\Delta\theta \tag{2.42}$$

Equation (2.42) represents the relationship between the dancer angular position and web tension under static equilibria. With this equation as the basis, we can determine a controller for the dancer that is equivalent to the controller with load-cell feedback. Figure 2.9 shows how the outer-loop controller with dancer position feedback is obtained. The load-cell based tension PI controller for the unwind roll that is

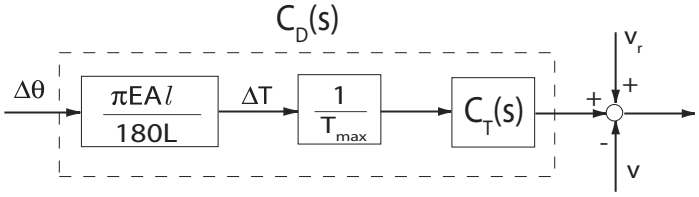

Figure 2.9: Equivalent Dancer Controller

implemented on the EWL is given by

$$C_T(s) = \frac{12(s+0.1)}{s} \tag{2.43}$$

Based on the above procedure, substitute the parameter values as $EA = 2800$ lbf, $l = 1.04$ ft, $L = 1.825$ ft, and $T_{max} = 50$ lbf, the equivalent dancer-based controller is

$$C_D(s) = \frac{4(s+0.1)}{s} \tag{2.44}$$

The pendulum dancer typically has lower resonant frequencies than the load-cell. So, the equivalent controller must be tuned to provide adequate performance. In the case of EWL, the dancer controller given by equation (2.44) delivers very good tension regulation.

2.3 Pendulum Dancer Pneumatic System

The pendulum dancer and its pneumatic system are shown in Figure 2.10. Fluctuations in pneumatic cylinder pressure inject disturbances into the pendulum dancer system. This affects web tension regulation with dancer position feedback. In order to dampen pressure fluctuations in the cylinder of the pneumatic actuator, an air reservoir is installed between the pressure regulator and the pneumatic cylinder as shown in Figure 2.10. The capacity of the air reservoir is calculated based on Boyle's law.

The pneumatic cylinder is of horizontal type and holds the dancer against torque due to pendulum inertia and web tension. The cylinder also contains a spring for retracting the cylinder, which also provides additional stiffness to the dancer system. The supply pressure is regulated by the mechanical regulator to the set point pressure in the pneumatic cylinder.

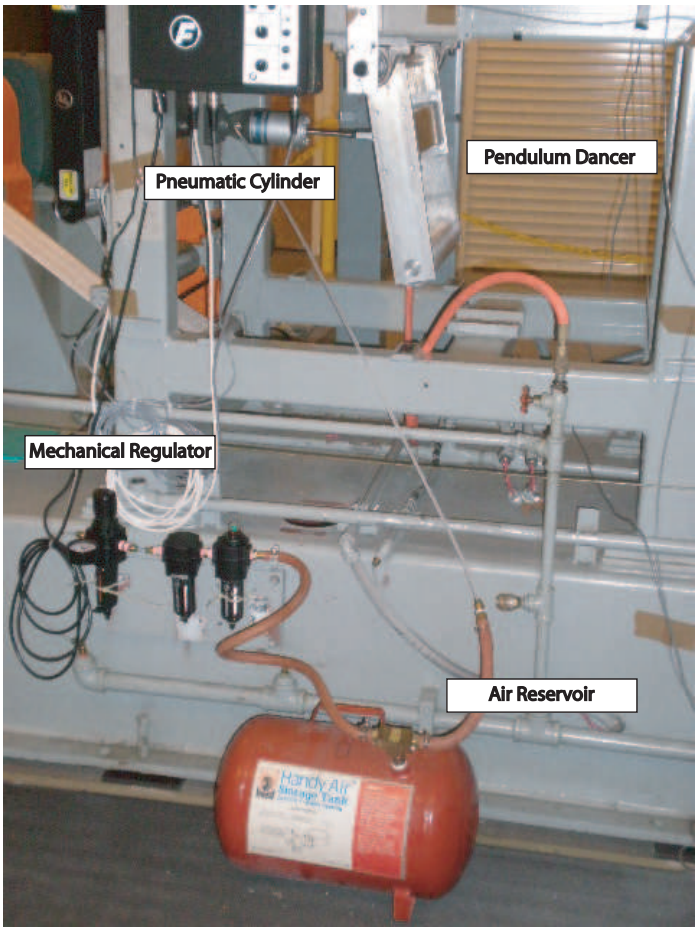

Figure 2.10: Pendulum Dancer Pneumatic System

2.4 Experimental Results

Figure 2.1 shows a sketch of the Euclid Web Line (EWL) experimental platform. The motors, drives, and controller on the EWL are from Rockwell Automation. Three phase, four pole, 15-HP capacity induction motors are used for the unwind and rewind rolls. Further, three 5-HP induction motors are used for each of S-Wrap lead, follower rollers and the pull roller.

The Euclid web line can be divided into four sections: Unwind section, S-wrap section, Pull roll section and Rewind section. The S-wrap and pull roll section act as master speed section. Pure speed regulation is used for both S-wrap rollers and pull roller to maintain the reference web speed. The unwind section contains load cells

on rollers 2 and 8 which can be used to provide tension feedback for the unwind roll control system. For load cell based control strategy, feedback from load cells on roller 2 was used for the unwind roll as this roller is immediately upstream of the dancer roller. There are eight idle rollers in the unwind section from the unwind roll to the S-wrap rollers. The radius of each idle roller is 0.125 ft and inertia is 0.003 lbf ft s^2. The web span lengths are given in Table 2.1. The web path for experimentation is

L_0	L_1	L_2	L_3	L_4	L_5	L_6	L_7	L_8
2.6	0.5	1.8	1.8	1.5	3.3	2.6	2.6	5.5

Table 2.1: Web Span Length (ft) of Unwind Zone

shown in Figure 2.3.

2.4.1 Time Domain Experiments

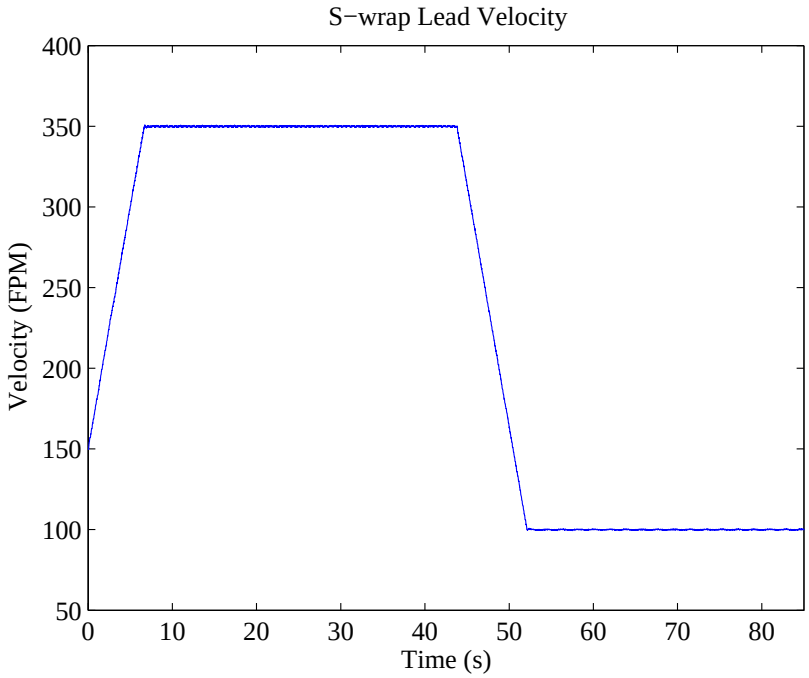

Figure 2.11: S-wrap Speed Profile

Time domain experiments were conducted with the pendulum dancer by giving a step/ramp speed input. The reference speed profile for the S-wrap is shown in Figure

2.11. The line is accelerated from 150 RPM to 350 RPM and decelerated back to 100 RPM. Web tension data is collected for the two cases, i.e., with dancer position and load cell tension controller strategies. Experiments were conducted in three different sets for acceleration and deceleration each. In the first set, dancer feedback is used and tension data was collected from load cells on roller 8. In the second set load cell feedback on roller 2 is used and tension data was collected from the same load cells on roller 2. The third set is similar to the second set except that load cells on roller 8 are utilized as feedback to the unwind roll. Tension PI controller and dancer position controller described by equations (2.43) and (2.44) are used. The unwind roll diameter is kept at 14 inches at the beginning of all experiments, ensuring uniform radius change in every set. The reference tension for tension control was set at 20 lbf and the reference dancer angle was set to zero.

During acceleration, the S-wrap speed changes from 150 RPM to 350 RPM. The tension data plots for both dancer and load cell feedback are shown in Figures 2.13 through 2.15. The calculated standard deviation indicates less tension variation with dancer feedback compared to load cell feedback. The control system based on load cell feedback is more sensitive to speed changes which results in higher tension fluctuations. During deceleration, when the S-wrap speed changes from 350 RPM to 100 RPM , the tension data plots are shown in Figures 2.16 through 2.18. Similar to the results with the acceleration of the line, it was found that the tension regulation performance was better with dancer feedback when compared with load cell feedback. The dancer seems to attenuate tension disturbances due to speed changes better than the load-cell system.

2.4.2 Frequency Response Experiments

The frequency response experiments were performed to verify if the minimum resonant frequency of the unwind section is predicted by the model. Experiments

were performed for both the dancer position based controller and load-cell based tension controller. The dancer feedback controller is given by (2.44). The unwind section contains eight idle rollers, including the dancer roller, from the unwind roll to the S-wrap driven rollers. The S-wrap reference speed V_{sr} is varied sinusoidally with different frequencies to collect tension data for this frequency response study. The S-wrap reference speed with a sinusoidal disturbance of the following form is chosen:

$$V_r = V_{sr} + M(\sin 2\pi\nu_1 t + \sin 2\pi\nu_2 t + \ldots + \sin 2\pi\nu_n t) \tag{2.45}$$

where $V_{sr} = 150$ FPM is the base reference velocity, $M = 5$ FPM is the amplitude, and ν_i is the frequency. Note that all the sinusoidal components are not implemented at once. A few frequencies are implemented at a time and the data is combined. In each experiment, tension behavior was investigated at 21 frequency points ranging from 0.5 Hz to 10 Hz.

Computer simulations were performed with the developed model by feeding sinusoidal frequency input to the model, and output tension response data is collected. In the case of experiments, tension data was collected from both load cells on roller 8 and roller 2.

Simulation and experimental results are shown in Figures 2.19 through 2.22. The frequencies corresponding to peaks in the tension signal FFT are resonant frequencies. The resonant frequencies from model simulations agree with those from the experiments. In the case of the load cell feedback, there was a close match (minimum resonant frequency was 5 Hz). In the case of dancer feedback, the minimum resonant frequency from experiments was 3.2 Hz and from model simulations was 3.5 Hz. Experimental results shown in Figures 2.23 and 2.24 reveal that the dancer system can damp low frequency tension disturbances.

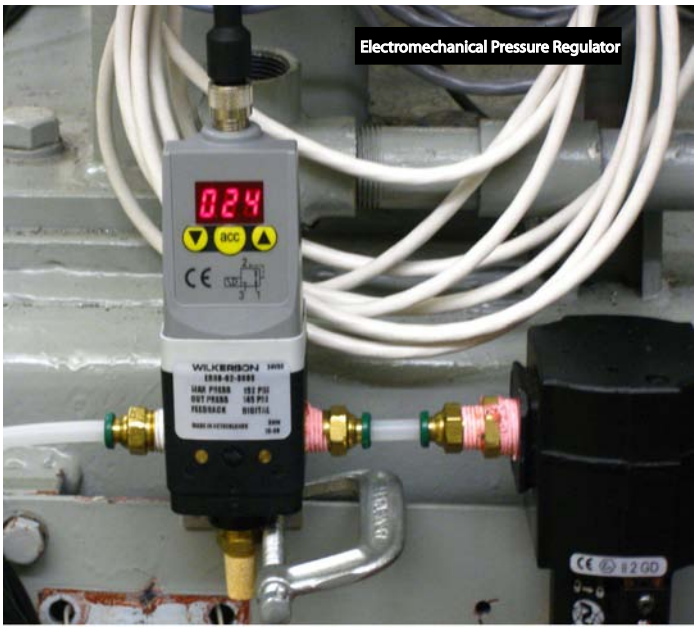

Figure 2.12: Electromechanical Pressure Regulator

2.5 Electromechanical Pressure Regulator Evaluation

A mechanical pressure regulator was used for supplying air to the pneumatic cylinder with required pressure. Since the mechanical regulator is an open loop system, it has limitations in regulating output pressure. The effects of back pressure and air flow variation can cause inconsistencies in the performance of pneumatic systems. Proportional regulators are used to eliminate these problems. In order to enhance the pendulum dancer system, the traditional mechanical regulator was replaced with an electromechanical pressure regulator (EPR). The chosen EPR is made by Wilkerson and contains an in built proportional controller. The ability of the EPR to provide precise pressure regulation and the flexibility to change parameters makes this unit well suited for dancer based feedback. With mechanical type regulators, the pressure set point is manually adjusted by a control knob. There is no mechanism to monitor the error between the set value and actual value of the output pressure. By using the EPR, the output pressure is continuously measured and is adjusted to the set value. The EPR has many other advantages over the traditional mechanical type regulator

in terms of fast response time, good linearity, high visibility LED display, flexibility with user friendly software. The EPR's output pressure can be set manually on the device panel or by an external voltage signal though a real time system. The EPR is integrated into the Rockwell controller on the EWL and the output pressure now can be set through a program in ControlLogix. The chosen EPR has an output pressure range of 0 to 150 psi corresponding to set value input signal of 0 to 10 V.

To evaluate the performance of the EPR, time domain and frequency domain experiments were conducted and compared to the earlier results based on the mechanical type pressure regulator. The same setup was used for both experiments. Comparison of the results show that with EPR, the tension variations are reduced by a considerable amount. This can be observed by comparing the frequency response results with the EPR shown in Figure 2.27 and those with the mechanical regulator as shown in Figure 2.19. Time domain experimental results indicate similar conclusions. Comparing the acceleration plots 2.25 with 2.13 and deceleration plots 2.26 with 2.16 show reduction in standard deviation of web span tension. Standard deviation of a data set is the square root of its variance and it shows how data varies from the average. A low standard deviation indicates that data points tend to be very close to the mean. The pendulum dancer torque balance variational equation (2.31) reveals that any pressure variation in the pneumatic cylinder from the set point causes dancer angle fluctuations which can cause oscillations in web tension. Inclusion of the EPR did not affect the location of the resonant frequencies in the frequency range used for testing.

2.6 Summary and Conclusion

A model is developed for a pendulum dancer system. The dynamic equations are linearized and expressed in a state space form. The ability of the developed model to predict resonant frequencies is verified by performing frequency response experiments.

Time and frequency domain experiments were performed for two control strategies, an outer-loop controller based on dancer position feedback and the other based on tension feedback from load cells mounted on a roller. The dancer position based feedback controller is normalized to the load cell based controller and tuned in order to reduce dancer oscillations. There was a very close match in terms of the minimum resonant frequency (5 Hz) between model simulations and experiments based on load-cell feedback. For the dancer based feedback, the minimum resonant frequency was 3.5 Hz with the model and 3.2 Hz from the experiments. Further, frequency response results also show that, in the low frequency range (0 to 3 Hz), tension variations with the dancer are much smaller compared to the load cell. The dancer was able to filter low frequency disturbances very well compared to the load cell. This was also evident from time domain results where the line was accelerated and decelerated to evaluate the performance of the two control systems. It was also shown that by precisely regulating air pressure in the pneumatic cylinder with electromechanical pressure regulator, the tension response is improved.

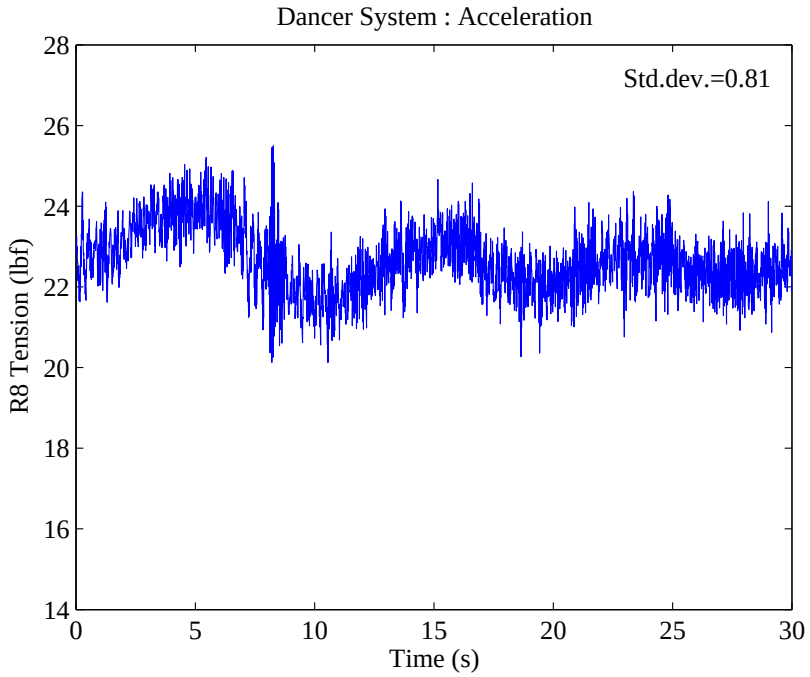

Figure 2.13: Web Tension with Dancer Position Feedback during Line Acceleration

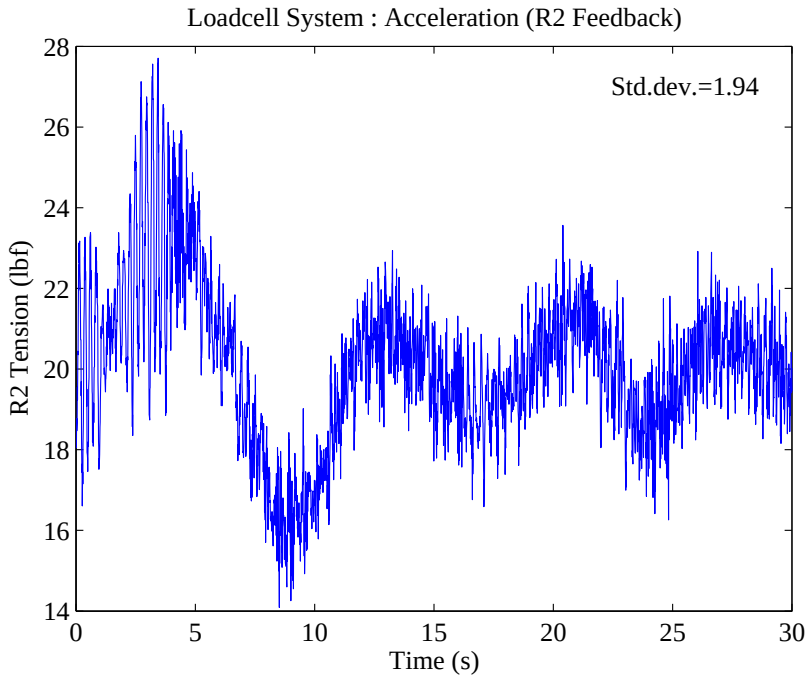

Figure 2.14: Web Tension with R2 Load Cell Feedback during Line Acceleration

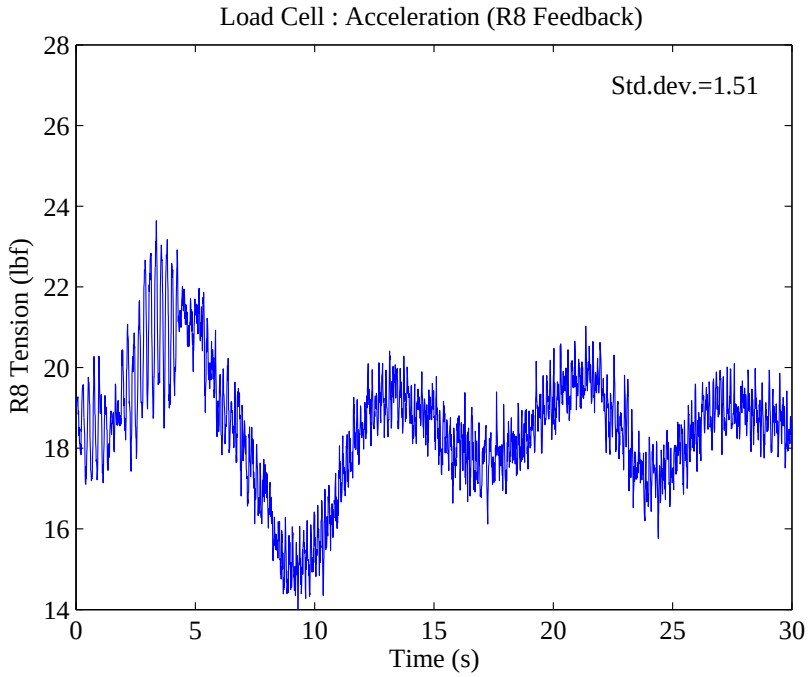

Figure 2.15: Web Tension with R8 Load Cell Feedback during Line Acceleration

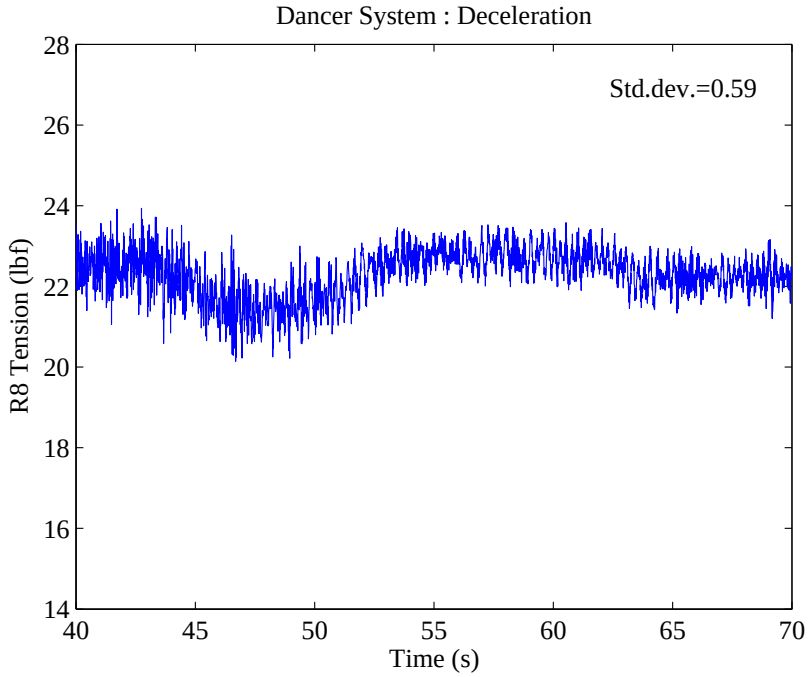

Figure 2.16: Web Tension with Dancer Position Feedback during Line Deceleration

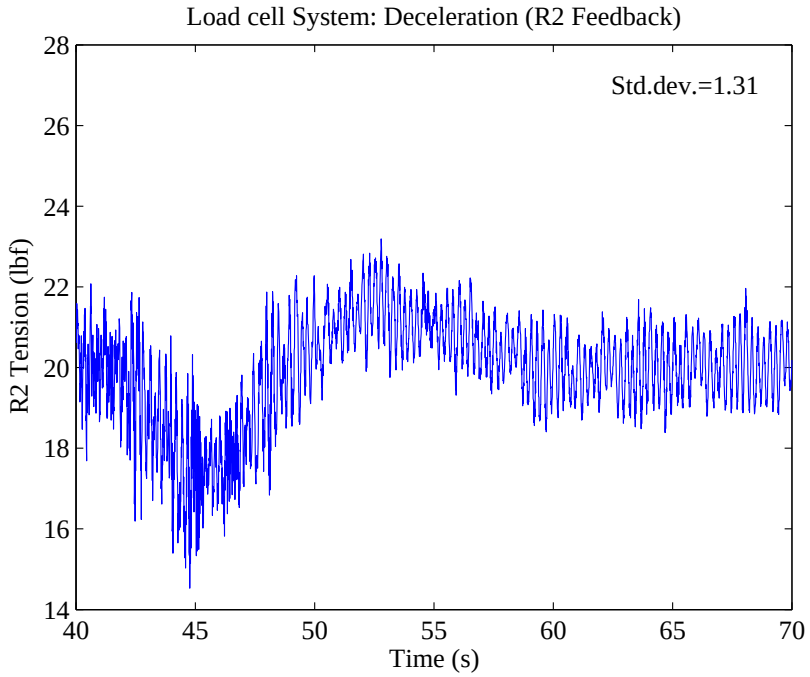

Figure 2.17: Web Tension with R2 Load Cell Feedback during Line Deceleration

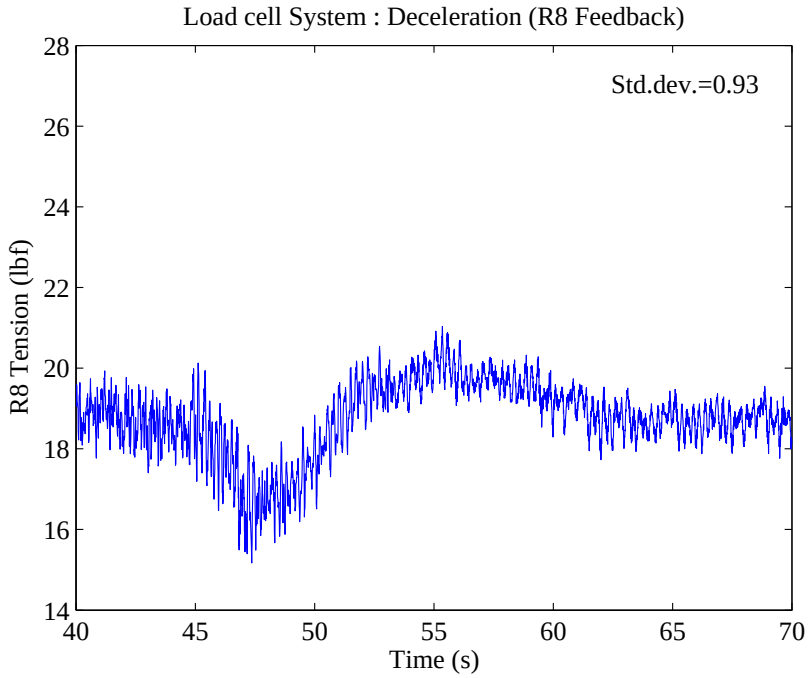

Figure 2.18: Web Tension with R8 Load Cell Feedback during Line Deceleration

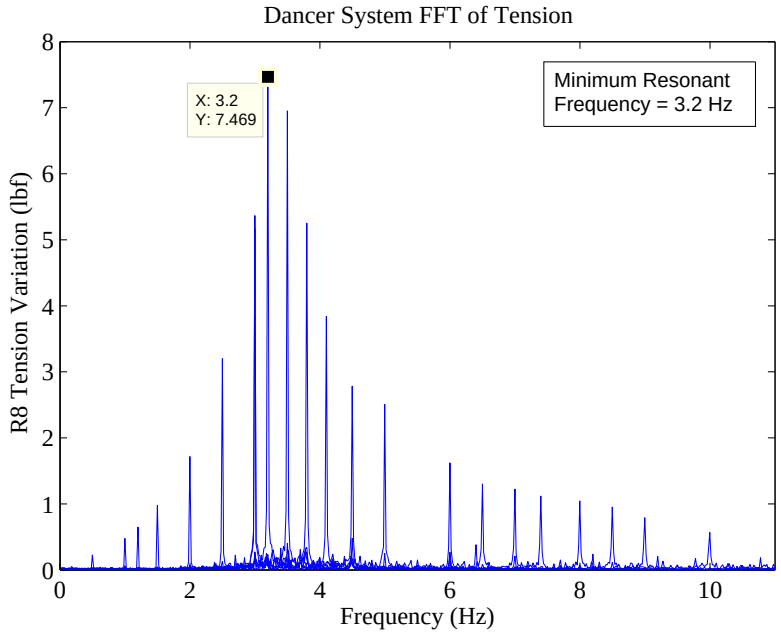

Figure 2.19: Experimental Results: FFT of Tension with Dancer Feedback (Tension from R8)

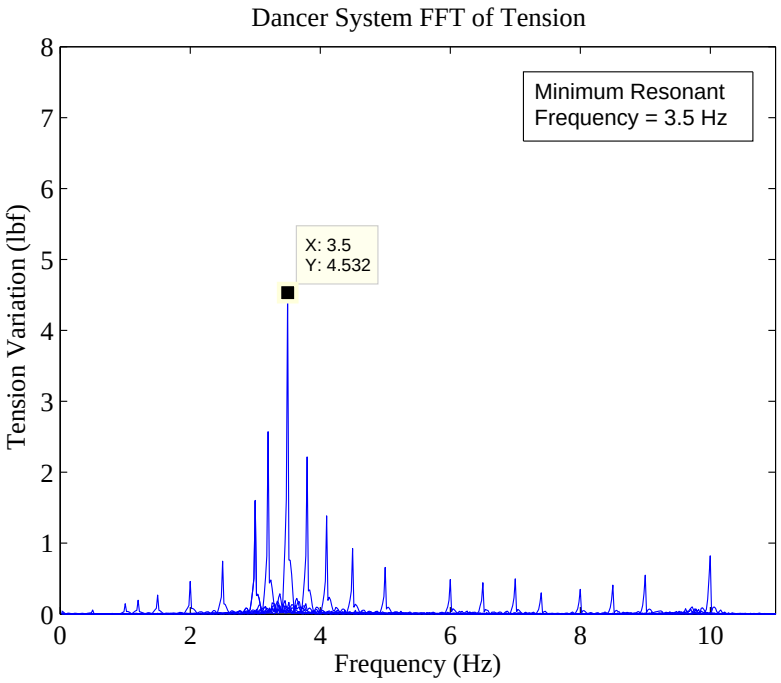

Figure 2.20: Model Simulation: FFT of Tension with Dancer Feedback

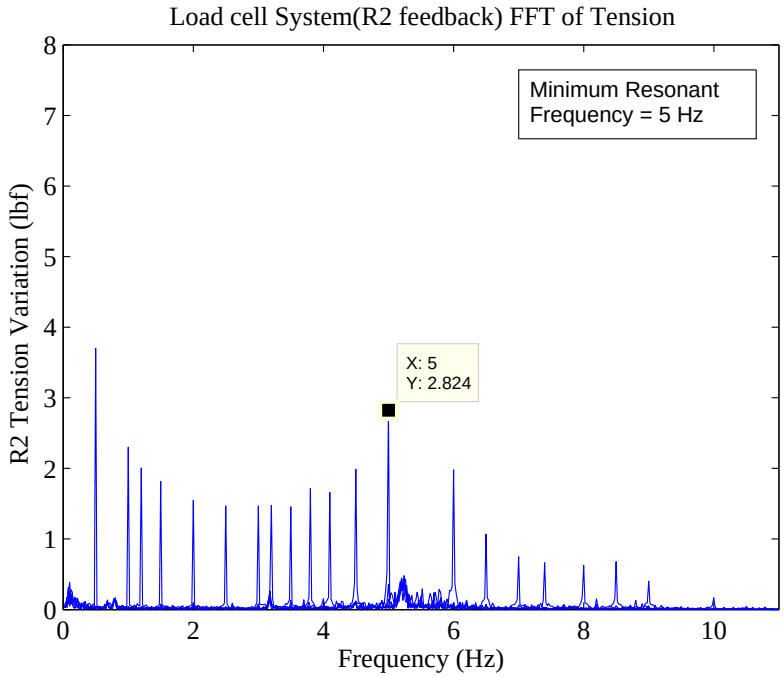

Figure 2.21: Experimental Results: FFT of Tension with Load Cell Feedback (Tension from R2)

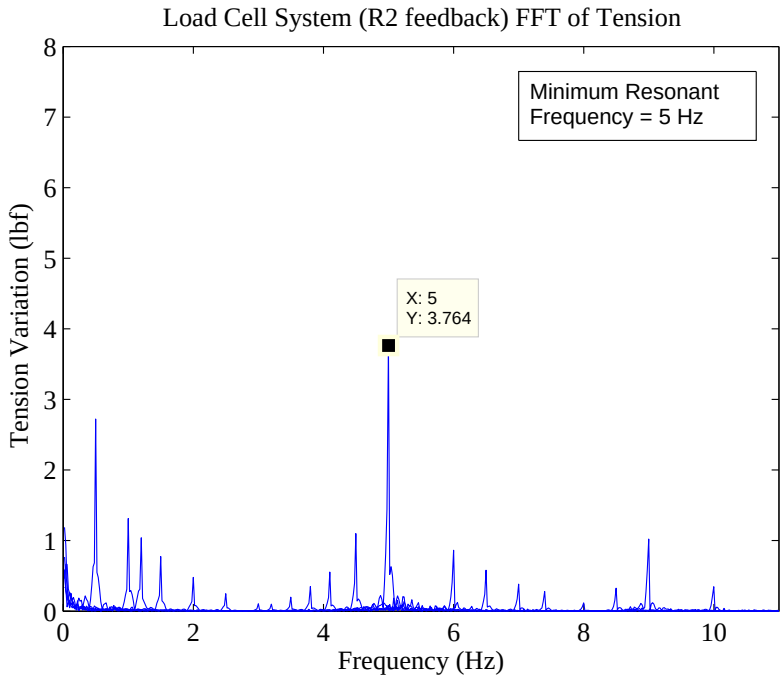

Figure 2.22: Model Simulation: FFT of Tension with Load Cell Feedback

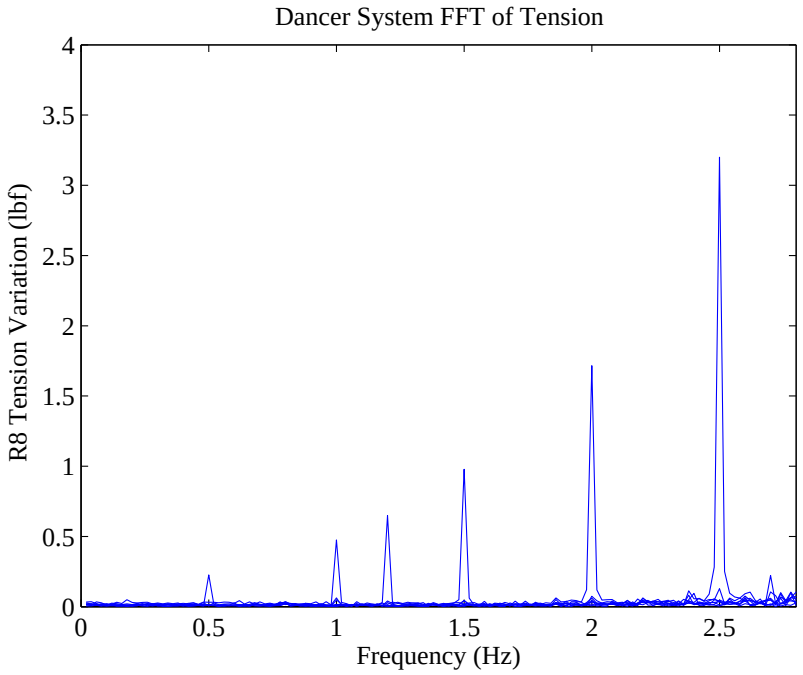

Figure 2.23: Low Frequency Content with Dancer Based Control System

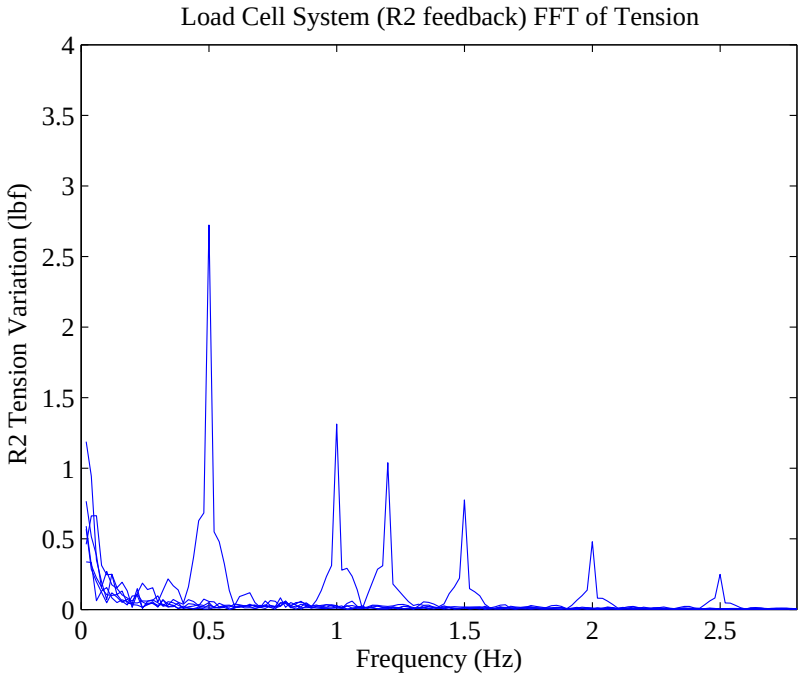

Figure 2.24: Low Frequency Content with Load Cell Based Control System

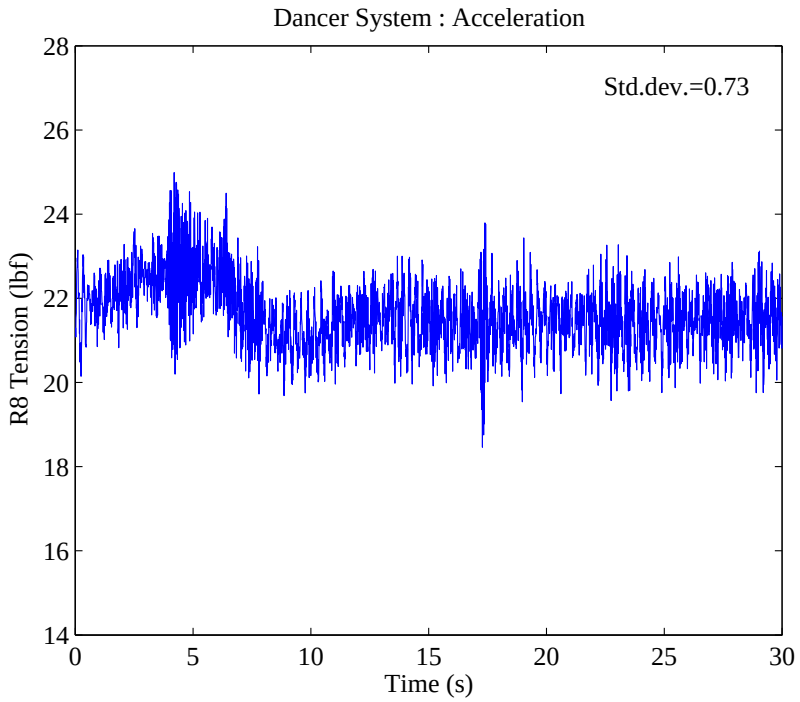

Figure 2.25: Web Tension with Dancer Position Feedback during Line Acceleration with EPR

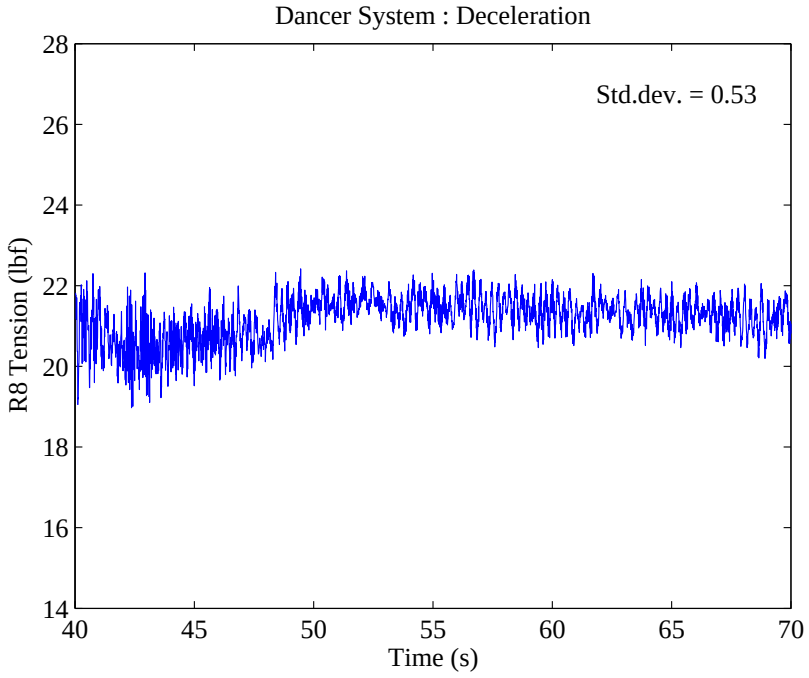

Figure 2.26: Web Tension with Dancer Position Feedback during Line Deceleration with EPR

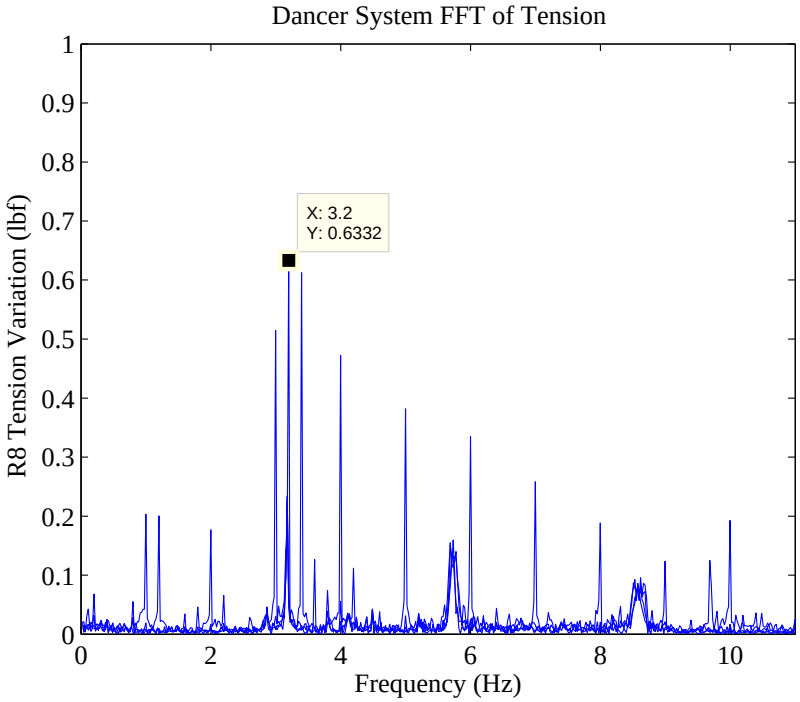

Figure 2.27: Experimental Results: FFT of Tension with EPR

CHAPTER 3

Dimensional Analysis of Longitudinal Web Dynamics

Application of the dimensional analysis technique for web transport systems is explored in this chapter. Dimensional analysis is a technique used to reduce complexity of variables in a system and to obtain relationships between the variables that characterized the system. Dimensional analysis technique can be applied to interconnected systems such as robotics, web handling systems, etc. This chapter contains basic concepts of dimensional analysis, Buckingham Pi theorem and its application to interconnected systems, dynamic equivalence condition and finally process parameters evaluation in dimensionless domain.

Our study on controller normalization described in Chapter 2, which compares load cell and dancer feedback control systems, led us to investigate dimensional analysis. Assuming that the web is elastic, the relation between dancer position and web tension can be evaluated. The goal of controller normalization was to match controller gains based on the relation between dancer position and tension. This controller normalization study gave rise to the following problem: can we obtain process parameters and controller gains for any general large-scale web line based on process parameters and controller gains available for a well tuned experimental web platform. This chapter explores this question about scaling process parameters and controller gains using dimensional analysis.

The rest of this chapter is organized as follows. Dimensions of physical quantities and unit schemes are discussed in Section 3.1. Dimensionless numbers and nondimensional space are described in Section 3.2. Dimensional analysis techniques are

explained in Section 3.3. Similitude, scaling laws and areas of applications of dimensional analysis are also highlighted in Section 3.3. Section 3.4 discusses dimensional analysis for web transport systems. The process parameters and the controller parameters scaling for a web system transporting different web materials is discussed in Section 3.5. Dimensional analysis of a web handling primitive element such as an accumulator is given in Section 3.6. Dimensional analysis technique is applied to a dancer system in Section 3.7.

3.1 Dimensional Analysis

Any physical quantity can be expressed in two forms: dimensional and dimensionless. A dimensional quantity is a number linked with dimension and unit. For example, speed is a dimensional quantity and can be expressed as '30 m/s'. This physical quantity has '30' as magnitude and 'm/s' as unit. The same physical quantity is described by a variety of units in different parts of the world. 'Mass' has units such as kilogram, pound, pound-mass, hyl and slug, etc. Since fundamental quantities are related with each other by physical laws, fundamental set of units are used to form units for all physical quantities. The known fundamental quantities are given in Table 3.1 with 'Standard International System' of units.

Dimension is a collection of fundamental quantities, joined by multiplication or division, and not by addition and subtraction, and is used to express any physical quantity. Dimension implies measurement unit of magnitude along with measurement method and nature of physical quantity. Dimensions are a different concept than units. A physical quantity may have a variety of units but is always presented with the same dimensional convention. Speed has unit 'm/s' and is expressed with two fundamental quantities, length and time. A square bracket notation is used to denote dimensions. The seven fundamental quantities given in Table 3.1 characterize any physical quantity.

Physical Quantity	Unit	Dimension
Mass	kilogram	[M]
Length	meter	[L]
Time	second	[T]
Current	ampere	[A]
Temperature	kelvin	[Θ]
Luminous intensity	candela	[cd]
Amount of substance	mole	[mol]

Table 3.1: Set of Fundamental Quantities

Dimension notations can be viewed as a vector space. The fundamental quantities can be treated as a basis for this vector space and corresponding powers represent coordinates of vector. Speed which is a combination of fundamental physical quantities would be dimensionally presented by $[\mathrm{L}][T]^{-1}$. Hence, speed is a $[0, 1, -1]^T$ vector corresponding to a basis of MLT fundamental quantities. The speed vector representation is shown in Figure 3.1.

$$[\text{speed}] = \begin{bmatrix} 0 \\ 1 \\ -1 \end{bmatrix}$$

The dimension of force is given as 'mass × acceleration' and is represented by $[\mathrm{M}][\mathrm{L}][T]^{-2}$.

$$[\text{force}] = \begin{bmatrix} 1 \\ 1 \\ -2 \end{bmatrix}$$

Most of the physical quantities are formulated with mass, length and time. This system is known as MLT dimensional system. In some situations force, length and time (FLT) are also used as fundamental quantities, and this usage is similar to a change of basis.

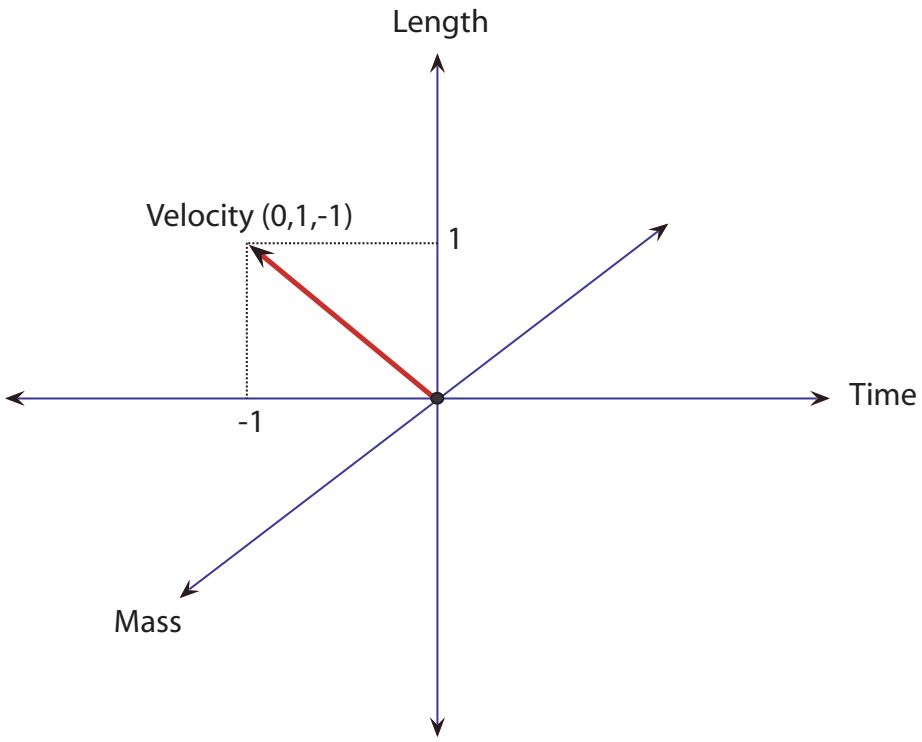

Figure 3.1: Representation of Speed Vector in Dimensional Space

3.2 Nondimensional Space

A nondimensional quantity is generally defined by a ratio or product of dimensional quantities. A nondimensional quantity does not have any unit, but in certain situations are expressed as ratio of units, such as 'lb/lb'. A nondimensional ratio has same value, independent of the system of units used for measurement. In a broad sense one can say that the universe is not calibrated in any set of units. The standards available around the world are created by humans for their own convenience. Most physical phenomena in the universe operate on groups of variables which are pure numbers, which are called as nondimensional quantities or parameters. For example, 'Mach number', an important phenomenon in fluid mechanics, is a nondimensional quantity which characterizes the relative velocity of sound 'c' in a flow of fluid of

velocity 'V'. In terms of fundamental dimensions

$$\text{Mach number} = \frac{V}{c} \equiv \frac{[M]^0[L][T]^{-1}}{[M]^0[L][T]^{-1}} \equiv [M]^0[L]^0[T]^0 \tag{3.1}$$

where c is the speed of sound in that particular fluid.

The dimensions of speed of fluid flow and speed of sound cancel each other and render Mach number dimensionless. The universe does not bother about the intensity of fluid flow speed, but is interested in speed of flow relative to the speed of sound in that fluid. Some other nondimensional parameters popularly used in engineering are Reynolds number, Nusselt number, Prandtl number, strain, etc. We will see later how nondimensional groups characterize and simplify governing equations for dynamic systems.

3.3 Dimensional Analysis Techniques

There are systematic techniques to form nondimensional parameters which can be used to characterize dynamic systems. One key requirement for performing dimensional analysis is that the governing equations of the given physical system must be dimensionally homogeneous.

3.3.1 Dimensional Homogeneity

The principle of dimensional homogeneity states that every equation meaningfully describing a physical system should be dimensionally homogeneous. A group of parameters, variables added or subtracted to form an equation of a physical system is dimensionally homogeneous, if every group has equivalent dimensions. Meaningful and valid physical systems, do not allow dimensionally dissimilar quantities to add, subtract or compare. Otherwise, such systems represent meaningless phenomena. Dimensionally similar quantities are also called commensurable quantities. For example, kinetic energy expression is dimensionally homogeneous, since both sides of equation

have equivalent units, that is,

$$\text{kinetic energy}(J) = \frac{1}{2} \times \text{mass}(kg) \times \text{velocity}^2(m^2/s^2) \tag{3.2}$$

In the case of a meaningful physical system, one type of energy can be added with another type of energy.

$$\text{Total energy of the system} = \text{Kinetic energy} + \text{Potential energy} \tag{3.3}$$

One cannot add force to energy to represent any physical system. For example, Newton's second law equation cannot be added with an equation of the first law of thermodynamics. Though both equations are dimensionally homogeneous but represent different dimensions. Hence, these dimensionally dissimilar quantities cannot be operated with addition or subtraction. An equation is correct if both sides are numerically as well as dimensionally equivalent.

Dimensional homogeneity is the necessary and essential condition for dimensional analysis techniques. Dimensional analysis techniques utilize the concept of dimensional homogeneity and reduce the number of variables for representing a physical system.

Dimensional analysis is a proven technique to scale parameters and express a system of equations in dimensionless variables. This technique is used to reduce complexity of variables in a system and to obtain relationships among the variables to form dimensionless numbers that characterize the physical system. Dimensional analysis appears to have added relevance in experimental work since it provides information about characteristic parameters which influence the physical phenomenon.

Two common techniques are used for dimensional analysis: Buckingham Pi method and Rayleigh method. These techniques require knowledge of variables which influence the physical system. The Buckingham Pi method is well known and is a widely used technique for dimensional analysis. It is a systematic approach and ensures a minimum number of dimensionless parameters.

The Rayleigh method and the Buckingham method approach are easy to apply, but sometimes knowledge of all variables influencing the system is not available. These approaches neglect unknown nondimensional groups characterizing system behavior from system description.

In the following subsections Rayleigh and Buckingham methods are described. But subsequent discussions are based on the Buckingham method due to its simplicity in application to complex interconnected systems.

3.3.2 Rayleigh Method

Rayleigh's method consist of formulating functional relationships between variables of a physical system in the form of exponential equations. Rayleigh's method involves a sequence of steps to generate dimensionless form from dimensional form, as proposed by Lord Rayleigh.

In order to apply Rayleigh's method, the knowledge about independent and dependent variables of the system is needed. A functional equation is formulated between dependent and independent variables based on system information. Suppose V_d is a variable that depends upon a number of independent variables V_n, then the functional equation can be written as

$$V_d = f(V_1, V_2, ...V_n) \tag{3.4}$$

The functional equation can be expressed as power equation of independent variables.

$$V_d = CV_1^a V_2^b ....V_n^k \tag{3.5}$$

where C is a nondimensional constant and $a, b, \ldots, k$ are arbitrary powers of independent variables. Dimensions are introduced in the power equation using any unit convention and presented in the form of fundamental units. Simultaneous equations involved with exponent powers, are obtained by using dimensional homogeneity. The

simultaneous equations are solved to evaluate the values for variable powers $a, b, \ldots, k$. The exponent values are substituted in the power equation and variables of similar exponent are combined to form nondimensional parameters.

For example, consider a spherical ball moving in a viscous fluid. The drag force exerted on the ball is influenced by the system parameters such as diameter size (D) and velocity of ball (V). The properties of the fluid medium such as density (ρ) and viscosity (μ) also influence the drag force. The Rayleigh's approach relates the variables by satisfying dimensional homogeneity. The drag force on the spherical ball can be written in the form of a functional equation as

$$F_d = f(D, V, \rho, \mu) \tag{3.6}$$

The functional equation can be expressed as the power equation

$$F_d = C D^a V^b \rho^c \mu^d \tag{3.7}$$

where C is dimensionless number and a, b, c, d are exponential power of independent variables. Dimensions for the variables are substituted with the MLT convention

$$\frac{[M][L]}{[T]^2} = [L]^a \frac{[L]^b}{[T]^b} \frac{[M]^c}{[L]^{3c}} \frac{[M]^d}{[L]^d [T]^d} \tag{3.8}$$

The dimensional homogeneity condition requires identical exponent power on both sides of the equation. Hence, equating the exponent powers on both sides of the equation we obtain

For L:

$$1 = a + b - 3c - d$$

For M:

$$1 = c + d$$

For T:

$$-2 = -b - d$$

Since, we have three equations and four unknowns, solve a, b and c in terms of d to get

$$a = 2 - d$$

$$b = 2 - d$$

$$c = 1 - d$$

Hence

$$F_d = CD^{2-d}V^{2-d}\rho^{1-d}\mu^d \tag{3.9}$$

Grouping similar exponent variables we can write

$$F_d = C(\rho)(D^2V^2)(\frac{VD\rho}{\mu})^{-d} \tag{3.10}$$

The nondimensional quantity formed is $\frac{VD\rho}{\mu}$ and is known as Reynolds number (R). The original functional equation (3.6) becomes

$$F_d = f(R)\rho D^2V^2 \tag{3.11}$$

The term $\frac{F_d}{\rho D^2V^2}$ is another dimensionless parameter and there is a relationship between the two nondimensional groups. The drag force depends on Reynolds number and the term ρD^2V^2. Nondimensional quantities formed by Rayleigh's method are used to characterize the system. Rayleigh's method requires knowledge of dependent and independent variables of a system which form the functional equation. In some complex systems, it is difficult to find the dependent and independent variables. In order to form dimensionless parameters, simultaneous equations are needed to solve. While in Buckingham Pi theorem, the evaluation of dimensionless parameters depend upon matrix calculation which is easy compared to solving simultaneous equations.

3.3.3 Buckingham Pi Theorem

The Buckingham Pi theorem provides a basis for dimensional analysis. This is a more generalized and systematic approach of determining the minimum number of dimensionless variables that characterize the system. The advantage of using this method is that it predicts the number of dimensionless groups at the initial stage of analysis.

The Buckingham Pi theorem states that, a dimensionally homogeneous equation containing 'n_d' dimensional variables/parameters, described by 'm_r' fundamental dimensions, can be grouped into '$n_d - m_r$' dimensionless groups. Formally, the theorem statement is the following.

Buckingham Pi Theorem: Let $f(V_1, V_2, ...V_n) = 0$ be a set of dimensional homogeneous equations with 'n_d' parameters and described by 'm_r' fundamental dimensions. The dimensional equation 'f' can be expressed by another set of equations 'F' with '$n_d - m_r$' dimensionless parameters. The nondimensional groups are referred to as 'Π' terms. The set of equations 'F' can be written as $F(\Pi_1, \Pi_2, ...\Pi_n) = 0$ and the nondimensional 'Π' terms characterize the system.

Proof: The dimension of each variable V_i can be expressed in terms of powers of fundamental quantities, say Q_i. Therefore

$$V_i = [Q_1]^{a_{1i}}[Q_2]^{a_{2i}} \dots [Q_m]^{a_{mi}} \tag{3.12}$$

Pi terms are formed by a combination of variables which characterize the system. Hence, Pi terms can be expressed in the form of powers of those variables:

$$\Pi_i = [V_1]^{b_1}[V_2]^{b_2} \dots [V_n]^{b_n} \tag{3.13}$$

But Pi terms are dimensionless and can be also expressed in terms of fundamental quantities with zero exponential powers:

$$\Pi_i = [Q_1]^0[Q_2]^0 \dots [Q_n]^0 \tag{3.14}$$

By substituting equation (3.12) in (3.13), each Pi term can be expressed as

$$\Pi_i = [Q_1]^{b_1a_{11}+b_2a_{21}+\ldots+b_na_{n1}} \ldots [Q_m]^{b_1a_{1m}+b_2a_{2m}+\ldots+b_na_{nm}} \tag{3.15}$$

Comparing the exponential terms for Pi parameters from equations (3.14) and (3.15), results in 'm_r' simultaneous equations

$$b_1a_{11} + b_2a_{21} + \ldots + b_na_{n1} = 0 \tag{3.16}$$

$$b_1a_{12} + b_2a_{22} + \ldots + b_na_{n2} = 0 \tag{3.17}$$

$$\vdots$$

$$b_1a_{1m} + b_2a_{2m} + \ldots + b_na_{nm} = 0 \tag{3.18}$$

In many practical systems, the number of fundamental quantities is less than the number of variables of the system. Hence, we have 'm_r' independent solutions and '$n_d - m_r$' are free variables. The values of the free variables can be selected arbitrarily. The arbitrary choice of variables form the different Pi groups equivalently characterizing the system. This completes the proof for the Buckingham Pi theorem.

Procedure to be followed to evaluate Pi parameters:

Step 1: List all the parameters which characterize the system. Suppose the list includes 'n_d' number of parameters. Based on empirical knowledge or engineering judgement less significant parameters can be dropped.

Step 2: Choose a set of fundamental dimensions suitable for the system. Seven fundamental units are listed in Table 3.1. Determine the number of fundamental parameters (say 'm_r') required to describe the system parameters from the listed Table 3.1.

Step 3: Express all the dimensional parameters in terms of fundamental quantities. The dimensions are written in the form of exponential powers of fundamental quantities. For example, Force = [Mass][Length][Time]$^{-2}$.

Step 4: Separate 'm_r' number of system parameters from the original list of 'n_d' number of parameters. This set must contain all the fundamental units used to describe the system. The set of 'm_r' parameters are called 'repeating parameters'. Do not choose the repeating parameters which are just multiples of each other. For example, Length (L) and area (L^2).

Step 5: Write the dimensions of non repeating physical variables in column form followed by dimensions of repeating variables. The matrix formed by nonrepeating parameters is called the dimensional matrix and is of the size '$m_r \times N_V$' where 'm_r' is the number of fundamental dimensions needed to express the variables and 'N_V' is the number of non repeating variables. The dimensional matrix is denoted by 'A'. Another matrix formed by repeating parameters is of size '$m_r \times m_r$' and is denoted by 'B'.

step 6: Calculate the number of nondimensional group '$n_d - m_r$'. Put the identity matrix 'D' below the dimensional matrix of size '$n_d - m_r$'. Compute the matrix 'C' using the relation

$$C = (-A^{-1}B)^T \tag{3.19}$$

Each row elements of matrix 'D' and 'C' gives the exponential power of non repeating variables and repeating variables, respectively, for dimensionless parameters. This completes the formation of dimensionless parameters.

Step 7: Verify that the formulated Pi parameters are dimensionless.

The given procedure is best illustrated by examples. Consider the drag force F_d exerted on a sphere due to movement through a viscous liquid. The variables involved in the process are drag force (F_d), velocity of sphere (V), diameter of sphere (D), density of liquid (ρ) and viscosity of liquid (μ). Units and dimensions of variables are given in Table 3.2. The relation between system variables is not known. We will

Variable	Units	Dimension
Drag Force (F_d)	m kg s^{-2}	[M][L][T]$^{-2}$
Velocity of sphere (V)	m s^{-1}	[L][T]$^{-1}$
Diameter of sphere (D)	m	[L]
Density of liquid (ρ)	m^{-3} kg	[M][L]$^{-3}$
Viscosity of liquid (μ)	m^{-1} kg s	[M][L]$^{-1}$[T]

Table 3.2: Units and Dimensions of Variables

rearrange the variables with unknown function of the form

$$f(F_d, \mu, L, V, \rho) = 0 \tag{3.20}$$

where f is the unknown function.

According to the Buckingham Pi Theorem, the 'n_d' variables of the system can be rearranged in '$n_d - m_r$' Pi dimensionless parameters and 'm_r' number of fundamental quantities needed to describe the system parameters. In this example, $n_d = 5$, $m_r = 3$. Hence, the system variables can be rearranged in two dimensionless parameters. The dimension matrix can be formed as shown in Figure 3.2.

The matrices 'C' and 'D' represent exponential powers of variables which group together to formulate dimensionless Pi parameters. The two dimensionless parameters are

$$\Pi_1 = \frac{F_d}{D^2 \rho V^2}$$

$$\Pi_2 = \frac{\mu V}{D^3 \rho} \tag{3.21}$$

Furthermore, the dimensionless functional equation can be written as

$$g(\Pi_1, \Pi_2) = 0 \tag{3.22}$$

The Buckingham theorem reduces the number of variables and presents the system equations in a simplified manner. In this example with dimensionless representation

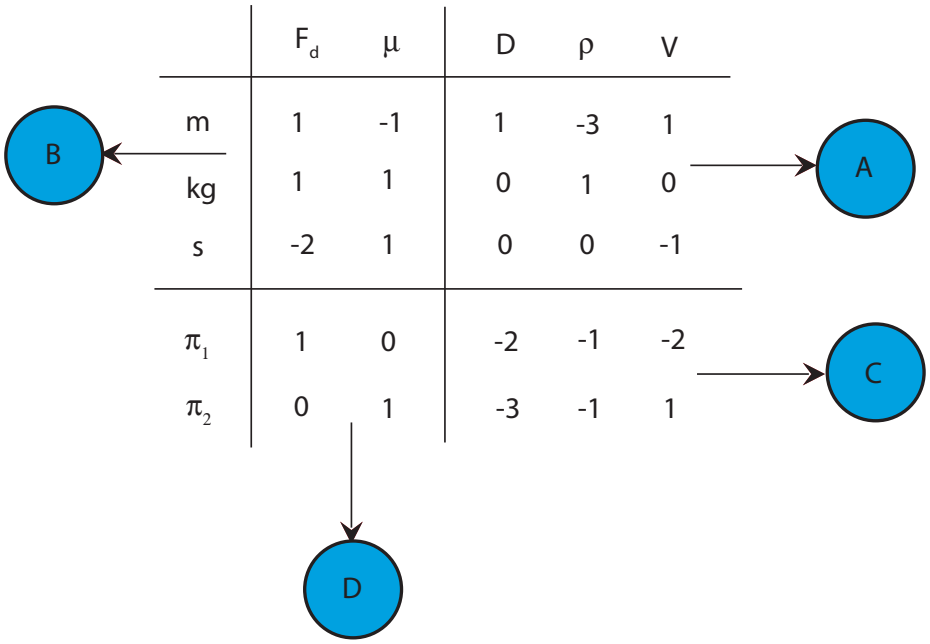

Figure 3.2: Dimensional Matrix

we have only two parameters to deal with. Dimensional analysis does not provide the relation between the two Pi parameters, i.e., the coefficient or powers of the Pi groups. The relation needs to be determined from theory or experiments.

3.3.4 Scaling Laws and Similitude

The principle of similarity relate physical systems of different sizes and are beneficial for scaling up or down of physical systems. In many applications it is advantageous to perform experiments on a small prototype before building the actual system. For example, aerodynamics, ship building, robotics, etc. Similitude ensures similar behavior between the scaled prototype and the actual system. The principle of similarity is a principle of nature while dimensional analysis is a technique by which the similarity principles are applied to different systems. There are three types of similarity: geometric similarity, kinematic similarity and dynamic similarity, which are discussed below.

Geometric Similarity:

Physical systems have generally three characteristics: size, shape and composition. These characteristics are independent of each other. Similarity can be stated in two ways, by specifying ratios of different measurements in a body or similar measurements in different bodies. Geometric similarity ensures identical scaling of linear dimensions between the prototype and the actual system. Two systems are said to be geometrically similar when every point in one system is corresponding to a point in the other system. Geometric similarity assures application of experimental results obtained from the prototype to the actual size system. Consider a point of one system in cartesian coordinates x, y, z and another point of a second system x', y', z' as shown in Figure 3.3. These points are related by

$$\frac{x'}{x} = \frac{y'}{y} = \frac{z'}{z} = L \tag{3.23}$$

where L is the scale ratio which is a constant.

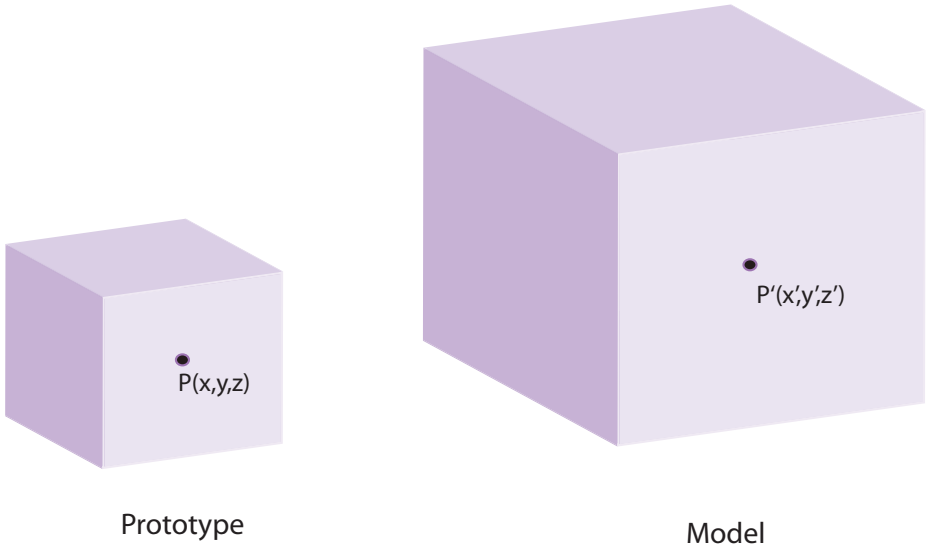

Figure 3.3: Geometric Similarity

The similarity in which scale ratios for two bodies are different in different directions is called distorted similarity. Distorted systems are described by two or more scale ratios.

Kinematic Similarity:

Kinematic similarity is concerned with the motion of a system. Kinematic similarity has additional dimension of time compared to three space coordinates of geometric similarity. Time is measured from arbitrary zero for every system and corresponding time measured by time scale ratio. Kinematic similarity ensures homologous time between the prototype and the actual system. A geometrically similar moving system is said to be kinematically similar when corresponding particles of the system trace geometrically similar paths in a specified interval of time. If the time scale is less than unity, the prototype behaves more slowly than the actual model.

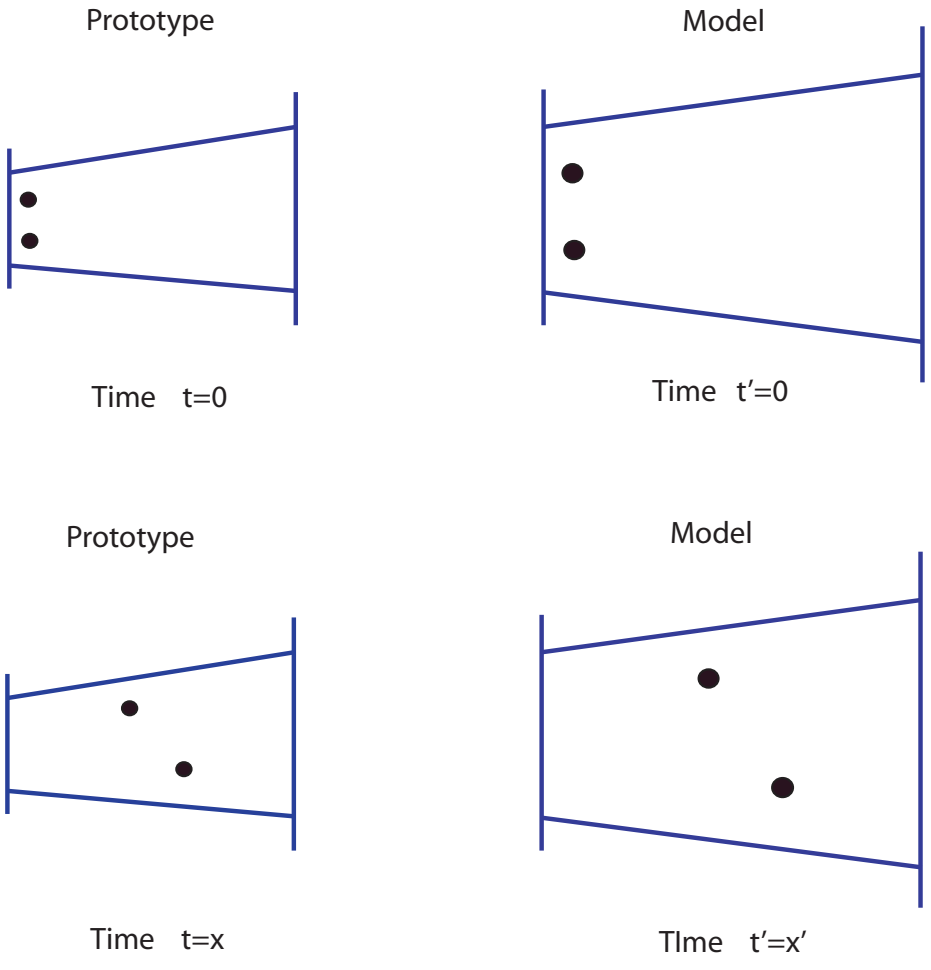

Figure 3.4: Kinematic Similarity

Dynamic Similarity:

Dynamic similarity is related to the forces acting on a system. Dynamic similarity means geometrically similar parts of the prototype and the actual system experience similar forces. In any system some forces cause motion while others may set static stresses. Geometrically similar moving systems are dynamically similar when the corresponding force ratios are equal.

$$\frac{F_1'}{F_1} = \frac{F_2'}{F_2} = \ldots = \frac{F_n'}{F_n} = \mathbf{F} \tag{3.24}$$

Dynamic similarity between two systems requires identical nondimensional dynamics. This means that nondimensional Pi parameters involved in that dynamics have equal values. Dynamic similarity does not imply geometric or kinematic similarity.

Dimensional analysis applies similarity conditions between the prototype and the actual system. The two systems are said to be dimensionally equivalent if all the nondimensional parameters have the same values for the prototype and the actual system.

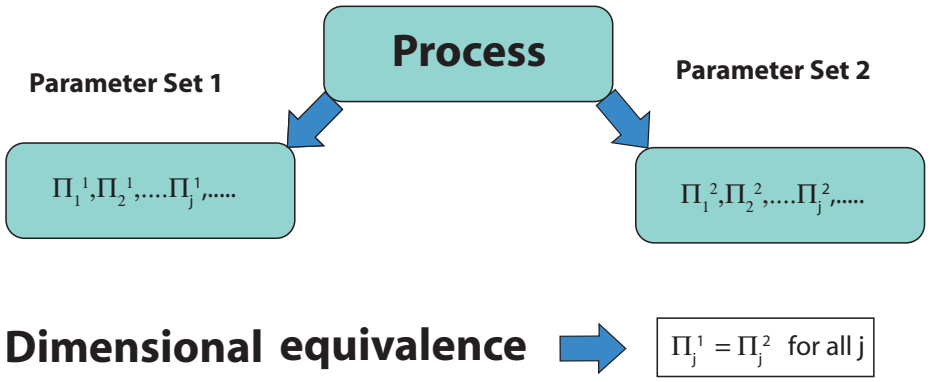

Figure 3.5: Dimensional Equivalence Between Two Systems

3.3.5 Application of Dimensional Analysis

Dimensional analysis is used in many fields for the purpose of reduction of number of variables and to simplify the system representation. Dimensional analysis is extensively used in the fields of fluid dynamics and thermodynamics. It is found to be effective in other fields like robotics, aerodynamics, ship design, structural dynamics, and economics.

Dimensional analysis can also be applied to web transport systems. Industrial web transport systems are large-scale interconnected systems. Dimensional analysis can be performed on a small-scale experimental platform and then scaled up to the actual industrial setup. Hence, it is possible to scale process parameters and controller parameters of the experimental platform with dimensional analysis techniques. This minimizes the period required to design a new web transport line, and also helps in designing controllers for industrial lines without much effort. Dimensional analysis can be used to determine time scaling, tension scaling and velocity scaling in a web transport system.

The remainder of this chapter describes the application of dimensional analysis technique (Buckingham Pi theorem) to web transport systems. The analysis output will be used in formulation of scaled process parameters and control laws for web transport systems.

3.4 Web Line Dimensional Analysis

A simplified three tension zone web line is shown in Figure 3.6. The simplified web line mimics many features of a general web transport system. The simplified web line is also a representation of the Euclid Web Line (EWL), an experimental platform available at WHRC. The web line shown in Figure 3.6 is divided into four sections: unwind section, master speed roller, process section and rewind section. In Figure 3.6, M_i denotes driving motors, v_i represents web transport velocity on the i^{th}

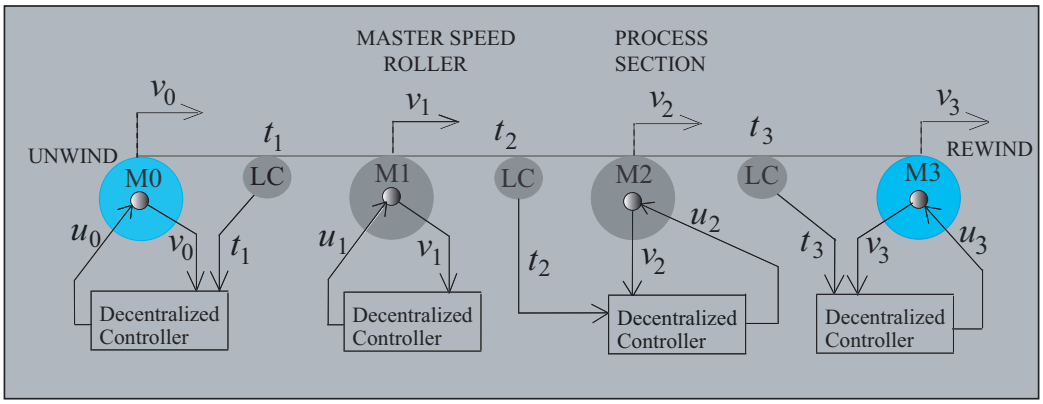

Figure 3.6: A Web line Sketch

roller, u_i represents input torque from the i^{th} motor, and t_i represents web tension between $i-1^{th}$ and i^{th} driven rollers. The master speed roller regulates reference speed for the web line and does not regulate tension in adjacent spans. The master speed roller operates under a single loop speed control. Unwind/rewind roll and pull roller is regulated by a cascaded tension and speed control system. The unwind and rewind zones release and accumulate web material, respectively. The dynamics of unwind/rewind contains time-varying parameters such as inertia and radii. The pull roll section contains downstream and upstream web span and a driven roller. A typical industrial web line is large in size and contains many pull roll sections repeated throughout the line. For the purpose of illustrating dimensional analysis, the pull roll section is chosen. It is also possible to perform dimensional analysis for unwind and rewind sections using the same procedure. Dimensional and nondimensional dynamics of the process section is presented in the following subsections.

3.4.1 Pull Roll Section Dimensional Equations

The pull roll section consists of two variables: tension in the upstream span t_2 and velocity of the pull roll v_2. The governing equation for web tension is given by

$$\dot{t}_2 = \frac{EA}{L_2}(v_2 - v_1) + \frac{t_1 v_1}{L_2} - \frac{t_2 v_2}{L_2} \tag{3.25}$$

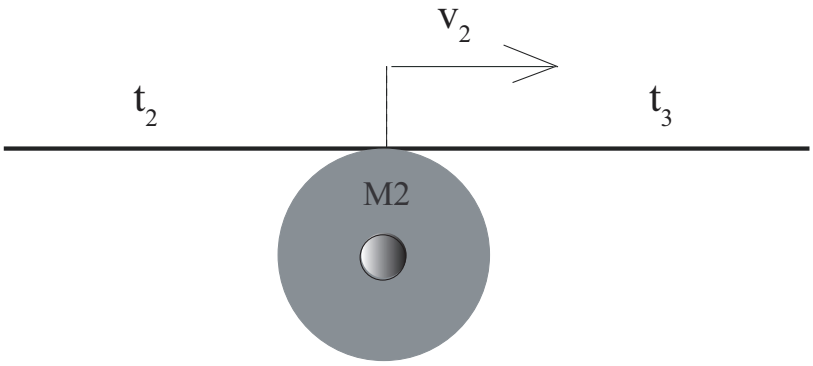

Figure 3.7: A Pull Roll

The governing equation for velocity on the roller is given by

$$\dot{v}_2 = \frac{R_2^2}{J_2}(t_3 - t_2) + \frac{R_2}{J_2} n_2 u_2 \tag{3.26}$$

where t_i : web tension in the i^{th} span, v_i : velocity of the i^{th} roll, R_2 : pull roll radius, n_2 : gear ratio, J_2 : inertia of the pull roll, E : elastic modulus of the web material, A : cross section area of the web, L_i : length of the i^{th} span, u_2 : torque input to pull roll.

3.4.2 Nondimensional Dynamics

The list of parameters for the pull roll system include tension in web spans (t_1, t_2, t_3), velocity of driven rollers (v_1, v_2), inertia of pull roll (J_2), radius of pull roll (R_2), length of web span (L_2), time (t), modulus of elasticity times area of cross section (EA), and input torque (u_2). Eleven parameters are influenced in the selected web zone. Three fundamental dimensions, length, force and time are chosen to describe the parameters. The unit system used for the fundamental dimensions are feet (ft), pound-force (lbf), and second (s), respectively. Using Buckingham Pi theorem there are eight nondimensional Pi parameters which characterize the dimensionless system.

The dimensional parameters can be expressed in terms of fundamental dimensions. For example, the tension variable can be written as $[L]^0[F]^1[T]^0$. So, the tension pa-

rameter forms the column vector with exponent of dimensions as $[0\ 1\ 0]^T$ which is used in dimensional representation. Three repeating parameters for dimensional analysis are selected from the list of parameters as R_2, $\frac{EA}{L_2}$, and $\frac{R_2}{J_2}$ since these parameters contain all the fundamental dimensions chosen to describe the system. These repeating parameters must be chosen such that the dimensional columns of repeating parameters are independent. Dimensional matrix is formed by writing non-repeating parameters in dimensional form followed by repeating parameters. For the pull roll section dimensional matrix size is 3×8 and non repeating parameters matrix is of size 3×3. Non repeating parameters matrix need to be non singular in nature.

Place the identity matrix 'D' of size 8×8 below the dimensional matrix. Matrix 'C' can be calculated by equation (3.19). The rows of matrix 'D' and 'C' represent exponent powers of repeating and non repeating parameters which group together to form dimensionless Pi parameters.

The Table 3.3 describes the dimensional matrix and formation of Pi groups.

	t	u_2	v_1	t_3	v_2	t_2	t_1	$\frac{1}{L_2}$	R_2	$\frac{EA}{L_2}$	$\frac{R_2}{J_2}$
ft	0	1	1	0	1	0	0	-1	1	-1	0
lbf	0	1	0	1	0	1	1	0	0	1	-1
s	1	0	-1	0	-1	0	0	0	0	0	-2
Π_1	1	0	0	0	0	0	0	0	0.5	0.5	0.5
Π_2	0	1	0	0	0	0	0	0	-2	-1	0
Π_3	0	0	1	0	0	0	0	0	-1.5	-0.5	-0.5
Π_4	0	0	0	1	0	0	0	0	-1	-1	0
Π_5	0	0	0	0	1	0	0	0	-1.5	-0.5	-0.5
Π_6	0	0	0	0	0	1	0	0	-1	-1	0
Π_7	0	0	0	0	0	0	1	0	-1	-1	0
Π_8	0	0	0	0	0	0	0	1	-1	0	0

Table 3.3: Dimensional Matrix For Web Dynamics

Referring to Table 3.3, the Pi parameters are given by

$$\Pi_1 = tR_2\sqrt{\frac{EA}{L_2J_2}} = \tau \tag{3.27}$$

$$\Pi_2 = u_2\frac{L_2}{R_2^2EA} = \overline{u}_2 \tag{3.28}$$

$$\Pi_3 = \frac{v_1}{R_2^2}\sqrt{\frac{L_2J_2}{EA}} = \overline{v}_1 \tag{3.29}$$

$$\Pi_4 = t_3\frac{L_2}{R_2EA} = \overline{t}_3 \tag{3.30}$$

$$\Pi_5 = \frac{v_2}{R_2^2}\sqrt{\frac{L_2J_2}{EA}} = \overline{v}_2 \tag{3.31}$$

$$\Pi_6 = t_2 \frac{L_2}{R_2 EA} = \overline{t}_2 \tag{3.32}$$

$$\Pi_7 = t_1 \frac{L_2}{R_2 EA} = \overline{t}_1 \tag{3.33}$$

$$\Pi_8 = \frac{R_2}{L_2} = \overline{c} \tag{3.34}$$

A qualitative interpretation of representative Pi group to maintain dynamic equivalence is given below,

$\Pi_1 = tR_2\sqrt{\frac{EA}{L_2 J_2}} = \tau$: This Pi parameter is used to moderate time scaling of two systems. The material parameter EA and system parameters L, R, and J make implications on time scale. As EA and R are increased, t must decrease to maintain dynamic equivalence. Similarly, increasing L and J will result in increasing the time span.

$\Pi_2 = u_2 \frac{L_2}{R_2^2 EA} = \overline{u}_2$: This Pi parameter represents control input scaling to the system. It ultimately scales the controller gains. The formed Pi group depends upon the material property EA and system parameters L and R. With an increase in the span length, control input needs to be decreased to maintain dynamic equivalence. If parameters R and EA are increased, then the control input must be increased to maintain dynamic equivalence.

$\Pi_3 = \frac{v_1}{R_2^2}\sqrt{\frac{L_2 J_2}{EA}} = \overline{v}_1$: This Pi parameter scales the web line speed. The speed scaling depends upon material properties EA and system parameters R, L, and J. With a higher modulus material, i.e., higher E value, one must increase line speed.

$\Pi_4 = t_3 \frac{L_2}{R_2 EA} = \overline{t}_3$: This Pi parameter scales web tension and is proportional to the span length. Tension scaling also depends upon R and EA.

$\Pi_8 = \frac{R_2}{L_2} = \overline{c}$: This Pi parameter represents a geometrical constraint on the system. In order to maintain dynamic equivalence, the ratio of roller radius to span length must remain the same.

The dimensionless dynamic model can be formed by substituting the above formed Pi groups in dimensional equations (3.25) and (3.26). The dimensionless equations are given by

$$\dot{\overline{t}}_2 = (\overline{v}_2 - \overline{v}_1) + \overline{c}(\overline{t}_1\overline{v}_1 - \overline{t}_2\overline{v}_2) \tag{3.35}$$

$$\dot{\overline{v}}_2 = \overline{t}_3 - \overline{t}_2 + n_2\overline{u}_2 \tag{3.36}$$

Clearly, the dimensionless tension and velocity dynamics with reduced number of variables are simple in representation compared to the dimensional model. The simple dynamic representation helps in analysis and design of controllers. The resultant dimensionless model given by equations (3.35) and (3.36) is also nonlinear.

The nonlinear dimensionless dynamics can be linearized in order to analyze and design simple controllers. Define the variables: tension variation $\overline{T}_i = \overline{t}_i - \overline{t}_{ri}$, velocity variation $\overline{V}_i = \overline{v}_i - \overline{v}_{ri}$, and control input variation $\overline{U}_i = \overline{u}_i - \overline{u}_{ieq}$. $\overline{t}_{ri}$ and $\overline{v}_{ri}$ are nondimensional tension and velocity references. Therefore, the linearized dynamics is given by

$$\dot{\overline{x}}_2 = \begin{bmatrix} \dot{\overline{T}}_2 \\ \dot{\overline{V}}_2 \end{bmatrix} = \overline{A}_2\overline{x}_2 + \overline{B}_2\overline{U}_2 + \sum_{j=1, j\neq 2}^{3} \overline{A}_{2j}\overline{x}_j \tag{3.37}$$

where

$$\overline{A}_2 = \begin{bmatrix} -\overline{CV}_{2r} & 1 \\ -1 & 0 \end{bmatrix}, \qquad \overline{B}_2 = \begin{bmatrix} 0 \\ 1 \end{bmatrix}$$

$$\overline{A}_{21} = \begin{bmatrix} \overline{CV}_{2r} & \overline{C}\overline{t}_{1r} - 1 \\ 0 & 0 \end{bmatrix}, \qquad \overline{A}_{23} = \begin{bmatrix} 0 & 0 \\ 1 & 0 \end{bmatrix}$$

The non dimensional speed and tension references are given by

$$\overline{v}_{2r} = \frac{v_{2r}}{R_2^2}\sqrt{\frac{L_2 J_2}{EA}} \quad \text{and} \quad \overline{t}_{1r} = t_{1r}\frac{L_2}{R_2 EA} \tag{3.38}$$

The nondimensional state matrices are in simpler form compared to the dimensional case. The simplified form may help in analysis and design of advanced controllers.

3.4.3 Controller Scaling

A scaling law for a PI control strategy will be determined in this section. Controller scaling can be extended to any type of controller with its characteristic parameters like H_2, H_∞ and sliding mode. The control strategy for the pull roll section is shown in Figure 3.8. The control signal for the outer loop is based on tension feedback and controller scaling laws are applied to the tension loop. The tension loop PI controller

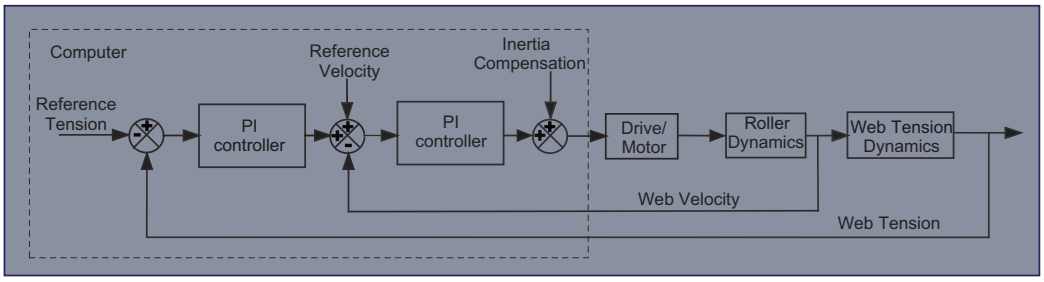

Figure 3.8: Pull Roll Control Strategy

can be expressed in frequency domain as:

$$C(s) = k_p\frac{s+\omega}{s} \tag{3.39}$$

where k_p: Proportional gain (ft), ω: Frequency (rad/sec), s: Frequency domain parameter (1/sec).

The set of parameters which characterize the PI controller is given by

$$\Phi = \{k_p, \omega, s\} \tag{3.40}$$

Scaling of the controller will require that these gains be scaled appropriately. The controller added three more parameters in the closed loop system and this introduced three dimensionless parameters in addition to the ones mention above. The controller parameters can be written in dimensional form as

$$k_p \equiv [L]^1[F]^0[T]^0 \tag{3.41}$$

$$\omega \equiv [L]^0[F]^0[T]^{-1} \tag{3.42}$$

$$s \equiv [L]^0[F]^0[T]^{-1} \tag{3.43}$$

Hence, by extending the Buckingham theorem to the closed loop system we get the following Pi parameters

$$\Pi_9 = \frac{k_p}{R_2} = \overline{k}_p \tag{3.44}$$

$$\Pi_{10} = s\frac{1}{R_2}\sqrt{\frac{L_2 J_2}{EA}} = \overline{s} \tag{3.45}$$

$$\Pi_{11} = \omega\frac{1}{R_2}\sqrt{\frac{L_2 J_2}{EA}} = \overline{\omega} \tag{3.46}$$

The Pi parameters implicate, proportional gain is inversely proportional to radius of roller. The Pi parameter corresponding to controller frequency depends on material properties EA and system parameters R, J, and L. Higher modulus materials require increase in frequency of controller to maintain dynamic equivalence. The nondimensional form of the controller is given by

$$\overline{C}(\overline{s}) = \overline{k}_p\frac{\overline{s}+\overline{\omega}}{\overline{s}} \tag{3.47}$$

This completes the non-dimensionalization of the controller. The nondimensional controller is a parametrization of the controller for a dynamically equivalent dimensional system. The controller scaling may expedite the process of tuning controller parameters for dynamically equivalent systems.

3.4.4 Model Law

The scaling law relates the parameters in the model and the prototype. Scale factor of particular parameter is defined as the ratio of the magnitude of that parameter for the candidate model to its magnitude for the base model. For example, the scale factor for length is

$$S_L = \frac{L_1}{L_2} \tag{3.48}$$

where L_1: length of prototype, L_2: length of model.

The model law is a relation or a set of relations between scale factors formed in a particular modeling. The relation between scale factors are formed on the basis of dimensionless Pi parameters. The model law can be formed very easily based on the Pi parameters. For example, the time scale Pi parameter is given by equation (3.27) and the model law for this is

$$S_t = S_{L_2}^{0.5} S_{J_2}^{0.5} S_{R_2}^{-1} S_{EA}^{-0.5} \tag{3.49}$$

where S_t: time scale factor, S_{L_2}: length scale factor, S_{J_2}: inertia scale factor, S_{R_2}: radius scale factor, S_{EA}: modulus and area scale factor.

Similarly, model law applied to web dynamics Pi parameters (3.28) to (3.34) and controller Pi parameters (3.44) to (3.46), gives the scale factor relations as

$$S_{u_2} = S_{R_2}^2 S_{EA} S_{L_2}^{-1} \tag{3.50}$$

$$S_{v_1} = S_{R_2}^2 S_{EA}^{0.5} S_{L_2}^{-0.5} S_{J_2}^{-0.5} \tag{3.51}$$

$$S_{t_3} = S_{R_2} S_{EA} S_{L_2}^{-1} \tag{3.52}$$

$$S_{v_2} = S_{R_2}^2 S_{EA}^{0.5} S_{L_2}^{-0.5} S_{J_2}^{-0.5} \tag{3.53}$$

$$S_{t_2} = S_{R_2} S_{EA} S_{L_2}^{-1} \tag{3.54}$$

$$S_{t_1} = S_{R_2} S_{EA} S_{L_2}^{-1} \tag{3.55}$$

$$S_{R_2} = S_{L_2} \tag{3.56}$$

$$S_{k_p} = S_{R_2} \tag{3.57}$$

$$S_s = S_{R_2} S_{EA}^{0.5} S_{L_2}^{-0.5} S_{J_2}^{-0.5} \tag{3.58}$$

$$S_\omega = S_{R_2} S_{EA}^{0.5} S_{L_2}^{-0.5} S_{J_2}^{-0.5} \tag{3.59}$$

The model law states the dimensional equivalence conditions for system parameters and variables. It restricts the application of scaling factors to any general web handling system. The implication can be explained by changing the web material in a web transport system. It implies change in material parameters like modulus of elasticity (E), density (ρ) etc. Dynamic equivalence conditions given by equations (3.51) and (3.55) show that the change in modulus results in a change in operating velocity and tension.

Equations (3.57) to (3.59) indicate that, for the same web platform i.e. geometrical similar systems, controller gains change only with a change in web material property values. Hence, controller gains can be scaled based on material properties for the same web line.

Dimensional analysis can be applied to dynamically equivalent systems with dif-

ferent materials, different tension feedback systems and web configurations. Some examples are given in the following sections.

3.5 Dimensional Analysis for Different Materials

The application of dimensional analysis can be illustrated by taking into account a web transport system processing different kinds of materials. The pull roll section of the EWL with outer tension loop and inner velocity loop is considered for this study. Therefore, the web transport system platform processing different materials is the same, which implies geometric similarity is maintained. The kinematic and dynamic similarity can be achieved by requiring equal dimensionless Pi parameters. The web materials chosen are Tyvek (EA = 2800 lbf), polyester (EA = 207 lbf), and polyethylene (EA = 263 lbf). To illustrate the controller scaling laws given by equations (3.57) to (3.59), a PI controller is tuned for Tyvek material and the controller gains are scaled for polyester and polyethylene.

System with Scaled Polyester:

For the system with Tyvek material, parameter specifications are L_i=2.7 ft, t_r=20 lbf, V_r=150 fpm, R_i=0.125 ft, and EA = 2800 lbf. Consider the system with polyester with L_i = 2.7 ft and EA = 207 lbf. All other parameters of both web systems are kept similar which results in unit scaled factors. The goal is to design a control system for the polyester web material system by scaling the tuned Tyvek web system. The model law for these two systems are given by equations (3.49) to (3.59) and the scale factor values of both systems are shown in Table 3.4. The scaled process parameters are, t_r=1.48 lbf, V_r=40.82 fpm. The scale factor values indicate that the proportional gain for both systems remains the same. Integral gain changes by a factor of '0.2721'. Time scale factor is '3.6747'. The controller gains tuned for Tyvek system on EWL are proportional gain, $k_p = 12$ and integral gain, $k_i = 1.2$. Hence, the scaled controller gains for the polyester web system are proportional gain, $k_p = 12$ and integral gain,

Scale Factor	Value	Scale Factor	Value
S_t	3.6747	S_{u_2}	0.074
S_{v_1}	0.2721	S_{t_3}	0.074
S_{R_2}	1	S_{k_p}	1
S_s	0.2721	S_ω	0.2721

Table 3.4: Scaled Factors for Polyester System

$k_i = 0.3265$. The system response is slow due to the scaled time factor.

System with Scaled Polyethylene:

In another simulation the existing Tyvek web system is replaced with polyethylene web material. The polyethylene system has span length $L_i = 2.7$ ft, $EA = 262.8$ lbf. The geometrical parameters of both web systems are kept similar which results in unit scaled factors. The model law for these two systems are given by equations (3.49) to (3.59) and scale factor values are given in Table 3.5.

Scale Factor	Value	Scale Factor	Value
S_t	3.2637	S_{u_2}	0.0938
S_{v_1}	0.3064	S_{t_3}	0.0938
S_{R_2}	1	S_{k_p}	1
S_s	0.3064	S_ω	0.3064

Table 3.5: Scaled Factors for Polyethylene System

The scaled process parameters are, $t_r = 1.88$ lbf, $V_r = 45.96$ fpm. Polyethylene control system has similar proportional gain value compared to Tyvek system. Integral gain changes by a factor of '0.3064'. Time scale factor is '3.2637'. The scaled controller gains for polyethylene web system are proportional gain, $k_p = 12$ and integral gain, $k_i = 0.3677$. The system response is slow due to the scaled time factor.

3.6 Dimensional Analysis of an Accumulator

The accumulator is one of the important primitive elements in web transport systems and plays a key role in continuous operation of web processing lines. Capacity of an accumulator is increased by increasing the carriage height. Dimensional analysis of an accumulator is performed in terms of capacity scaling. A simplified dynamic model of the accumulator is taken into consideration, that includes accumulator carriage dynamics, average web tension dynamics in accumulator web spans, driven roller dynamics at entry and process sides. We consider accumulator carriage control in conjunction with entry and process driven rollers. A schematic of accumulator is shown

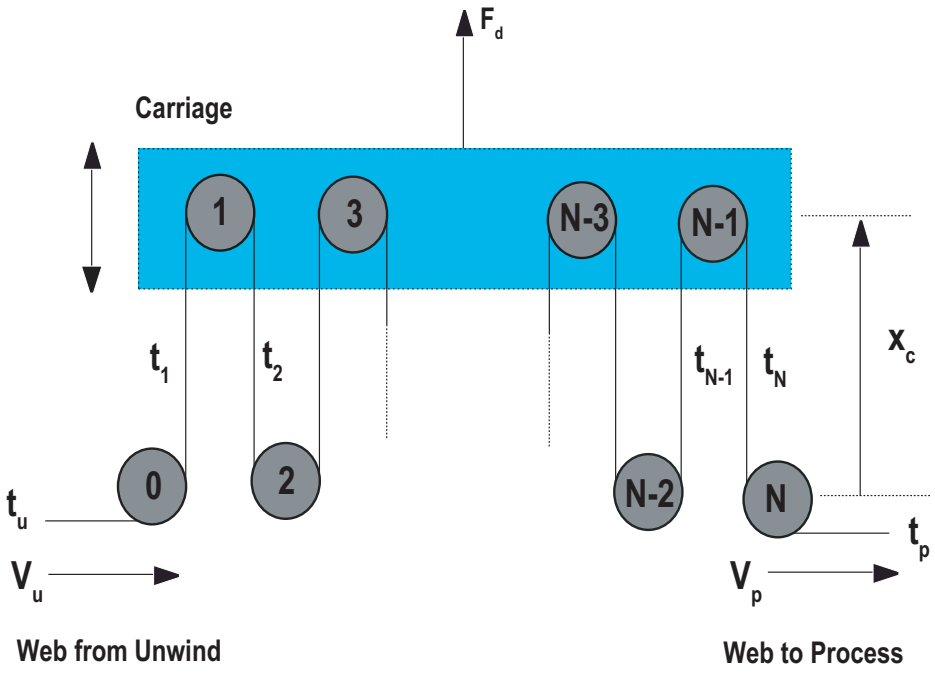

Figure 3.9: Schematic of an Entry Accumulator

in Figure 3.9 which includes carriage, web spans and rollers.

The carriage dynamics of the accumulator is given by

$$M_c \frac{d^2 x_c(t)}{dt^2} = u_c(t) - F_d(t) - M_c g - N t_c(t) \tag{3.60}$$

where u_c is the controlled force; F_d is the disturbance force due to friction in hydraulic cylinder and rod seals, friction in carriage guides, and external forces on carriage; M_c is the mass of carriage; t_c is the average tension in the accumulator spans; and N is the number of spans in the accumulator.

The average tension dynamics in accumulator web spans is given by

$$\frac{dt_c}{dt} = \frac{AE}{x_c}\frac{1}{N}(v_p(t) - v_u(t)) + \frac{AE}{x_c}\dot{x}_c(t) \tag{3.61}$$

Assuming that there is no slip between the web and the roller, roller angular velocities and web velocities are related as: $v_u = R\omega_0$ and $v_p = R\omega_N$, where R is the radius of roller.

The entry and process web velocities are given by

$$\dot{v}_u = \frac{1}{J}(-B_{fu}v_u(t) + R^2(t_c(t) - t_r) + RK_u u_u(t) \tag{3.62}$$

$$\dot{v}_p = \frac{1}{J}(-B_{fp}v_p(t) + R^2(t_r - t_c(t)) + RK_p u_p(t) \tag{3.63}$$

where B_{fp} and B_{fu} are coefficients of viscous friction, t_r is reference tension in entry and process web span i.e. $t_r = t_u = t_p$, u_p and u_u are the control inputs to driven roller actuators, and K_p and K_u are actuators gains.

For the described system, application of Buckingham Pi theorem results in the following dimensionless groups

$$\Pi_1 = t\sqrt{\frac{AER}{J}} \qquad \Pi_2 = \frac{u_p}{AER}$$

$$\Pi_3 = K_p \qquad \Pi_4 = \frac{u_u}{AER}$$

$$\Pi_5 = K_u \qquad \Pi_6 = \frac{u_c}{AE}$$

$$
\begin{aligned}
\Pi_7 &= \frac{M_c}{J}R^2 & \Pi_8 &= \frac{F_d}{AE} \\
\Pi_9 &= \frac{gJ}{AER^2} & \Pi_{10} &= \frac{t_c}{AE} \\
\Pi_{11} &= \frac{x_c}{R} & \Pi_{12} &= \frac{v_u}{R}\sqrt{\frac{J}{AER}} \\
\Pi_{13} &= \frac{v_p}{R}\sqrt{\frac{J}{AER}} & \Pi_{14} &= \frac{t_u}{AE} \\
\Pi_{15} &= \frac{t_p}{AE} & \Pi_{16} &= \frac{B_{fu}}{\sqrt{JAER}} \\
\Pi_{17} &= \frac{B_{fp}}{\sqrt{JAER}} & \Pi_{18} &= N
\end{aligned}
\tag{3.64}
$$

The Pi groups impose geometrical and material constraints on the accumulator system. Dimensionless equations can be formed with the derived Pi parameters for the accumulator system. Dimensionless dynamic equations are simple in representation and easy to analyze. The simplified form helps in controller design for a scaled accumulator. A scaling law for a scaled capacity accumulator system will be determined. In this case, the accumulator height is doubled to scale up the capacity.

Consider the accumulator with a scaled-up capacity. Scaling laws establish relations between the model and the prototype parameters. The model law applied to the accumulator equations gives the scale factor relations as

$$
\begin{aligned}
S_t &= S_{AE}^{-0.5} S_R^{-0.5} S_J^{0.5} & S_{K_u} &= 1 \\
S_{u_p} &= S_{AE} S_R & S_{u_c} &= S_{AE} \\
S_{K_p} &= 1 & S_{M_c} &= S_J S_R^{-2} \\
S_{u_u} &= S_{AE} S_R & S_{F_d} &= S_{AE} \\
S_g &= S_{AE} S_R^2 S_J^{-1} & S_{t_c} &= S_{AE}
\end{aligned}
\tag{3.65}
$$

$$S_{x_c} = S_R \qquad S_{v_u} = S_R^{1.5} S_{AE}^{0.5} S_J^{-0.5}$$

$$S_{v_p} = S_R^{1.5} S_{AE}^{0.5} S_J^{-0.5} \qquad S_{t_u} = S_{AE}$$

$$S_{t_p} = S_{AE} \qquad S_{B_{fu}} = S_J^{0.5} S_{AE}^{0.5} S_R^{0.5}$$

$$S_{B_{fp}} = S_J^{0.5} S_{AE}^{0.5} S_R^{0.5} \qquad S_N = 1$$

The model law was used to evaluate the dynamic equivalence conditions. The dynamic equivalence can be achieved by maintaining similar Pi parameters values. The model law helps in calculating scaled controller gains for the scaled up accumulator.

For existing accumulator the parameter values used are $M_c = 7310\ kgs,\ A = 3.27 \times 10^{-4}\ m^2,\ E = 6.9 \times 10^{10}\ N/m^2,\ N = 34,\ v_f = 35.037 \times 10^5\ N - s/m,\ R = 0.1524\ m,\ J = 2.1542\ kg - m^2,\ B_f = 0.02,\ t_r = 5180\ N$. The desired process speed is 3.3 m/s. A sinusoidal disturbance (amplitude 0.25 m/s^2 and frequency 0.5 Hz) is used as the disturbance force on the carriage. A typical scenario of entry speed during unwind roll change is shown in Figure 3.10. The desired profile for carriage velocity is given by

$$v_c^d = \frac{v_u^d - v_p^d}{N} \tag{3.66}$$

The control objective is to track the desired trajectory for the carriage position, entry velocity, and process velocity while maintaining the average web tension. The common industrial PI controller is used to evaluate the system. Simulations are performed with actuator gain values $K_p = K_u = 10$ and driven roller proportional and integral gain values $k_{pu} = 396,\ k_{iu} = 19.2,\ k_{pp} = 387,\ k_{ip} = 8.3$. The controlled carriage position response is shown in Figure 3.11.

For the scaled up accumulator, roller radius is increased to twice the value used for the original system and other system parameters are kept constant. The scale

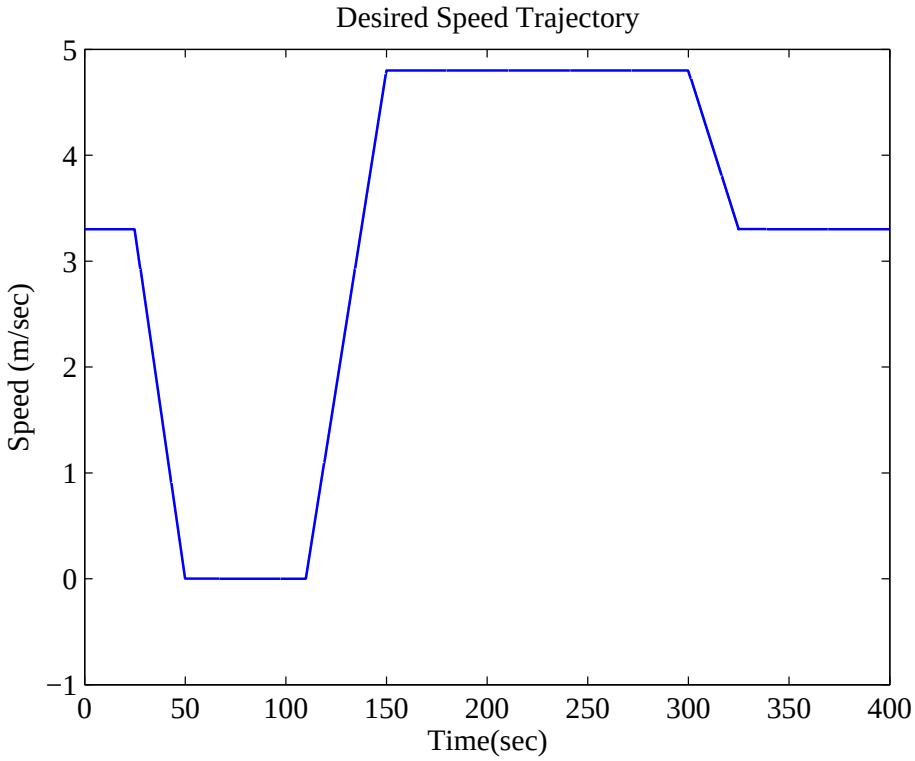

Figure 3.10: Desired Entry Speed Trajectory

factors with the modified system are

$$
\begin{aligned}
S_t &= \sqrt{2} & S_{u_p} &= 2 \\
S_{K_p} &= 1 & S_{u_u} &= 2 \\
S_{K_u} &= 1 & S_{u_c} &= 1 \\
S_{M_c} &= 1 & S_{F_d} &= 1 \\
S_g &= 1 & S_{t_c} &= 1 \\
S_{xc} &= 2 & S_{v_u} &= \sqrt{2} \\
S_{t_u} &= 1 & S_{t_c} &= 1 \\
S_{B_{fu}} &= 2\sqrt{2} & S_{B_{fp}} &= 2\sqrt{2} \\
S_N &= 1 & S_{v_p} &= \sqrt{2}
\end{aligned}
\tag{3.67}
$$

The model law indicates that integral gains for both systems remain the same.

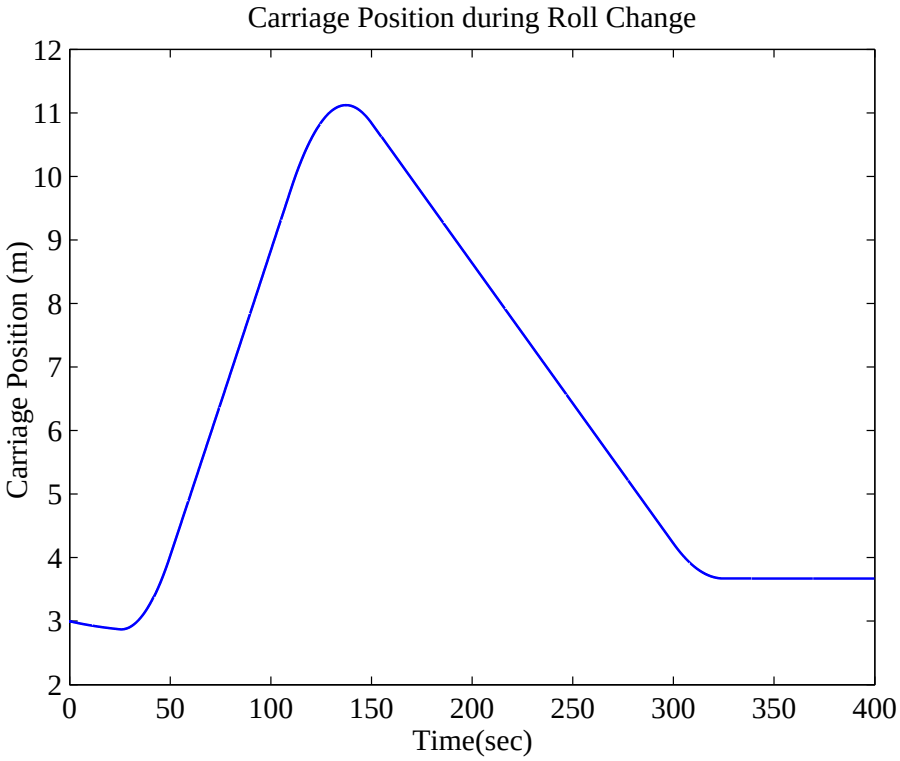

Figure 3.11: Carriage Position during Roll change

Proportional gains change by a factor of $\sqrt{2}$. Control effort is scaled by a factor of 2. The new accumulator system is simulated with scaled controller gains. The plots shown in Figures 3.12 and 3.13 show scaled desired entry speed and scaled carriage position during unwind/rewind roll change. The scaled capacity is twice that of the original system. The scaled control scheme achieved the desired position by matching the original system performance. Though the scaled system is slow, dimensional analysis gives scaled controller gains which serve the purpose for the modified accumulator.

3.7 Dimensional Analysis of Pendulum Dancer

A schematic of the pendulum dancer is shown in Figure 2.2. The pendulum dancer is widely used in industry as a tension sensing element and plays an important role in

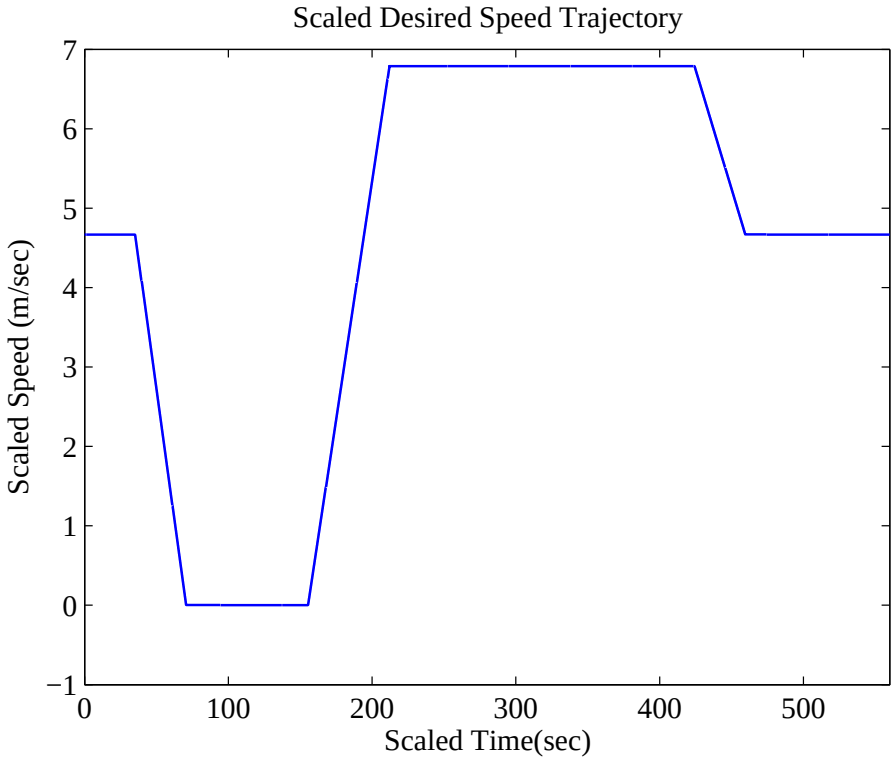

Figure 3.12: Scaled Desired Entry Speed Trajectory

many web processing lines. Dimensional analysis of a pendulum dancer is performed in terms of scaling of geometrical parameters for a web line transporting different web materials. A dynamic model of pendulum dancer includes span tension dynamics with time varying length, dancer rotational dynamics, and roller dynamics. The web velocity dynamics on the dancer roller (neglecting friction) are given by

$$\dot{v}_2 = \frac{R_2^2}{J_2}(t_2 - t_1) \tag{3.68}$$

Web tension dynamics for the upstream and downstream spans of the dancer are given by

$$\dot{L}_1(t)\dot{t_1} = EA(v_2 - v_1) + t_0 v_1 - t_1 v_2 + (AE - t_1)\dot{L}_1 \tag{3.69}$$

$$\dot{L}_2(t)\dot{t_2} = EA(v_3 - v_2) + t_1 v_2 - t_2 v_3 + (AE - t_2)\dot{L}_2 \tag{3.70}$$

The pendulum dancer dynamics (neglecting friction) are given by

$$J_p\ddot{\theta} + M_p g z(\sin\theta) + F_s y - F_p y + t_2 l\cos(\theta - \alpha_2) + t_1(l + d)\cos(\theta - \alpha_1) = 0 \tag{3.71}$$

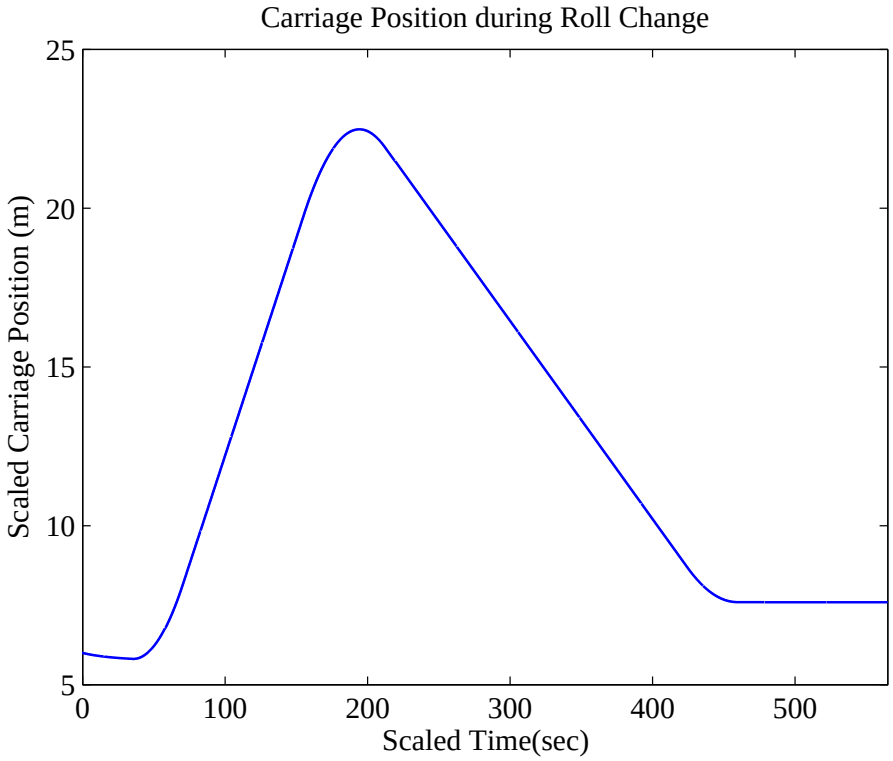

Figure 3.13: Scaled Carriage Position during Roll change

The dimensionless parameters are formed by Buckingham theorem and are defined as

$$\Pi_1 = t\sqrt{\frac{AER}{J_2}} \qquad \Pi_2 = \frac{t_1}{AE}$$

$$\Pi_3 = \frac{t_2}{AE} \qquad \Pi_4 = \frac{L_1}{R_2}$$

$$\Pi_5 = \frac{L_2}{R_2} \qquad \Pi_6 = \frac{v_1}{R_2}\sqrt{\frac{J_2}{AER_2}}$$

$$\Pi_7 = \frac{v_2}{R_2}\sqrt{\frac{J_2}{AER_2}} \qquad \Pi_8 = \frac{t_0}{AE}$$

$$\Pi_9 = \frac{v_3}{R_2}\sqrt{\frac{J_2}{AER_2}} \qquad \Pi_{10} = \frac{J_p}{J_0}$$
$$\Pi_{11} = \frac{l}{R_2} \qquad \Pi_{12} = \frac{M_p g}{AE}$$
$$\Pi_{13} = \frac{z}{R_2} \qquad \Pi_{14} = \frac{F_s}{AE}$$
$$\Pi_{15} = \frac{F_p}{AE} \qquad \Pi_{16} = \frac{y}{R_2}$$
$$\Pi_{17} = \frac{d}{R_2} \tag{3.72}$$

Dimensionless governing equations can be formed with the derived Pi parameters for the pendulum dancer system. The Pi parameters impose geometrical and material constraints on the pendulum dancer system. The simplified dimensional form can be used to scale geometrical and material parameters for the pendulum dancer system. A scaling law for the scaled pendulum dancer system is given below.

The pendulum dancer is scaled for different materials, having considerably different values of elastic modulus. Scaling laws establish relations between base model and candidate model parameters. Model law applied to pendulum dancer dynamics gives the scale factor relations as

$$S_t = S_{AE}^{-0.5} S_{R_2}^{-0.5} S_{J_2}^{0.5} \qquad S_{t_1} = S_{AE}$$
$$S_{t_2} = S_{AE} \qquad S_{L_1} = S_{R_2}$$
$$S_{L_2} = S_{R_2} \qquad S_{v_1} = S_{R_2}^{1.5} S_{AE}^{0.5} S_{J_2}^{-0.5}$$
$$S_{v_2} = S_{R_2}^{1.5} S_{AE}^{0.5} S_{J_2}^{-0.5} \qquad S_{t_0} = S_{AE}$$
$$S_{v_3} = S_{R_2}^{1.5} S_{AE}^{0.5} S_{J_2}^{-0.5} \qquad S_{J_p} = S_{J_0} \tag{3.73}$$
$$S_l = S_{R_2} \qquad S_{M_p g} = S_{AE}$$
$$S_z = S_{R_2} \qquad S_{F_s} = S_{AE}$$
$$S_{F_p} = S_{AE} \qquad S_y = S_{R_2}$$
$$S_d = S_{R_2}$$

Dynamics equivalence between the base model and the candidate model can be

achieved by maintaining similar Pi parameters values. The model law evaluates the dynamic equivalence conditions. The model law helps in calculating scaled geometrical parameters for scaled pendulum dancer. For example, consider the base material as Tyvek: elastic modulus constant, $AE = 2800$ lbf. Scaling is performed by considering aluminium as the candidate material : elastic modulus constant, $AE = 5.07 \times 10^6$ lbf. The model law indicates that the change in modulus constant places a constraint on mass of the pendulum dancer. For higher modulus candidate materials such as aluminium, mass of the pendulum needs to be increased. The increase in the pendulum dancer mass results in increase in the pendulum inertia. The model law reveals the relation between pendulum inertia and roller inertia. Hence, ultimately dancer roller geometrical parameters need to be modified for the new design. The change in roller radius affects the pendulum geometrical parameters. Dimensional analysis expedites the process of designing a pendulum dancer for modified material parameters.

CHAPTER 4

Model Reference Adaptive Controllers for Web Tension Control

An adaptive controller can modify closed loop system behavior by compensating for the changes in system dynamics. An adaptive controller has adjustable parameters against the fixed parameters in traditional controllers and a mechanism for adjusting the system parameters. Most adaptive controllers are nonlinear due to nonlinear parameter adjusting mechanisms. A number of adaptive schemes are used in practice such as gain scheduling, self-tuning regulators, and model reference adaptive control, etc.

In the gain scheduling approach, the variables causing the changes in system dynamics are considered to evaluate the controller parameters. For example, in flight control, altitude and Mach number are measured with air sensors and used to calculate controller gain parameters. A schematic of the gain scheduling approach is shown in Figure 4.1. The main problem involved in this scheme is that suitable gain scheduling variables that characterize the system need to be found.

A self-tuning regulator (STR) is a controller that automatically tunes its parameters in order to achieve desired performance. The STR is composed of two loops. The inner loop is ordinary feedback control loop. While the outer loop estimates the process parameters and compares with the parameter specifications. Based on the comparison, controller parameters are calculated. The performance of the controller depends on the given parameter specifications. A schematic of the STR approach is shown in Figure 4.2.

Model reference adaptive control (MRAC) is an important approach in adaptive

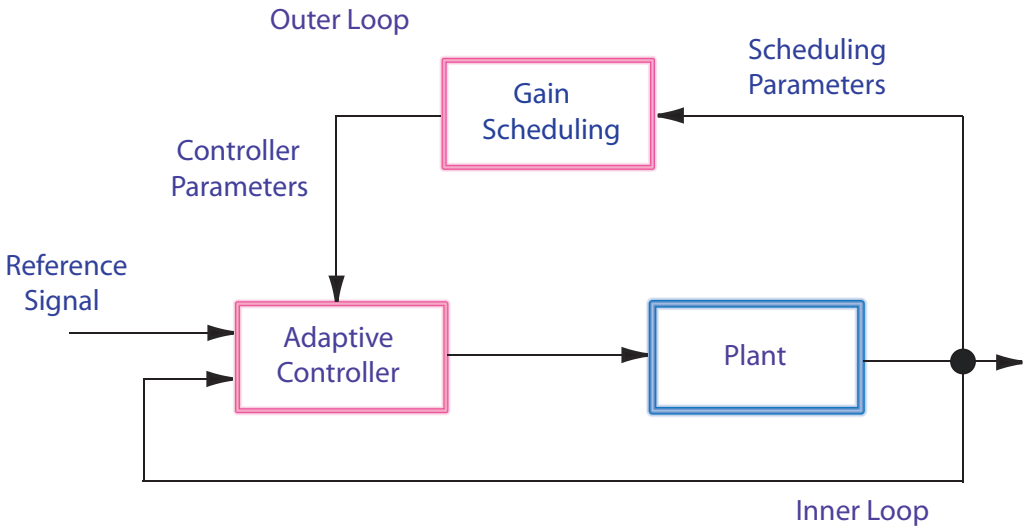

Figure 4.1: Schematic of System with Gain Scheduling

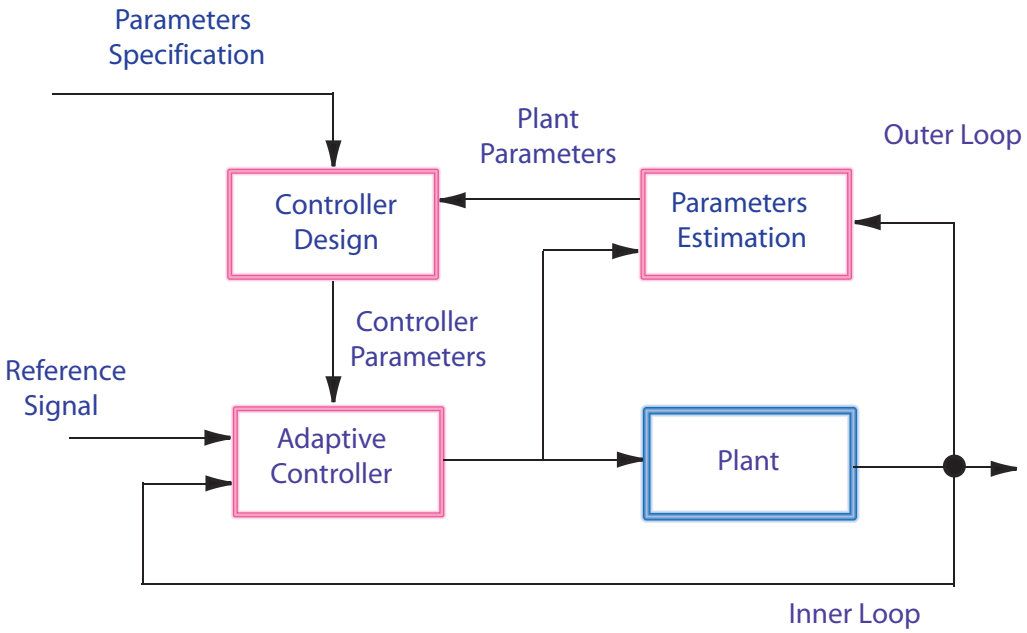

Figure 4.2: Schematic of a Self Tuning Regulator

control. MRAC was first introduced in flight control. The reference model is chosen to generate a desired trajectory and guide the system for ideal response with given reference command. The MRAC method is composed of two loops similar to the self tuning regulator. The inner loop is an ordinary feedback control loop. The outer loop is a controller parameters adjustment loop. The controller parameters are

adjusted based on certain variables like error between the actual system output and the model output, control input to the system, and the actual output of the system. The parameter adjustment mechanism can be generated in two ways: by using a gradient method or with stability theory such as Lyapunov stability. The goal is to find an adjustment mechanism, to obtain zero error between the reference model output and the actual system output. A schematic of the MRAC approach is shown in Figure 4.3.

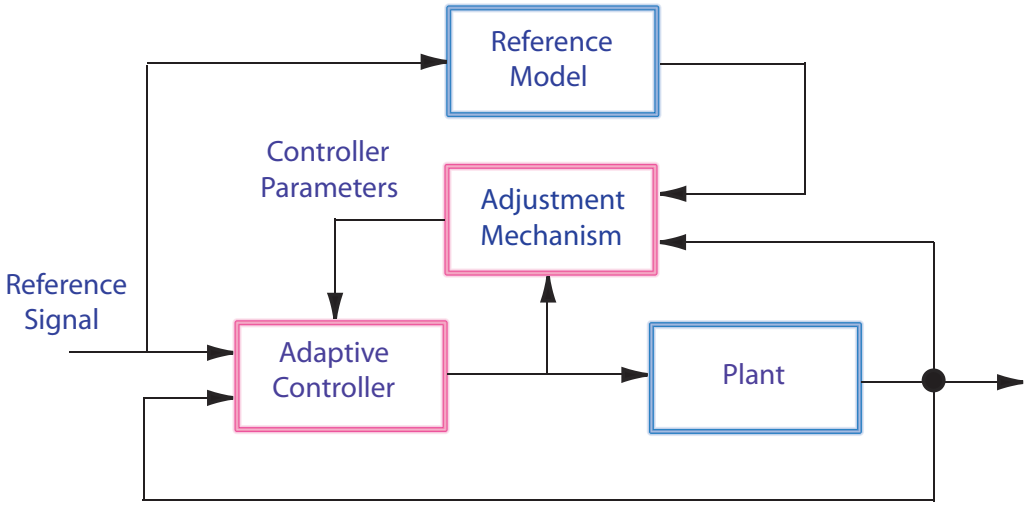

Figure 4.3: Schematic of Model Reference Adaptive System

The MRAC approach can be divided into direct and indirect adaptive schemes. In most of the applications, system parameters are unknown and need to be estimated in order to design effective control schemes. The estimation of parameters is governed by the adaptive law. In direct MRAC control, the plant is parameterized in terms of controller parameters. The controller parameters are updated directly by an adaptive law. Whereas, indirect MRAC schemes formulate a relation between controller parameters and online estimation of plant parameters. Plant parameters are estimated based on an adaptive law and controller parameters are calculated indirectly based on the relation formulated. In subsequent study of adaptive control to a web transport system, model reference schemes are chosen. The reference model

specifies desired performance and guides the adaptive controller such that the closed loop system behaves as the reference model. The designed model reference adaptive schemes are decentralized in nature.

In this chapter, direct and indirect model reference adaptive controllers are designed and experimental results are presented. The designed direct and indirect controllers are decentralized in nature for a class of large-scale interconnected systems. A simple direct adaptive controller based on the gradient method is also presented. Adaptive control schemes using MRAC is described in Section 4.1. The MRAC direct and indirect approaches and the gradient method are studied in Sections 4.2 to 4.4. Experimental procedure and results are presented in Sections 4.5 and 4.6, respectively.

4.1 Adaptive Control Schemes Using MRAC

Adaptive laws can be designed using the Lyapunov stability approach. The problem of adaptive gain evaluation is similar to the problem of online parameter identification. The gains can obtained by parameterization of the plant.

Consider a simple first order scalar plant:

$$\dot{x} = ax + u, \quad x(0) = x_0 \tag{4.1}$$

where a is an unknown plant parameter, x is the state as well as the output, and u is the input to the system. The goal is to estimate the unknown parameter and design the control input u so that the state x of the plant remains bounded and converges to zero for any given initial condition. Let a_m be any arbitrary positive model reference parameter with $\dot{x} = -a_m x$ being a stable system.

To develop a control scheme for the plant with known a is easier and the following feedback control can be selected:

$$u = -kx \tag{4.2}$$

where $k = a + a_m$ and the closed loop system becomes

$$\dot{x} = -a_m x \tag{4.3}$$

Hence, the resultant system is stable with the equilibrium at zero.

But in many practical cases, system parameters are unknown. The unknown plant and the controller parameters need to be estimated in order to implement the control scheme. Let $\hat{k}$ be the estimate of the controller parameter. Add and subtract the desired control input given by equation (4.2) in the plant equation (4.1).

$$\dot{x} = ax - kx + kx + u \tag{4.4}$$

Since $a - k = -a_m$, the plant equation (4.4) can be written as,

$$x(s) = \frac{1}{s + a_m}(u + kx(s)) \tag{4.5}$$

The plant is parameterized in terms of controller parameters. The estimated controller parameter generates estimated plant output as

$$\hat{x}(s) = \frac{1}{s + a_m}(u + \hat{k}x(s)) \tag{4.6}$$

By substituting the estimated control input $u = -\hat{k}x$ in equation (4.6), the estimated plant output becomes zero. Define the plant output estimation error as $\epsilon = x - \hat{x}$. Due to zero estimation output, the estimation error is the regulation error i.e. $\epsilon = x$. Define parameter error $\tilde{k} = \hat{k} - k$ and substitute estimated control input $u = -\hat{k}x$ in equation (4.5) to obtain

$$\dot{\epsilon} = -a_m \epsilon - \tilde{k}x \tag{4.7}$$

In the frequency-domain

$$\epsilon(s) = \frac{1}{s + a_m}(-\tilde{k}x(s)) \tag{4.8}$$

Assume the adaptive law to be in the form

$$\dot{\tilde{k}} = \dot{\hat{k}} = f(\hat{x}, x, u) \tag{4.9}$$

Now choose the Lyapunov function as

$$V = \frac{\epsilon^2}{2} + \frac{\tilde{k}^2}{2\gamma} \tag{4.10}$$

where $\gamma > 0$ is the adaptive gain. The time derivative of the Lyapunov function is

$$\dot{V} = -a_m \epsilon^2 - \tilde{k}\epsilon x + \frac{\tilde{k} f}{\gamma} \tag{4.11}$$

Define the function f as

$$f = \dot{\hat{k}} = \gamma \epsilon x = \gamma x^2, \quad \tilde{k}(0) = \tilde{k}_0 \tag{4.12}$$

Substitute the function f in equation (4.11) to get

$$\dot{V} = -a_m \epsilon^2 \leq 0 \tag{4.13}$$

The Lyapunov approach that is used, proves the stability of the control scheme with the selected controller parameter update law. The combination of the control law (4.2) and the adaptive law (4.12) regulate the plant and ensure state convergence to zero.

In parameter identification, the system parameter converges to its nominal value. In the case of adaptive control, it is not necessary to converge controller parameters to true values. The control objective of zero error can be achieved without convergence of the parameter values to their true values. Larger values for the adaptive gain lead to faster convergence of parameter value to true value. But larger gain make the system more sensitive to measurement noise and error. So proper selection of the adaptive gain is a trade-off.

4.1.1 Sigma (σ) switching

In large scale interconnected systems, the problem of parameter drifting occurs due to interaction between subsystems. The issue of parameter drifting can be avoided

by using σ switching. The σ switching can be defined as

$$\sigma = \begin{cases} \sigma_0 & \text{if } \| \hat{k} \| > \hat{k} \\ 0 & \text{if } \| \hat{k} \| \leq \hat{k} \end{cases} \tag{4.14}$$

The adaptive law described by equation (4.12) can be modified as

$$\dot{\hat{k}} = -\gamma \epsilon x - \sigma \gamma (1 + x^2) \hat{k} \tag{4.15}$$

4.2 Direct MRAC for Web Transport System

Consider a single input single output (SISO), linear time invariant (LTI) system:

$$\begin{aligned} \dot{x}_p &= A_p x_p + B_p u_p, \quad x_p(0) = x_0 \\ y_p &= {C_p}^T x_p \end{aligned} \tag{4.16}$$

where x_p: state vector, u_p: input to system, A_p: state matrix, B_p: input matrix, y_p: system output.

The plant transfer function is

$$G_p(s) = k_p \frac{Z_p(s)}{R_p(s)} \tag{4.17}$$

where Z_p, R_p are monic polynomials and k_p is the high frequency gain.

The reference model in state space representation is

$$\begin{aligned} \dot{x}_m &= A_m x_m + B_m u_m, \quad x_m(0) = x_0 \\ y_m &= {C_m}^T x_m \end{aligned} \tag{4.18}$$

where x_m: state vector, u_m: input to model, A_m: state matrix, B_m: input matrix, y_m: model output.

The reference model transfer function is

$$W_m(s) = k_m \frac{Z_m(s)}{R_m(s)} \tag{4.19}$$

where Z_m, R_m are monic polynomials and k_m is a constant.

The goal of model reference control is to evaluate system input u_p so that the system output y_p tracks the reference model output y_m for a given command reference input r. The general structure of the direct MRAC scheme is shown in Figure 4.4.

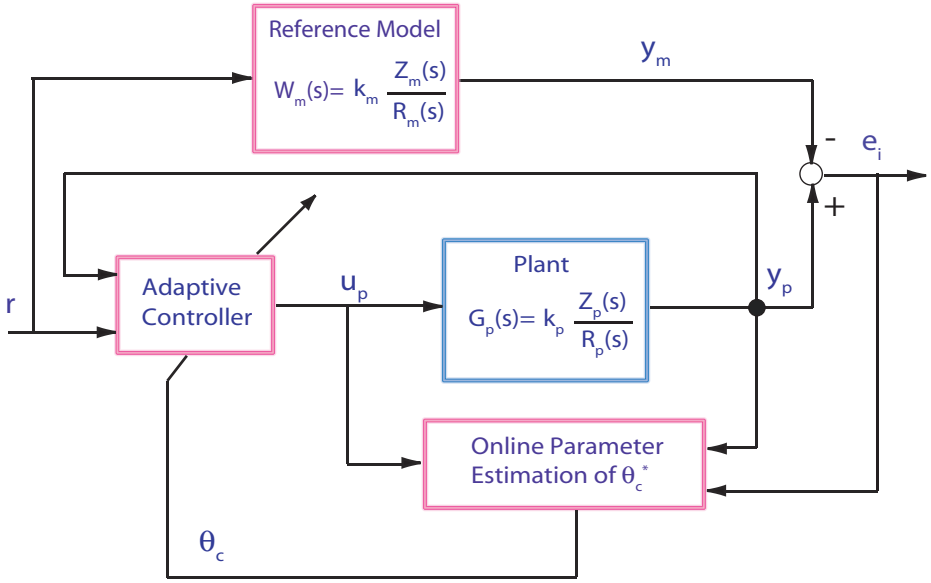

Figure 4.4: Schematic of Direct Model Reference Adaptive System

In model reference control one has to impose some assumptions on plant and reference model so that the control input is free of differentiators and depend on measurable signals. The assumptions on plant and model are as follows:

1. 'n' is an upper bound on degree 'r_p' of R_p, and is known.

2. Z_p is monic Hurwitz of degree 'z_p', that means plant should be minimum phase.

3. Relative degree of the plant $n_p = r_p - z_p$ is known.

4. The sign of the high frequency gain k_p is known.

5. $Z_m(s)$, $R_m(s)$ are monic Hurwitz polynomials of degree z_m and r_m, respectively and $r_m \leq n$.

6. The relative degree of the reference model, n_m is equal to the plant relative degree n_p.

The important characteristics of model reference adaptive control are that the adaptive law depends on the state estimation error, that is, regulation error, and the designed adaptive law ensures internal stability of system.

4.2.1 Design of a Direct MRAC Scheme for Web Tension Control

A schematic of a simplified web transport system is shown in Figure 3.6. Design of the direct MRAC for control of tension in the unwind section is presented here. This approach can be followed for other sections.

The web tension dynamics of i^{th} span is given by

$$\dot{t}_i = \frac{EA}{L_i}(v_i - v_{i-1}) + \frac{1}{L_i}(t_{i-1}v_{i-1} - t_i v_i) \tag{4.20}$$

The governing equation for web velocity on the i^{th} driven roller is given by

$$\dot{v}_i = \frac{R_i^2}{J_i}(t_{i+1} - t_i) + \frac{R_i}{J_i}n_i u_i - \frac{b_{fi}}{J_i}v_i \tag{4.21}$$

The linearized web span tension dynamics in frequency domain is given by

$$T_i(s) = \frac{EA/V_r}{\tau_{\omega i}s + 1}(V_i(s) - V_{i-1}(s)) + \frac{1}{\tau_{\omega i}s + 1}T_{i-1}(s) \tag{4.22}$$

where $\tau_{\omega i} = \frac{L_i}{V_r}$ is the span time constant. T_i and V_i are tension and velocity variations, respectively. The web span tension T_i is the output and the roller velocity V_i is the input. For the unwind zone, the tension variation T_{i-1} in web roll is assumed to be zero. The transfer function from the velocity input to the span tension is

$$G_p(s) = \frac{EA/V_r}{\tau_{\omega i}s + 1} \tag{4.23}$$

The linearized equation reduces the number of estimated parameters in adaptive control design and will be used in the following.

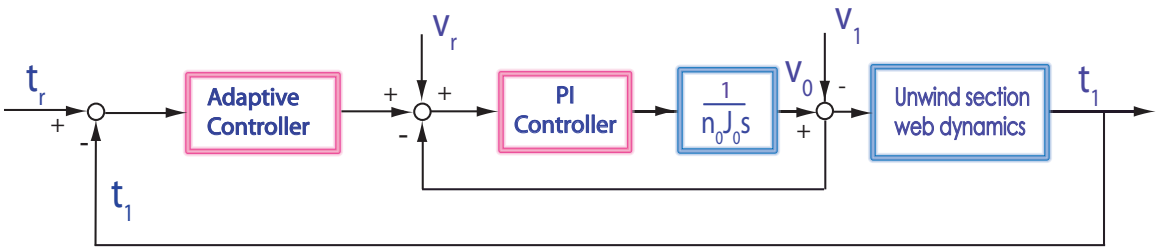

Figure 4.5: Control Strategy for Unwind Section

The control strategy for the unwind roll is shown in Figure 4.5. The unwind roll is controlled by a cascaded control strategy. The inner loop is the velocity loop which is regulated by a well-tuned PI controller. The outer loop is the tension loop and contains the adaptive controller.

The velocity open loop transfer function is given

$$G_v(s) = \frac{k_v(s+\omega_v)}{s}\frac{1}{n_0 J_0 s} \tag{4.24}$$

where k_v is proportional gain and ω_v is cutoff frequency.

The closed loop velocity transfer function is

$$G_{cv}(s) = \frac{k_{rf}(s+\omega_v)}{s^2 + k_{rf}s + k_{rf}\omega_v} \tag{4.25}$$

where $k_{rf} = \frac{k_v}{n_0 J_0}$ is the reference gain, $\omega_v = \frac{k_{rf}}{4\zeta^2}$ is the cut-off frequency, ζ is the damping ratio of the system.

The plant transfer function (4.23) in conjunction with the closed loop velocity transfer function (4.25) gives the following combined system transfer function from the velocity reference correction provided by the outer tension loop controller and the tension output

$$W(s) = G_{cv}G_p \tag{4.26}$$

The resulting transfer function has relative degree two.

In order to design a direct MRAC for the tension loop, we select a second order system with relative degree two as the reference model. The upper bound 'n' for the

combined plant is selected to be three. The reference model transfer function can be expressed as

$$W_m(s) = \frac{\omega_n^2}{s^2 + 2\zeta_m\omega_n s + \omega_n^2} \tag{4.27}$$

where ω_n is the natural frequency and ζ_m is the damping ratio of the reference model.

The model output is given by

$$t_m = W_m(s)t_r \tag{4.28}$$

The estimation error between model and the tension output is defined as

$$e_1 = t_1 - t_m \tag{4.29}$$

Let us consider the combined feedback and fedforward control law so that the closed loop plant response matches that of the reference model. The control law is chosen as

$$u_p = \theta_{c1}^{*T}\frac{\alpha(s)}{\Lambda(s)}u_p + \theta_{c2}^{*T}\frac{\alpha(s)}{\Lambda(s)}t_1 + \theta_{c3}^{*}t_1 + \theta_{c4}^{*}t_r \tag{4.30}$$

where

$\alpha(s) \equiv \alpha_{n-2}(s) = [s^{n-2}, s^{n-3}, \ldots, 1]^T \quad \text{for } n \geq 2,$

$\Lambda(s) = \Lambda_0(s)Z_m(s)$ is any monic Hurwitz polynomial, and

$\theta_{c1}^*, \theta_{c2}^* \; \varepsilon \; \Re^{n-1}$ and $\theta_{c3}^*, \theta_{c4}^* \; \varepsilon \; \Re^1$ are constant controller parameters to be designed.

The controller parameters vector

$$\theta_c^* = [\theta_{c1}^{*T}, \theta_{c2}^{*T}, \theta_{c3}^{*}, \theta_{c4}^{*}]^T \tag{4.31}$$

is selected in such a way that the closed loop plant transfer function asymptotically tends to the model reference transfer function.

Control Law

For a relative degree two model, the control law is given by

$$\dot{\omega}_1 = F\omega_1 + gu_p, \quad \omega_1(0) = 0$$

$$\dot{\omega}_2 = F\omega_2 + gu_p, \quad \omega_2(0) = 0$$

$$\dot{\phi} = -p_0\phi + \omega, \quad \phi(0) = 0 \tag{4.32}$$

where $\omega_i \, \varepsilon \, \Re^{n-1}$ are the filters, p_0 is chosen such that $W_m(s)(s+p_0)$ is strictly positive real, (F,g) is a state space realization of the transfer function $\frac{\alpha(s)}{\Lambda(s)}$.

The control input is

$$u_p = \theta_c^T\omega + \dot{\theta}_c^{\,T}\phi \tag{4.33}$$

where ω is the vector of filter parameters given by

$$\omega = \begin{bmatrix} \omega_1^T & \omega_2^T & t_1 & t_r \end{bmatrix}^T \tag{4.34}$$

The control input has an additional term $\dot{\theta}_c^{\,T}\phi$ compared a relative degree one design, this is discussed in detail in the next subsection.

Adaptive Law

A state space representation of the closed loop system by combining plant (4.16) and adaptive controller (4.32) can be presented as

$$\dot{Y}_c = A_cY_c + B_cu_p, \quad Y_c(0) = Y_0$$

$$t_1 = C_c^TY_c \tag{4.35}$$

where

$$Y_c = \begin{bmatrix} x_p^T & \omega_1^T & \omega_2^T \end{bmatrix} \qquad A_c = \begin{bmatrix} A_p & 0 & 0 \\ 0 & F & 0 \\ gC_p & 0 & F \end{bmatrix}$$

$$B_c = \begin{bmatrix} B_p \\ g \\ 0 \end{bmatrix} \qquad C_c^T = \begin{bmatrix} C_p^T & 0 & 0 \end{bmatrix}$$

Define the state error $e = Y_c - x_m$ and the tracking error $e_1 = t_1 - t_m$. The governing equation for error is given by

$$\dot{e} = A_c e + B_c(u_p - \theta_c^T \omega) \tag{4.36}$$

$$e_1 = C_c^T e = W_m(s)\rho(u_p - \theta_c^T \omega) \tag{4.37}$$

where $\rho = \frac{k_p}{k_m}$ is an unknown constant, θ_c is estimated controller parameters. With a relative degree two system, W_m cannot be designed to be strictly positive real with the control law $u_p = \theta_c^T \omega$. We need to rewrite the error equation as

$$\begin{aligned} \dot{e} &= A_c e + \bar{B}_c(s + p_0)\rho(u_f - \theta_c^T \phi) \\ e_1 &= W_m(s)(s + p_0)\rho(u_f - \theta_c^T \phi) \end{aligned} \tag{4.38}$$

where u_f is the filtered input.

The state error can also be represented as

$$\bar{e} = e - B_c \rho \tilde{\theta_c}^T \phi \tag{4.39}$$

where $\tilde{\theta}_c = \theta_c - \theta_c^*$ is the parameter estimation error.

Choose the control input as

$$u_p = (s + p_0)u_f = \theta_c^T \omega + \dot{\theta_c}^T \phi \tag{4.40}$$

Now, the Lyapunov function can be selected as

$$V = \frac{\bar{e}^T P \bar{e}}{2} + \frac{\tilde{\theta_c}^T \Gamma^{-1} \tilde{\theta}_c \rho}{2} \tag{4.41}$$

where $\Gamma \geq 0$ is any arbitrary positive constant and $P > 0$ satisfies the algebraic equation

$$P A_c + A_c^T P = -Q Q^T - \nu_c L_c \tag{4.42}$$

where Q is any vector, $L_c > 0$ and $\nu_c > 0$.

By choosing the parameter adaptation law as

$$\dot{\tilde{\theta}}_c = \dot{\theta}_c = -\Gamma e_1 \phi sgn(\rho) = -\Gamma e_1 \phi sgn(k_p/k_m) \tag{4.43}$$

the time derivative of the Lyapunov function is given by

$$\dot{V} = -\frac{\bar{e}^T Q Q^T \bar{e}}{2} - \frac{\nu_c}{2} \bar{e}^T L_c \bar{e} \leq 0 \tag{4.44}$$

Lyapunov stability ensures all signals in the closed loop system to be bounded and the model error e_1 converges to zero asymptotically.

The controller implementation for direct MRAC scheme is shown in Figure 4.6.

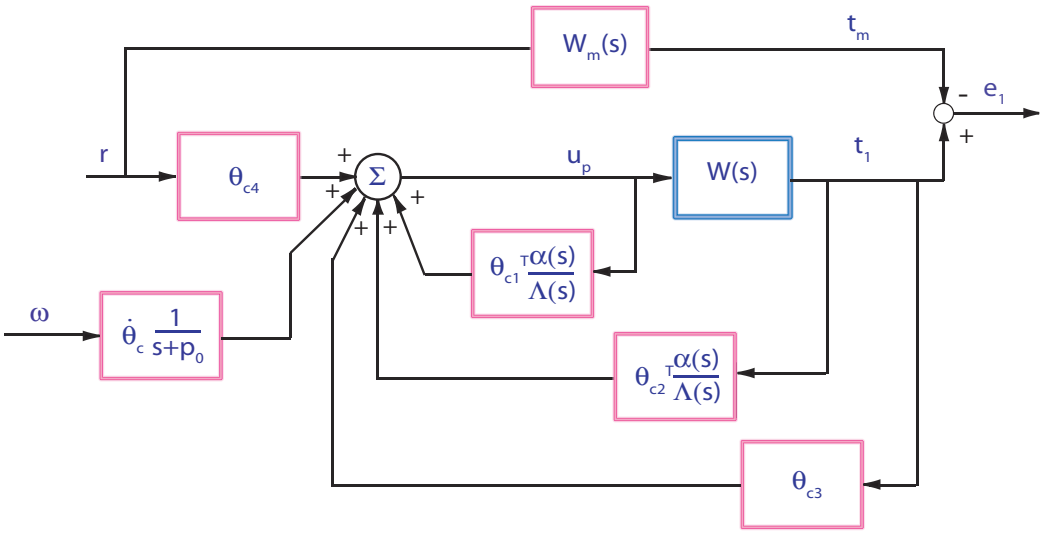

Figure 4.6: Implementation of Direct Model Reference Adaptive Control

4.3 MRAC Indirect Adaptive Controller for Web Tension Control

In the previous section, we designed a direct adaptive controller for web span tension control with unknown parameters by directly estimating the controller parameters. Alternatively, one could estimate the plant parameters which can be used to calculate the controller parameters. This approach is called the indirect MRAC scheme since the controller parameters are calculated indirectly using plant parameters estimates. A schematic of the indirect MRAC scheme is shown in Figure 4.7.

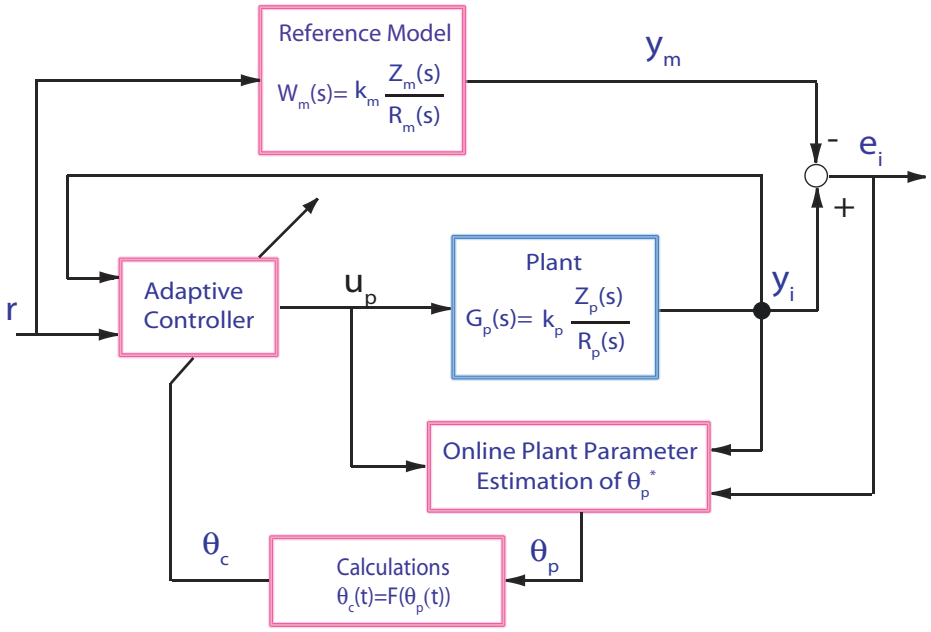

Figure 4.7: Schematic of Indirect Model Reference Adaptive System

The parameter vector consists of the high frequency gain of the plant and coefficients of plant transfer function polynomials. The adaptive law uses the filtered values of the plant output and the control input to estimate plant parameters.

Similar to the direct MRAC control design, the plant dynamics is given by (4.20) and (4.21). A second order model with relative degree two is selected as a reference and described by equation (4.27). The unwind control strategy is as shown in Figure 4.5. The combined plant and velocity closed loop transfer function is given by equation (4.26). The resultant system is of relative degree two. The upper bound 'n' for plant transfer function is selected as three.

Consider again the combined feedback and fedforward control law

$$u_p = \theta_{c1}^T \frac{\alpha(s)}{\Lambda(s)} u_p + \theta_{c2}^T \frac{\alpha(s)}{\Lambda(s)} t_1 + \theta_{c3} t_1 + \theta_{c4} t_r \tag{4.45}$$

where

$\alpha(s) \equiv \alpha_{n-2}(s) = [s^{n-2}, s^{n-3}, \ldots, 1]^T \quad$ for $n \geq 2$,

$\Lambda(s) = \Lambda_0(s) Z_m(s)$ is any monic Hurwitz polynomial, and

$\theta_{c1}^*, \theta_{c2}^* \; \varepsilon \; \Re^{n-1}$ and $\theta_{c3}^*, \theta_{c4}^* \; \varepsilon \; \Re^1$ are constant controller parameters to be designed.

The controller parameter vector is

$$\theta_c = [\theta_{c1}^T, \theta_{c2}^T, \theta_{c3}, \theta_{c4}]^T \tag{4.46}$$

Control Law

We propose the same control law used in direct MRAC scheme for the plant of relative degree two.

$$\begin{aligned}
\dot{\omega}_1 &= F\omega_1 + gu_p, \quad \omega_1(0) = 0 \\
\dot{\omega}_2 &= F\omega_2 + gu_p, \quad \omega_2(0) = 0 \\
\dot{\phi} &= -p_0\phi + \omega, \quad \phi(0) = 0
\end{aligned} \tag{4.47}$$

where $\omega_i \; \varepsilon \; \Re^{n-1}$ are the filters, p_0 is chosen such that $W_m(s)(s+p_0)$ become strictly positive real, (F,g) is state realization of $\frac{\alpha(s)}{\Lambda(s)}$.

The control input is

$$u_p = \theta_c^T\omega + \dot{\theta}_c^T\phi \tag{4.48}$$

where ω is the vector of filter parameters given by

$$\omega = \begin{bmatrix} \omega_1^T & \omega_2^T & t_1 & t_r \end{bmatrix}^T \tag{4.49}$$

The control input has an additional term $\dot{\theta_c}^T\phi$ compared a relative degree one design, this is discussed in detail in the next subsection.

Adaptive Law

The plant parameter adaptation law is given by

$$\dot{\theta}_p = -\Gamma e_1 \phi sgn(k_p/k_m) \tag{4.50}$$

where $\Gamma \; > 0$ (any arbitrary positive number), $e_1 = t_1 - t_m$ is the model error, and $k_p, \; k_m$ are high frequency gains of the plant and the model, respectively.

Define $Q(s)$ to be the quotient of $\frac{\Lambda_0 R_m}{R_p}$, $p_1 = [p_{11}, p_{12}]^T$, $p_2 = [p_{21}, p_{22}]^T$, $\nu = [\nu_1, \nu_2]^T$, and $\lambda = [\lambda_1, \lambda_2]^T$. Then, we can write

$$Z_p(s)Q(s) = s^{n-1} + p_1^T \alpha_{n-2}(s) \tag{4.51}$$

$$R_p(s)Q(s) = s^{n+1} + a_n s^n + a_{n-1}s^{n-1} + p_2^T \alpha_{n-2}(s) \tag{4.52}$$

$$\Lambda(s) = s^{n-1} + \lambda^T \alpha_{n-2}(s) \tag{4.53}$$

$$\Lambda_0 R_m(s) = s^{n+1} + r_n s^n + r_{n-1}s^{n-1} + \nu^T \alpha_{n-2}(s) \tag{4.54}$$

The plant high frequency gain is estimated using the adaptation law

$$\dot{\hat{k}}_p = -\gamma_p e_1 \xi_1 \quad \text{if} \quad |\hat{k_p}| > k_0 \tag{4.55}$$

The coefficient of the plant transfer function are estimated as

$$\dot{\hat{a}}_{n-1} = -\gamma_1 e_1 \xi_2 \tag{4.56}$$

$$\dot{\hat{p}}_1 = \Gamma_1 e_1 \omega_1 sgn(k_p) \tag{4.57}$$

$$\dot{\hat{p}}_2 = -\Gamma_2 e_1 \omega_2 \tag{4.58}$$

where

$$\xi_1 = \lambda^T \omega_1 - u_p - \hat{p}_1^T \omega_1$$

$$\xi_2 = t_1 - \lambda^T \omega_2$$

$$e_1 = t_1 - t_m$$

Based on the plant parameter estimation, controller parameters are calculated as

$$\theta_{c11} = \lambda_1 - \hat{p}_{11} \tag{4.59}$$

$$\theta_{c12} = \lambda_2 - \hat{p}_{12} \tag{4.60}$$

$$\theta_{c21} = \frac{\hat{p}_{21} - \nu_1 - \lambda_1(\hat{a}_{n-1} - r_{n-1})}{\hat{k}_p(t)} \tag{4.61}$$

$$\theta_{c22} = \frac{\hat{p}_{22} - \nu_2 - \lambda_2(\hat{a}_{n-1} - r_{n-1})}{\hat{k}_p(t)} \tag{4.62}$$

$$\theta_{c3} = \frac{\hat{a}_{n-1} - r_{n-1}}{\hat{k}_p(t)} \tag{4.63}$$

$$\theta_{c4} = \frac{k_m}{\hat{k}_p(t)} \tag{4.64}$$

The indirect MRAC scheme guarantees internal stability of the system, i.e. all signals are bounded, and convergence of the tracking error e_1 to zero asymptotically.

The controller implementation for the indirect MRAC tension control scheme is shown in Figure 4.8.

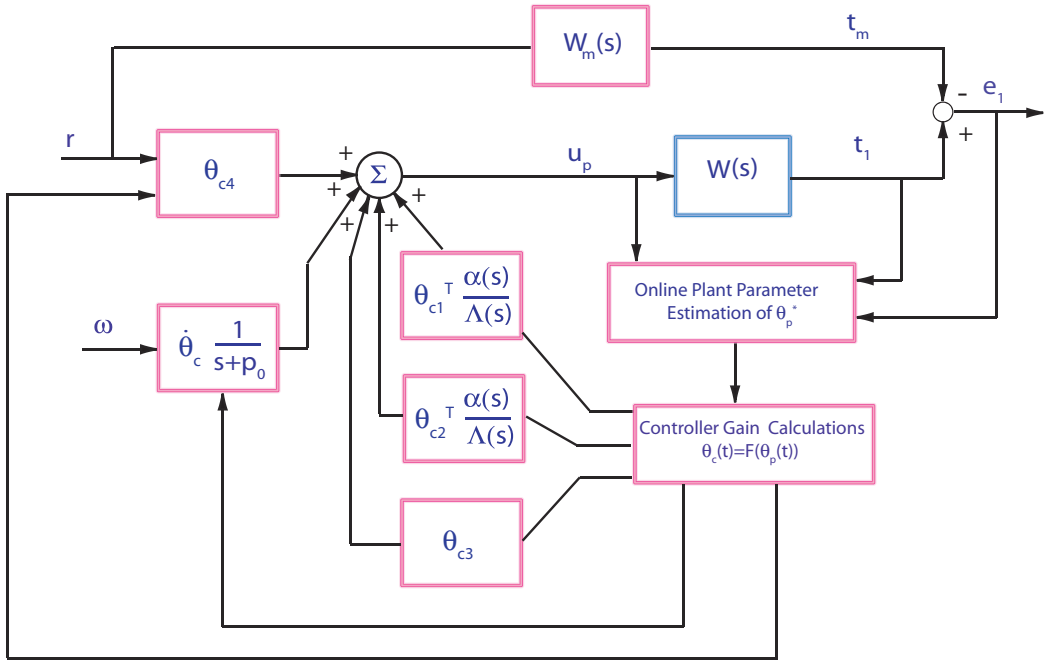

Figure 4.8: Implementation of Indirect Model Reference Adaptive Control

4.4 A Simple Adaptive PI Controller for Web Tension Control

Both Direct and indirect MRAC schemes for tension regulation require estimation of six parameters. There is a need for a simple adaptive scheme which has fewer parameters to be estimated. Adaptive PI scheme is developed based on directly estimating the gains of the PI controller by gradient method. The simple adaptive PI

requires estimation of only two parameters. The simple adaptive PI controller does not give a guarantee of stability. Since a regular PI controller also does not assure stability with a linearized model, the designed adaptive PI is a better option. The simple adaptive PI controller does not require extensive tuning.

The adaptive PI controller has only two adjustable parameters i.e., the proportional gain and the integral gain. The parameters can be adjusted by minimizing the loss function corresponding to the model error $e_1 = t_1 - t_m$

$$J(\theta) = \frac{1}{2} e_1^2 \tag{4.65}$$

where parameter vector $\theta = \begin{bmatrix} k_p & k_i \end{bmatrix}^T$ is a function of the controller, k_p and k_i are the proportional and integral gain, respectively. To minimize the loss function, it is reasonable to change the adjustable parameter in the direction of the negative gradient of J, i.e.,

$$\frac{d\theta}{dt} = -\gamma \frac{\partial J}{\partial \theta} = -\gamma e_1 \frac{\partial e_1}{\partial \theta} \tag{4.66}$$

where $\frac{\partial e_1}{\partial \theta}$ is called the sensitivity of the system. Equation (4.66) is generally called the MIT rule in adaptive control literature. The sensitivity of the system can be further simplified as

$$\dot{\theta} = \frac{\partial (t_1 - t_m)}{\partial \theta} = \frac{\partial t_1}{\partial \theta} \tag{4.67}$$

With the combined plant as given by equation (4.26), the closed loop transfer function with the adaptive PI control scheme is given by

$$G_c(s) = \frac{(sk_p + k_i)W(s)}{s + (sk_p + k_i)W(s)} \tag{4.68}$$

The output of the closed loop system is the actual web span tension t_1 and the input is the reference tension t_r, i.e.,

$$t_1 = \frac{(sk_p + k_i)W(s)}{s + (sk_p + k_i)W(s)} t_r \tag{4.69}$$

where the transfer function composed of the linearized tension dynamics and velocity loop is

$$W(s) = \frac{k_{rf}(s+\omega_v)}{s^2 + k_{rf}s + k_{rf}\omega_v} \frac{EA/V_r}{\tau_{\omega i}s + 1} \tag{4.70}$$

The relative degree of this transfer function is two. We can select a reference model with relative degree two and having the same number of poles and zeros as the transfer function (4.68), i.e.,

$$W_m(s) = \frac{k_m(as+z_1)(s+z_2)}{(s+p_1)(s+p_2)(s+p_3)(s+p_4)} \tag{4.71}$$

where the model parameters a, z_i and p_i are known and can be selected to provide the desired performance.

Applying the MIT rule, we can derive the adaptive law for controller parameters as

$$sk_p = -\gamma_p e_1 \frac{s(t_r - t_1)(EA/V_r)(k_{rf}s + k_{rf}^2/4\zeta^2)}{s(s^2 + k_{rf}s + k_{rf}^2/4\zeta^2)(\tau_{\omega i}s+1) + (k_p s + k_i)(EA/V_r)(k_{rf}s + k_{rf}^2/4\zeta^2)} \tag{4.72}$$

$$sk_i = -\gamma_i e_1 \frac{(t_r - t_1)(EA/V_r)(k_{rf}s + k_{rf}^2/4\zeta^2)}{s(s^2 + k_{rf}s + k_{rf}^2/4\zeta^2)(\tau_{\omega i}s+1) + (k_p s + k_i)(EA/V_r)(k_{rf}s + k_{rf}^2/4\zeta^2)} \tag{4.73}$$

In adaptive PI controller design, it is assumed that the system parameters are not known. So the exact formulae that are derived using the MIT rule (4.66) cannot be used. Comparing the closed loop adaptive control system with the reference model, the controller parameter estimates are given by

$$sk_p = -\gamma_p e_1 \frac{s(t_r - t_1)k_m(s+z_2)}{(s+p_1)(s+p_2)(s+p_3)(s+p_4)} \tag{4.74}$$

$$sk_i = -\gamma_i e_1 \frac{(t_r - t_1)k_m(s+z_2)}{(s+p_1)(s+p_2)(s+p_3)(s+p_4)} \tag{4.75}$$

The designed controller does not guarantee the stability of the closed loop system. The designed adaptive PI controller scheme is shown in Figure 4.9. This provides a scope to design an adaptive PI controller which ensures the stability as well.

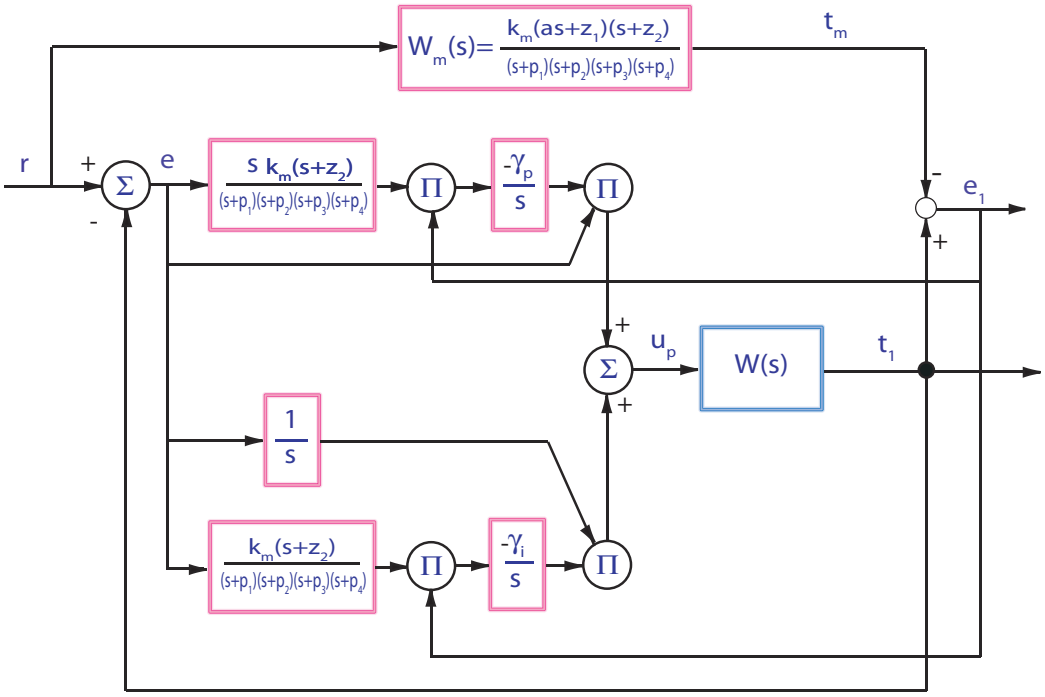

Figure 4.9: Implementation of Adaptive PI Model Reference Control

4.5 Experimental Procedure

The experimental platform used for implementation of a designed adaptive controller was shown in Figure 2.1. The details about the experimental platform were described in Section 2.4. The controllers were implemented for the unwind section of the EWL. The material used for all experiments was the polymer Tyvek manufactured by Dupont. The experiments were performed for both load cell and dancer feedback control strategies. The tension data was collected from the load cell on roller R8, which is shown in the experimental platform schematic Figure 2.1. The experiments were carried out at two line speeds: 150 FPM and 200 FPM. Initially, 20 lbf tension is maintained at zero line velocity. The line velocity is accelerated to 150 FPM or 200 FPM as shown by the velocity profile for the 150 FPM case in Figure 4.10.

The nominal values of key plant parameters are given in the Table 4.1.

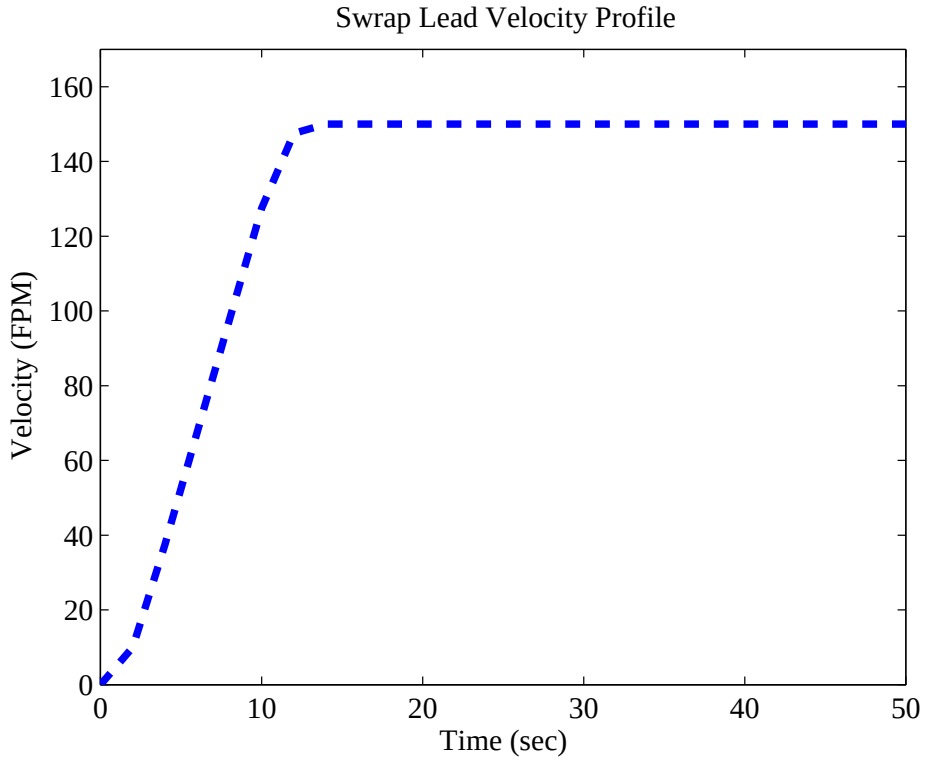

Figure 4.10: Velocity Profile Used for Experimentation

Parameter	Notation	Numerical Values (FPS units)
Modulus constant	EA	2800 lbf
Roller inertia	J	0.003 lbf - ft - s^2
Pendulum dancer inertia	J_p	0.4210 lbf - ft - s^2
Roller radius	R	0.125 ft
Web width	w	0.5 ft
Web thickness	w	0.007 ft
Pendulum dancer span length	L_i	1.825 ft

Table 4.1: Plant Parameter Nominal Values

4.6 Experimental Results

Implementation of the designed decentralized model reference adaptive controllers on the Euclid Web Line (EWL) is presented in this section. Three types of decentral-

ized model reference adaptive controller schemes along with a well-tuned PI controller were implemented and their performance was evaluated through extensive experimentation.

- Industrial PI Controller
- Direct Model Reference Adaptive Controller
- Indirect Model Reference Adaptive Controller
- Adaptive PI Controller

4.6.1 Experimental Results with the PI Controller

An often used PI control strategy for the unwind roll is shown in Figure 4.5. The control strategy is a cascaded outer loop PI controller to regulate tension and inner velocity control loop. The output of the tension controller becomes a reference velocity error correction for the inner velocity loop. The outer loop tension controller responds to tension variation and generates velocity correction to the inner velocity loop. The non-ideal effects, such as out of roundness, eccentricity of unwind roll, continuously inject disturbances into the system. This causes variations in web span tension.

Experiments were performed for load cell and dancer feedback strategies with well-tuned proportional and integral gains. The tuned values of the gains are given in Table 4.2.

	Load cell	Dancer
k_p	12	4
ω_i	0.1	0.1

Table 4.2: Finely Tuned PI Controller Gains

Web tension as measured by load cells on roller number 8 for load cell and dancer feedback for two line speed reference values of 150 FPM and 200 FPM are shown in Figures 4.11 through 4.14.

The standard deviation is evaluated for steady-state tension values. The standard deviation values indicate that the web tension in the unwind section at steady state varies between ±2.5 lbf with both load cell and dancer feedback control strategies.

4.6.2 Experimental Results with the Direct MRAC Scheme

The control strategy for direct adaptive control is as shown in Figure 4.5. The plant given by equation (4.26) has relative degree two and the upper bound 'n' for the plant denominator degree is selected as three. The direct MRAC scheme contains six controller parameters 'θ_{ci}' for the plant with the selection of the upper bound as three. The filter parameters are chosen as follows:

$$\alpha(s) = \begin{bmatrix} s & 1 \end{bmatrix}^T, \qquad \Lambda(s) = s^2 + 2s + 1$$

where $\Lambda(s)$ is a monic Hurwitz polynomial.

The state space representation of the filter gives the state matrix and input matrix as

$$F = \begin{bmatrix} -2 & -1 \\ 1 & 0 \end{bmatrix}, \quad g = \begin{bmatrix} 1 \\ 0 \end{bmatrix} \tag{4.76}$$

The strict positive real condition of $(s + p_0)W_m(s)$ can be fulfilled by choosing $p_0 = 1$. Experiments were performed for load cell feedback at 150 FPM and 200 FPM, and tension data was collected using the load cells on the roller 8 in the unwind section. The initial estimates of the controller parameters were chosen to be zero. Based on the tension performance in the transient and steady state, the initial estimates of the controller parameters were tuned. The adaptive gain rates were chosen as $\Gamma = [15, 15, 15, 15, 25, 25]^T$ and the tuned initial values of the controller parameter

Controller Parameter	θ_{11}	θ_{12}	θ_{21}	θ_{22}	θ_3	θ_4
Initial Value	1.6	-0.3	-0.96	-1.6	11.5	-9.0

Table 4.3: Direct MRAC Controller Parameter Initial Value Estimates

estimates were given in Table 4.4. The tension signal for load cell feedback at 150 FPM and 200 FPM are shown in Figures 4.15 and 4.16. With the direct MRAC scheme, tension was regulated to within ±1.5 lbf.

4.6.3 Experimental Results with the Indirect MRAC Scheme

The indirect adaptive control strategy is shown in Figure 4.5. The plant described by equation (4.26) has relative degree two and the upper bound 'n' is selected as three, similar to the direct adaptive design. The indirect MRAC scheme also involves six controller parameters 'θ_{ci}' which can be calculated based on the estimation of plant parameters.

The filter parameters are chosen as

$$\alpha(s) = \begin{bmatrix} s & 1 \end{bmatrix}^T, \quad \Lambda(s) = s^2 + 2s + 1$$

where $\Lambda(s)$ is a monic Hurwitz polynomial.

The state space representation of the filter gives the state matrix and the input matrix as

$$F = \begin{bmatrix} -2 & -1 \\ 1 & 0 \end{bmatrix}, \quad g = \begin{bmatrix} 1 \\ 0 \end{bmatrix} \tag{4.77}$$

Experiments were performed for load cell feedback at 150 FPM and 200 FPM and tension data was collected using the load cells on roller 8 in the unwind section. The strict positive real condition of $W_m(s)(s + p_0)$ can be fulfilled by choosing $p_0 = 1$. The initial estimates of the plant parameter were chosen to be zero. Based on the tension performance in the transient and steady state, the initial estimates of the plant parameters were tuned. The tuned plant parameter coefficient values were

selected as $\lambda = [2, 1]^T$, $\nu = [2.092, 0.1014]^T$. The adaptive gain rates were $\Gamma = [-10, 10, 10, -10, -10, -10]^T$ and initial estimates of plant controller parameters are given in Table 4.4.

Plant Parameters	k_p	a_n	p_{11}	p_{12}	p_{21}	p_{22}
Initial Values	1900	5	-1	-0.8	-1	6

Table 4.4: Indirect MRAC Plant Parameter Initial Estimates

The tension response for load cell feedback at 150 FPM and 200 FPM are shown in Figures 4.17 and 4.18. Indirect MRAC regulates the tension for the unwind section within ± 1.5 lbf.

4.6.4 Direct Adaptive PI Controller

The implementation of adaptive PI control is shown in Figure 4.9. The selected reference model has relative degree two. The poles and zeros of the reference model can be selected based on the actual model parameter nominal values. The selected reference model can be simulated to verify the desired performance. The reference model selected for the design is

$$W_m(s) = \frac{0.25(4s + 1.6)(20s + 100)}{(0.4s + 1.6)(s + 0.5)(s + 0.5)(5s + 100)} \tag{4.78}$$

The adaptive PI controller is easy to implement since only two parameters need to be estimated. This controller is simple in design compared to the direct and indirect MRAC strategies. Experiments were performed for load cell and dancer feedback at 150 FPM and 200 FPM. The implementation procedure for adaptive PI is given below.

Step 1: Choose a reference model which gives desired performance, i.e., fast transient response, low percentage overshoot, etc. The selection of poles and zeros of the reference model can be based on the nominal values of the plant parameters.

Step 2: Perform computer simulations to evaluate the selected reference model.

Computer simulations help in adjusting the reference model parameters.

Step 3: Choose initial controller gain estimates to be zero. Choose the adaptive gain rate to be one. The selected initial gains is a good starting point for load cell and dancer feedback systems.

Step 4: The initial value of the proportional gain may be increased in steps until desired response is achieved.

Step 5: In the presence of steady state error, increase the integral gain initial value.

The system with load cell feedback is stiff and requires larger initial estimates of proportional gain. The tension data for load cell feedback at 150 FPM and 200 FPM are shown in Figures 4.19 and 4.20.

Same adaptive PI structure is implemented for the dancer feedback system. Initial estimates for adaptive gains are set to zero as mentioned in the above implementation procedure. Adaptive gain rates are kept at one. With the dancer system, the adaptive gain estimates converge close to the well-tuned PI parameters values used for dancer feedback. The proportional gain reaches the value of 4 and integral gain reaches to 0.2. The tension data for dancer feedback at 150 FPM and 200 FPM are shown in Figures 4.19 and 4.20. The evolution of the estimates of controller parameters are shown in Figures 4.23 through 4.26. The adaptive PI control performs similarly to a well-tuned PI controller in both, load cell and dancer feedback systems.

4.6.5 Comparison of PI and Model Reference Adaptive Control Schemes with Load Cell Feedback

Compared to an existing well-tuned PI controller, the proposed adaptive schemes show improvements in tension regulation. The standard deviation of the steady-state tension data is used as a performance metric. The Tables 4.5 through 4.6 show the standard deviations for PI and adaptive control schemes implemented with

load cell feedback at 150 FPM and 200 FPM. One can observe that the adaptive control schemes perform better than a well-tuned PI controller in steady state and the transient corresponding to acceleration and deceleration of the line seem to be better for the adaptive schemes. The industrial PI controller requires extensive tuning during the initial implementation phase. The tuned PI controller is not robust enough for the changes in web transport system such as web configuration, feedback system, web materials. Extensive tuning can be avoided at later stages by using MRAC schemes.

Control Scheme	Standard Deviation
PI	0.71
Direct Adaptive	0.57
Indirect Adaptive	0.52
Adaptive PI	0.45

Table 4.5: Standard Deviations with Load cell Feedback at 150 FPM

Control Scheme	Standard Deviation
PI	1.21
Direct Adaptive	0.73
Indirect Adaptive	0.63
Adaptive PI	0.47

Table 4.6: Standard Deviations with Loadcell Feedback at 200 FPM

4.6.6 Comparison of PI and Adaptive PI Control Schemes with Dancer Feedback

The Table 4.7 shows the standard deviation for fixed PI and adaptive PI control schemes with dancer feedback at 150 FPM and 200 FPM. It can be seen from the standard deviation values that adaptive PI is performing similar to a well-tuned PI

controller. The adaptive PI controller has an advantage over a fixed gain industrial PI control scheme, that extensive tuning is not necessary. Adaptive PI controller has adjustable characteristics to compensate for changes in sensing system, web configurations, and web materials. The adaptive PI has only two parameters to be estimated. It is simple in design and implementation. One limitation of the adaptive PI scheme with gradient based adaptation scheme over Lyapunov based MRAC schemes is that there are no stability results associated with the gradient based scheme.

Control Scheme	Standard Deviation	
	150 FPM	200 FPM
PI	0.45	0.46
Adaptive PI	0.49	0.44

Table 4.7: Standard Deviations with Dancer Feedback

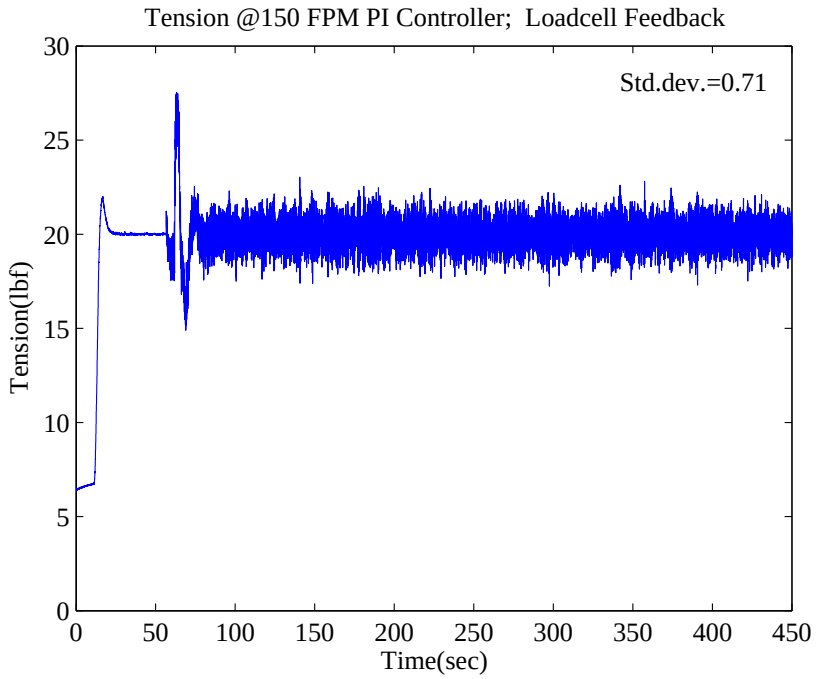

Figure 4.11: Tension at 150 FPM with PI Controller and Load cell feedback

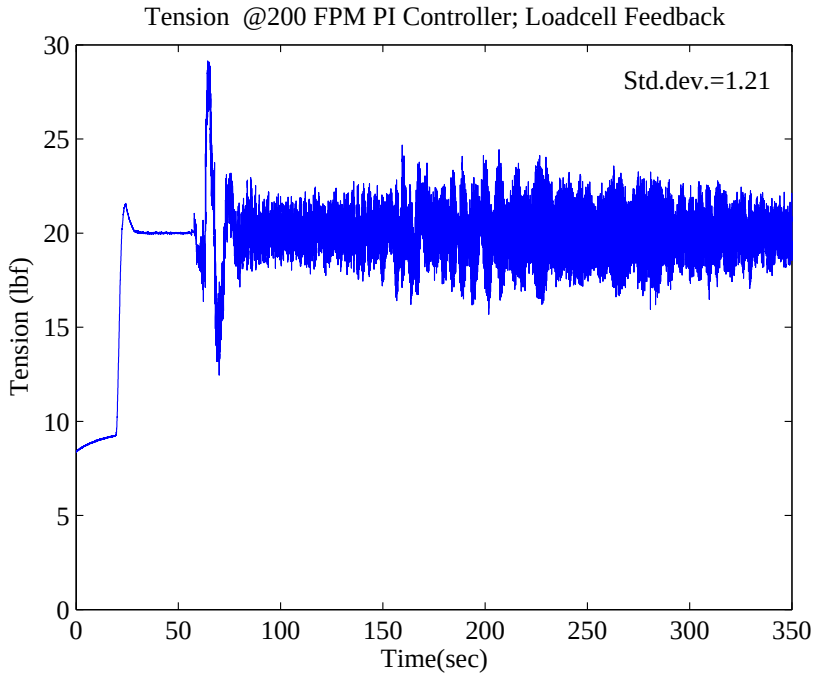

Figure 4.12: Tension at 200 FPM with PI Controller and Load cell feedback

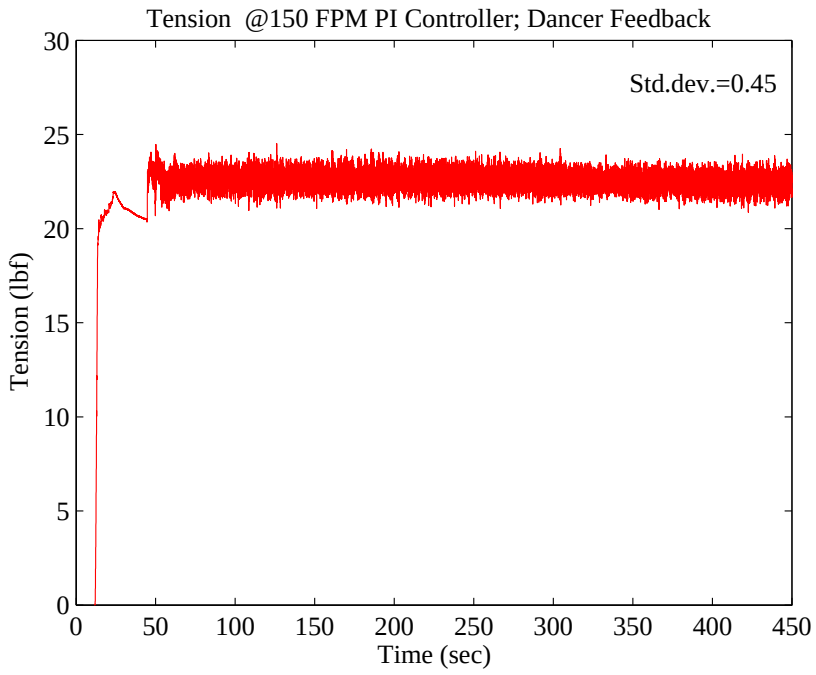

Figure 4.13: Tension at 150 FPM with PI Controller and Dancer feedback

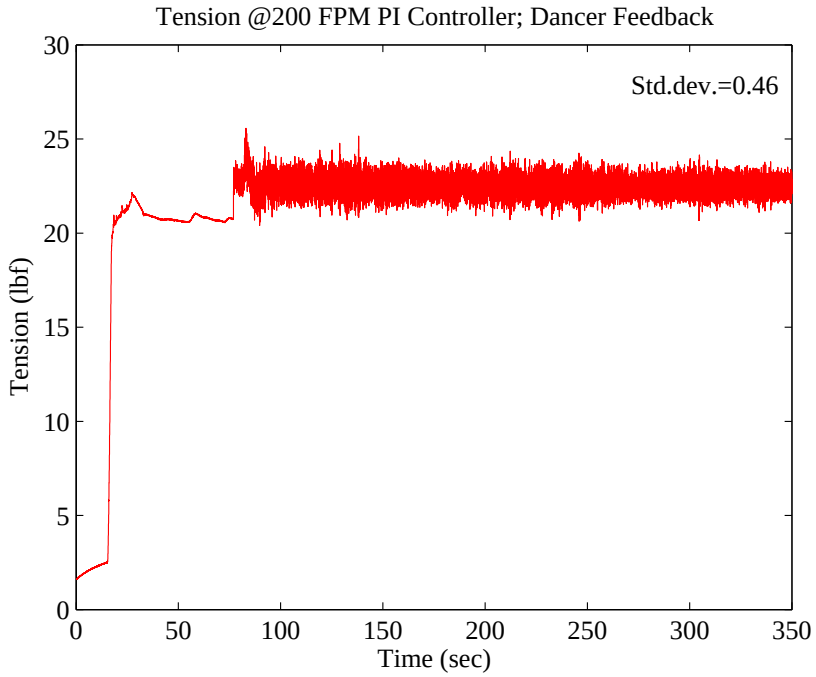

Figure 4.14: Tension at 200 FPM with PI Controller and Dancer feedback

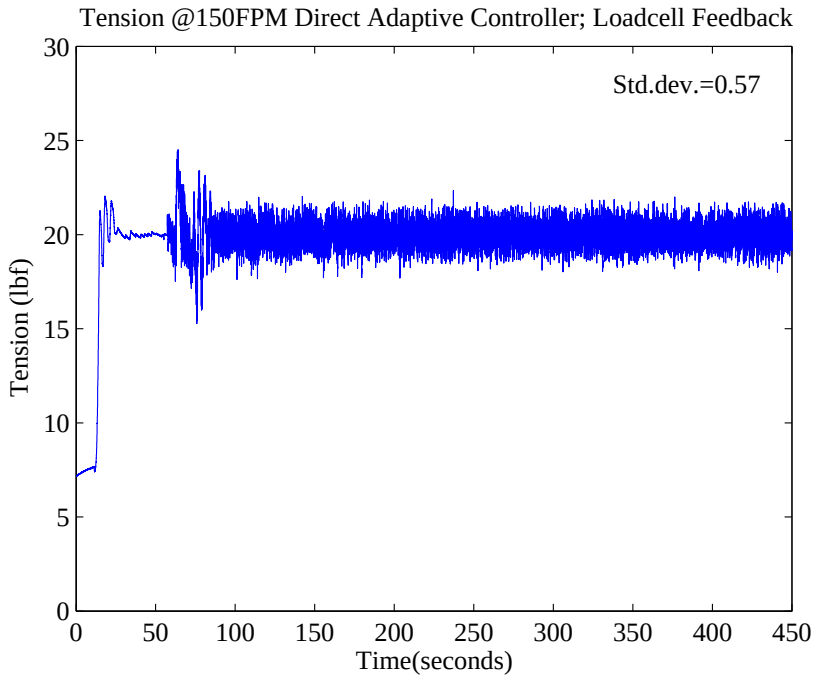

Figure 4.15: Tension at 150 FPM with Direct MRAC Controller and Load cell feedback

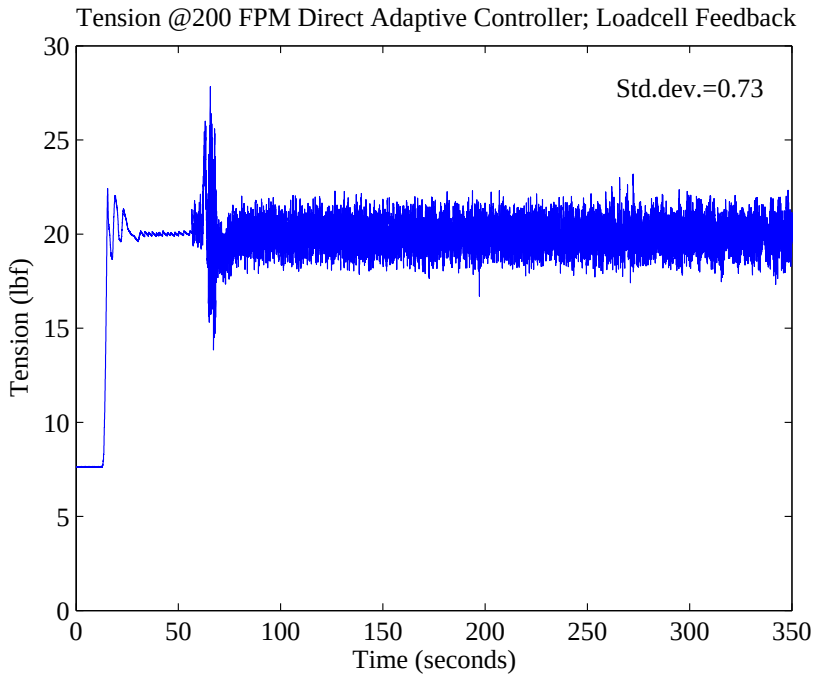

Figure 4.16: Tension at 200 FPM with Direct MRAC Controller and Load cell feedback

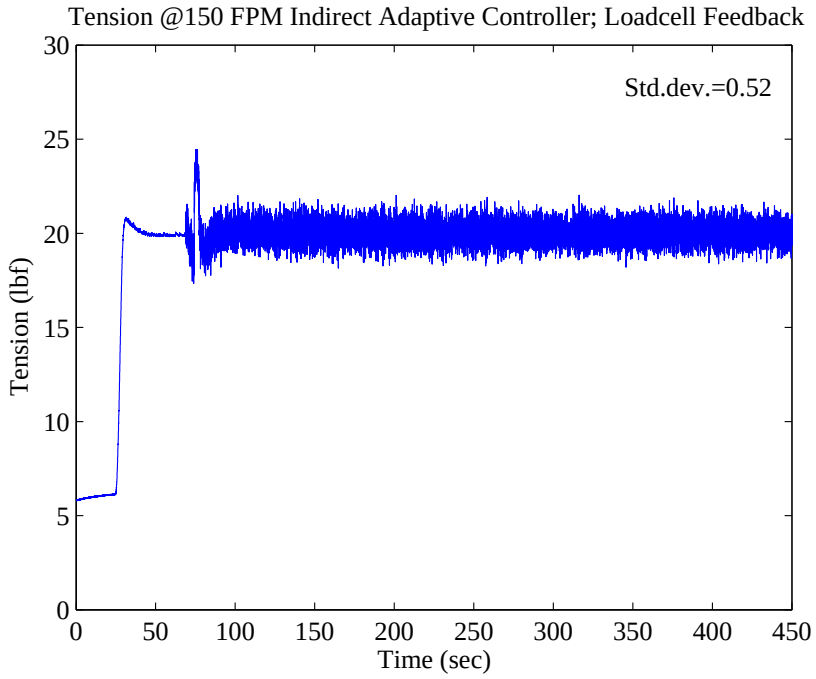

Figure 4.17: Tension at 150 FPM with Indirect MRAC Controller and Load cell feedback

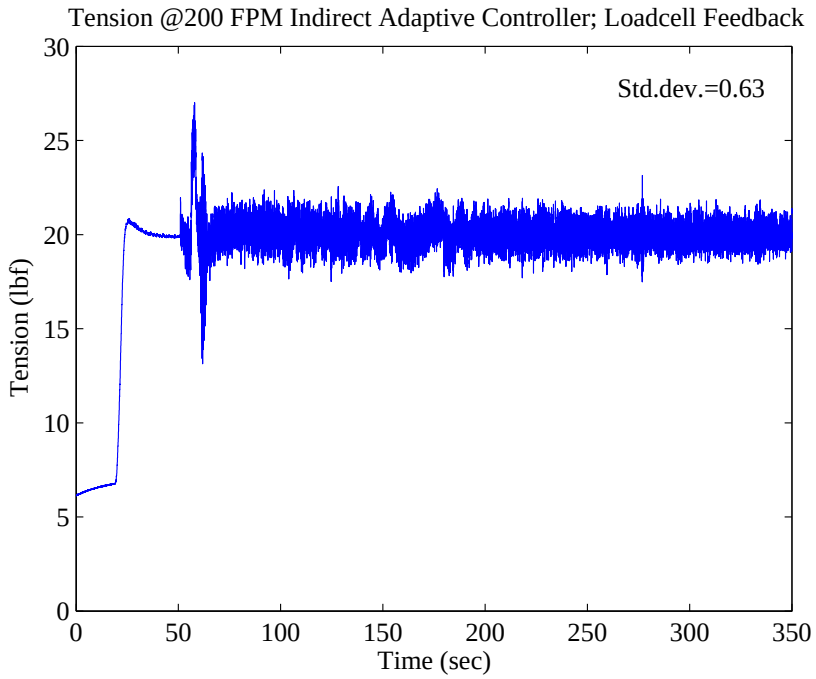

Figure 4.18: Tension at 200 FPM with Indirect MRAC Controller and Load cell feedback

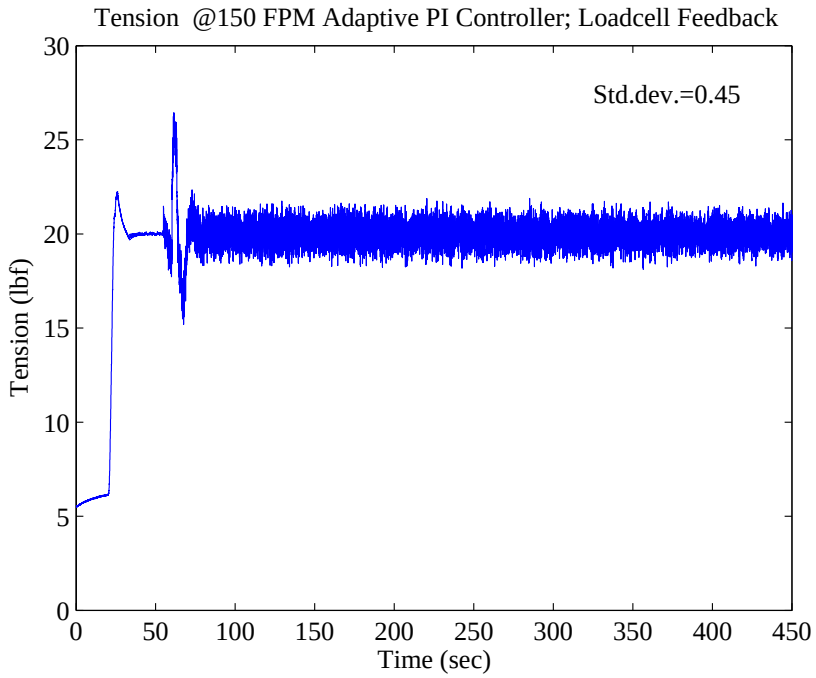

Figure 4.19: Tension at 150 FPM with Adaptive PI Controller and Load cell feedback

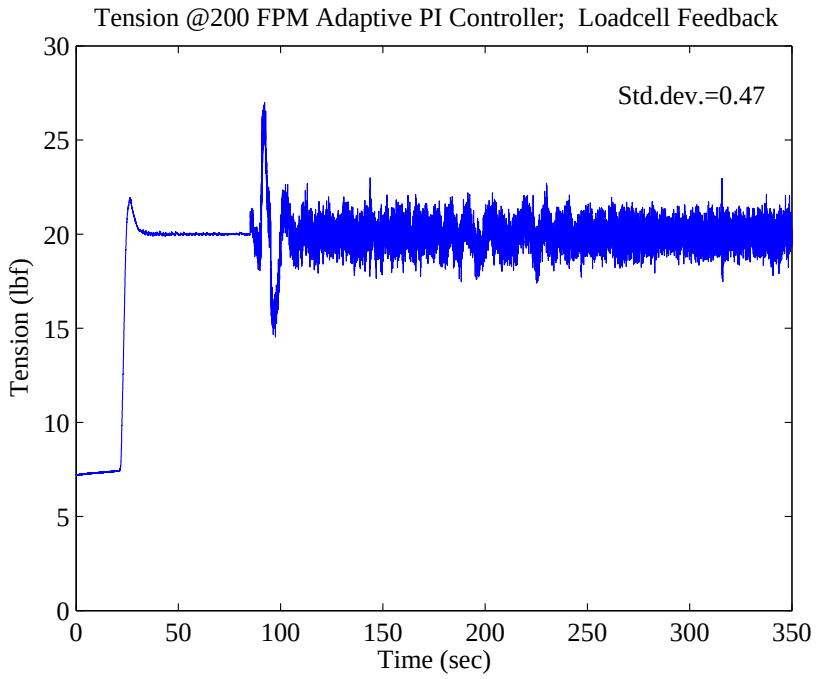

Figure 4.20: Tension at 200 FPM with Adaptive PI Controller and Load cell feedback

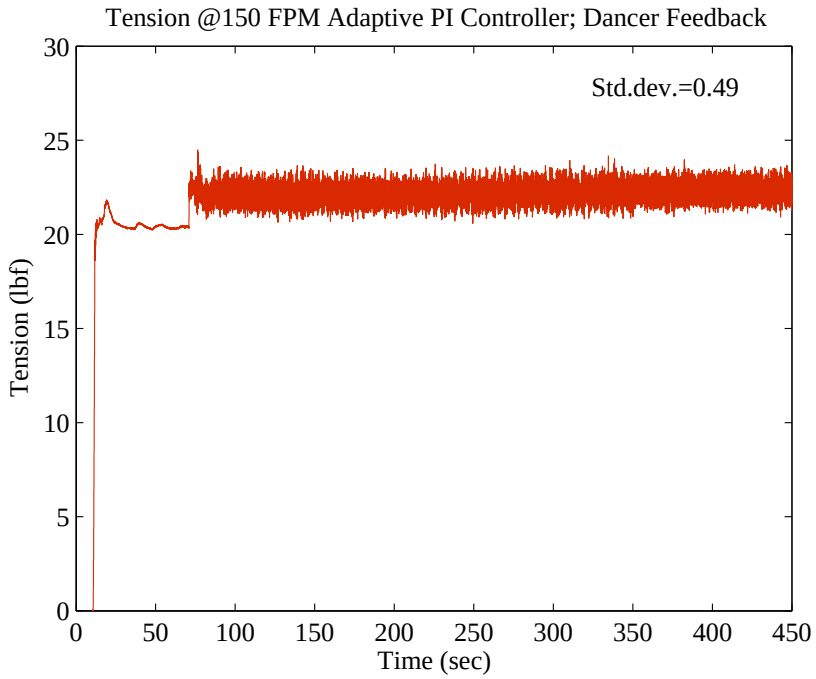

Figure 4.21: Tension at 150 FPM with Adaptive PI Controller and Dancer feedback

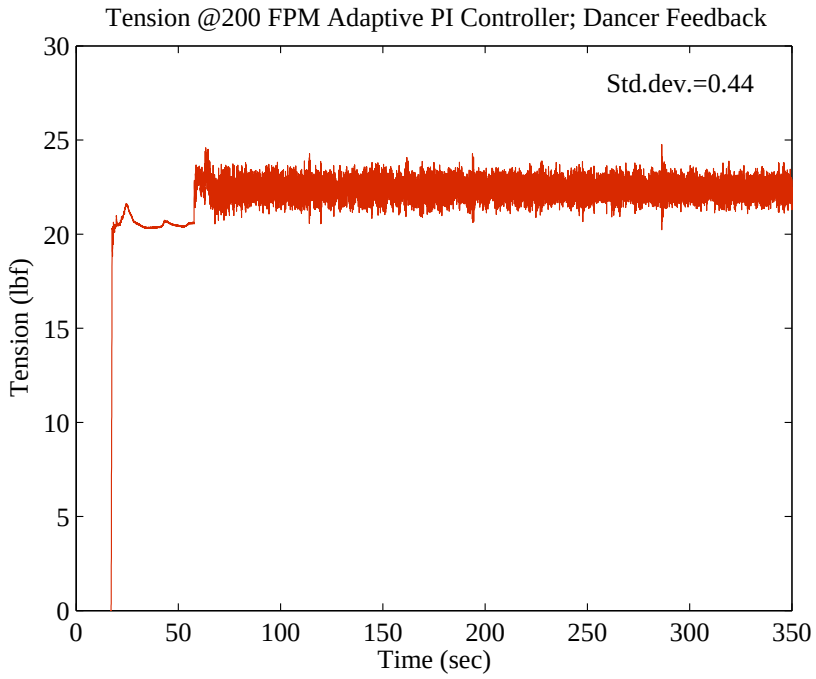

Figure 4.22: Tension at 200 FPM with Adaptive PI Controller and Dancer feedback

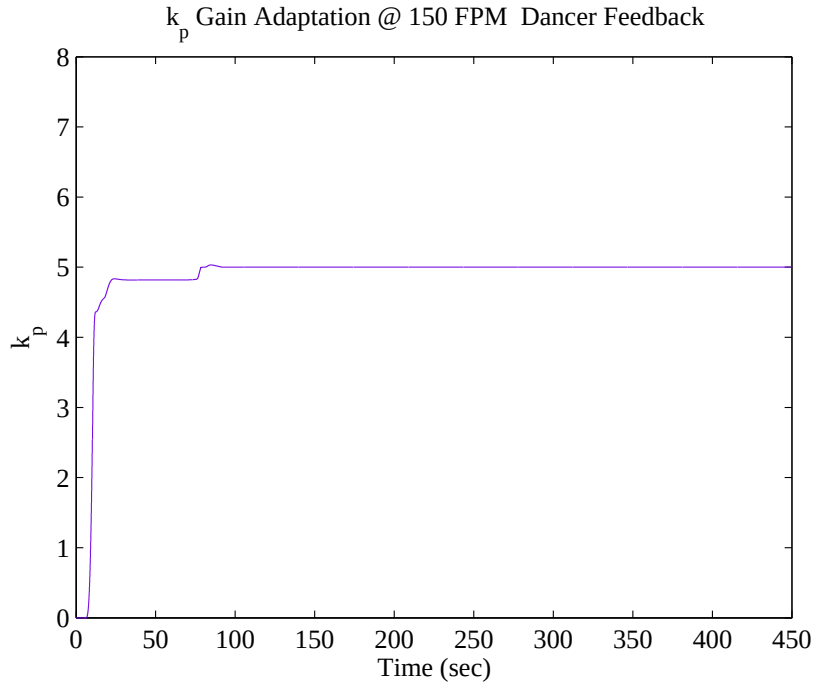

Figure 4.23: Proportional Gain Adaptation at 150 FPM with Dancer feedback

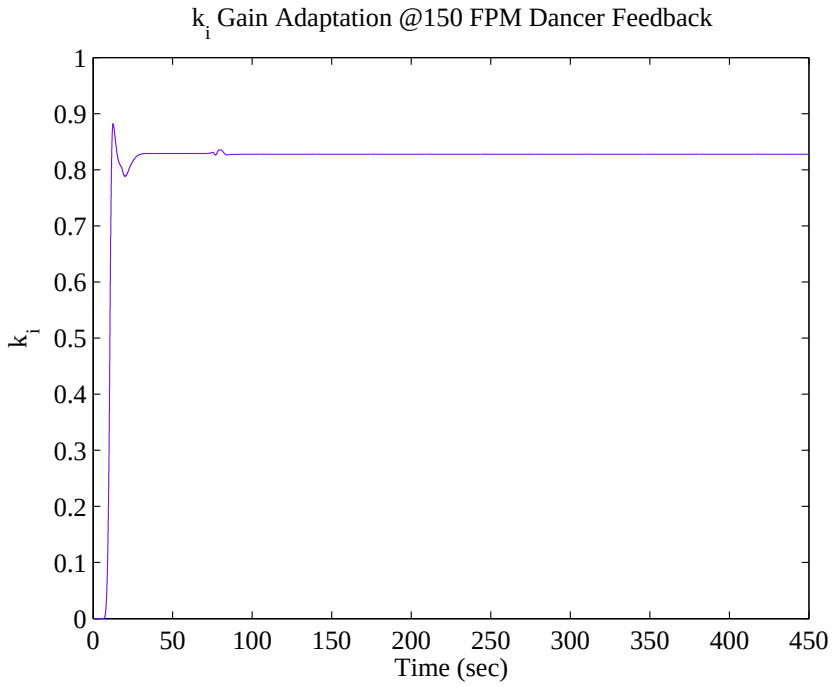

Figure 4.24: Integral Gain Adaptation at 150 FPM with Dancer feedback

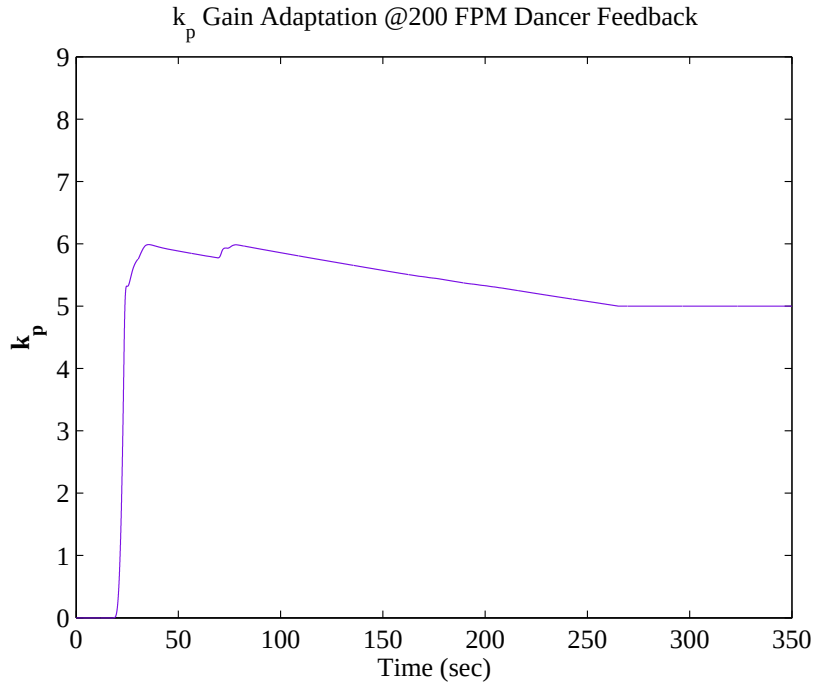

Figure 4.25: Proportional Gain Adaptation at 200 FPM with Dancer feedback

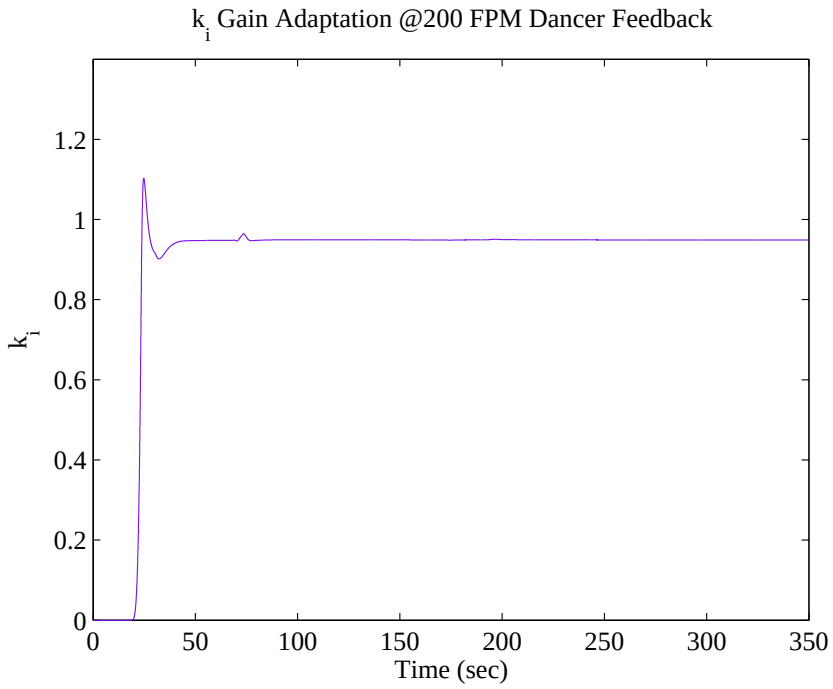

Figure 4.26: Integral Gain Adaptation at 200 FPM with Dancer feedback

CHAPTER 5

Summary and Future Work

5.1 Summary

Longitudinal dynamics of the web plays an important role in web transport systems. It is essential to maintain tension in the longitudinal direction (machine direction), since tension variations directly affect web transport and the quality of the final product. A number of problems are involved with longitudinal dynamic behavior of a web, such as dynamic interaction between web spans, use of dancer and load cell for tension regulation, and tension regulation in the presence of mechanical resonances. In this thesis, research work was conducted to understand web tension behavior and improve tension control schemes. Frequency response and time domain experiments were conducted to evaluate dancer and load cell performance. Controller normalization is performed in order to obtain dancer system controller gains based on a load cell feedback control scheme. The concept of normalization motivates the study of dimensional analysis for the web transport system. Adaptive control strategies were developed that give satisfactory performance for tension regulation and can be readily used in situations where process and machine changes are made. A chapter by chapter summary is given in following paragraphs:

In Chapter 2, a mathematical model is developed for a pendulum dancer system. The ability of the developed model to predict resonant frequencies is evaluated by performing frequency response experiments. Time and frequency domain experiments were performed for the dancer and load cell control strategies, which reveal tension regulation ability of both systems. The dancer position based feedback controller is

normalized based on load cell controller. A close match in terms of the minimum resonant frequency between model simulations and experiments is observed for load-cell and dancer feedback systems. The dancer based system was able to filter low frequency disturbances very well compared to the load cell. The time domain results indicate that the dancer control scheme regulates tension better than load cell during line acceleration and deceleration. It was observed that by precisely regulating air pressure in the pneumatic cylinder with electromechanical pressure regulator, the tension response can be improved. One limitation of the dancer based scheme over a load cell based scheme is that the minimum resonant frequency is much lower, which may excite resonances.

In Chapter 3, dimensional analysis is performed for web transport systems. Dimensionless tension and roller velocity dynamic equations are developed. The dimensionless equations are simple, and contain fewer variables than dimensional equations. The dimensionless equations are used to scale the process parameters. The scaling is based on the dynamic equivalence condition applied between two systems. A numerical example is provided to investigate the web system operating on a different kind of materials for process parameter scaling. The parameter scaling depends upon the model law developed with dimensionless Pi parameters. Dimensional analysis is also performed for two primitive elements, accumulator and dancer. The process parameters are evaluated for scaled-up capacity of the accumulator.

In Chapter 4, model reference adaptive control is considered for implementation on the Euclid web line. A web system is a large scale system with many interconnections. Decentralized MRAC strategies are considered and implemented in the unwind section of the Euclid Web Line. Three types of adaptive strategies are designed and implemented:

- Direct model reference adaptive control
- Indirect model reference adaptive control

- Adaptive PI control

Extensive experiments are performed to verify the tension regulation ability of the adaptive control schemes. An adaptive PI controller is implemented for both, dancer and load-cell control strategies. The proposed adaptive control schemes are compared with a well-tuned traditional fixed gain PI controller on the Euclid Web Line. Standard deviations calculated for the steady state tension data show improvement in tension regulation with the adaptive schemes.

5.2 Future Work

The frequency response study was performed for the dancer and load cell feedback systems. The minimum resonant frequency for the dancer and load cell system is evaluated in this thesis. The experiments were performed for Tyvek material manufactured by Dupont. The developed mathematical model of a pendulum dancer must be verified with different web materials. A detailed study is required to determine the sources of various frequencies observed. This study should help in finding the sources of oscillations in tension and velocity and to get remedies to eliminate oscillations. The frequency response study can also assist in selection of better filters in the adaptive control design. Based on the frequency response results, systematic guidelines for better tension control systems need to be developed.

Dimensional analysis simplifies the governing equation of a system. A model law formulates the process of parameter scaling. The numerical example provided in the thesis for the web lines transporting different kinds of materials should be experimentally verified to substantiate conclusions derived from dimensional analysis. The effectiveness of the scaled parameters need to be evaluated for the scaled system. Similar experimental verification should be performed for dimensional analysis of an accumulator. Further, the scope of dimensional analysis can be expanded for many primitive web handling elements. Dimensional analysis as known currently

cannot be applied for generalized system scaling, and constraints are imposed with dynamic equivalence conditions. Future study on dimensional analysis should focus on generalization of process parameters scaling and overcome the constraints applied by dimensional equivalence. There is also potential in using dimensional analysis to design the reference model in model reference adaptive control schemes for the scaled systems.

The proposed adaptive strategies are experimentally evaluated for Tyvek material. Adaptive control strategies should be investigated for (i) different types of materials; (ii) different web configuration by changing web path, and number of rollers. The proposed adaptive algorithms give similar or better tension regulation compared to a well-tuned PI controller as seen from experiments on the Euclid Web Line. The adaptive PI scheme based on the gradient method does not guarantee stability of the system. A simple adaptive PI scheme based on Lyapunov design should be pursued to ensure overall system stability.

BIBLIOGRAPHY

[1] D. P. Campbell, *Dynamic Behavior of the Production Process, Process Dynamics*. John Wiley and Sons Inc., New York, first ed., 1958.

[2] D. King, "The mathematical model of a newspaper press," *Newspaper Techniques*, pp. 3–7, December 1969.

[3] G. Brandenberg, "New mathematical models for web tension and register error," *International IFAC Conference on Instrumentation and Automation in the Paper Rubber and Plastics Industry*, vol. 1, pp. 411–438, December 1977.

[4] J. J. Shelton, "Dynamics of web tension control with velocity or torque control," *Proceedings of the American Control Conference*, pp. 1423–1427, June 1986.

[5] K. Shin, *Distributed control of tension in multi-span web transport systems*. PhD thesis, Oklahoma State University, Stillwater, May 1991.

[6] G. Young and K. Reid, "Lateral and longitudinal dynamic behavior and control of moving webs," *ASME Journal of Dynamics Systems, Measurement, and Control*, vol. 115, pp. 309–317, June 1993.

[7] W. Wolfermann, "Tension control of webs, a review of the problems and solutions in the present and future," *Proceedings of the Third International conference on Web Handling*, pp. 198–229, June 1995.

[8] D. Schroder and W. Wolfermann, "Application of decoupling and state space control in processing machines with continuous moving webs," *Proceedings International federation of Automatic Control*, pp. 198–229, June 1987.

[9] J. J. Shelton, "Limitations to sensing of web tension by means of roller reaction forces," *in proceedings of the Fifth International Conference on Web handling*, June 1999.

[10] D. H. Carlson, "Consideratios in the selection of a dancer or load cell based tension regulation strategy," *in proceedings of the Sixth International Conference on Web handling*, June 2001.

[11] Y. Diao, "Resonant frequencies in web lines and filtering of web tension," Master's thesis, Oklahoma State University, Stillwater, December 2008.

[12] T. Szirtes, *Applied dimensional analysis and modeling*. McGraw-Hill, New York, 2nd ed., 1998.

[13] S. Brennan, *On size and control: The use of dimensional anlysis in controller design*. PhD thesis, University of Illinois, Urbana-Champaign, November 2002.

[14] P. R. Pagilla, S. S. Garimella, L. H. Dreinhoefer, and E. O. King, "Dynamics and control of accumulators in continuous strip processing lines," *IEEE Transactions on Industry Applications*, vol. 37, pp. 934–940, June 2001.

[15] M. Aoki, "On feedback stabilizability of decentralized dynamics system," *Automatica, Pergamon press*, vol. 8, pp. 163–173, June 1972.

[16] D. D. Siljak, *Large-scale dynamic systems*. Elsevier North-Holland,Inc., 1978.

[17] R. V. Monopoli, "Model reference adaptive control with an augmented error signal," *IEEE transactions on automatic control*, vol. 19, pp. 474–484, 1974.

[18] A. Feuer and A. S. Morse, "Adaptive control of single-input, single-output linear systems," *IEEE transactions on automatic control*, vol. 23, pp. 557–569, 1978.

[19] D. T. Gavel and D. D. Siljak, "Decentralized adaptive control: Structural conditions for stability," *IEEE Transactions on Automatic Control*, vol. 34, pp. 413–426, April 1989.

[20] K. S. Narendra and N. O. Oleng, "Exact output tracking in decentralized adaptive control systems," *IEEE Transactions on Automatic Control*, vol. 47, pp. 390–395, February 2002.

[21] P. A. Ioannou, "Decentralized adaptive control of interconnected systems," *IEEE Transactions on Automatic Control*, vol. AC-31, pp. 291–298, April 1986.

[22] K. S. Narendra, *Stable adaptive systems*. Englewood cliffs, N.J., 1989.

[23] K. J. Astrom and B. Wittenmark, *Adaptive control*. Pearson Education Inc., 2nd ed., 2003.

[24] N. B. Siraskar, "Decentralized control of large-scale interconnected systems with application to web processing machines," Master's thesis, Oklahoma State University, Stillwater, December 2004.

[25] P. R. Pagilla, N. B. Siraskar, and R. V. Dwivedula, "Decentralized control of web proceesing lines," *IEEE Transactions on Control Systems Technology*, vol. 15, pp. 106–117, January 2007.

[26] R. V. Dwivedula, *Modeling the effects of belt compliance, backlash, and slip on web tension and new methods for decentralized control of web processing lines*. PhD thesis, Oklahoma State University, Stillwater, December 2005.

[27] P. R. Pagilla, R. V. Dwivedula, and N. B. Siraskar, "A decentralized model reference adaptive controller for large-scale systems," *IEEE Transactions on Mechatronics*, vol. 12, pp. 154–163, April 2007.

VITA

Pramod R. Raul

Candidate for the Degree of

Master of Science

Thesis: FREQUENCY RESPONSE OF WEB SYSTEMS CONTAINING LOAD CELLS AND DANCERS, DIMENSIONAL ANALYSIS, AND MODEL REFERENCE ADAPTIVE SCHEMES FOR TENSION CONTROL

Major Field: Mechanical and Aerospace Engineering

Biographical:

Personal Data: Born in Maharashtra, India, on December 12, 1980, the son of Rajaram V. Raul and Shobha R. Raul.

Education: Received the B.E. degree from Government College of Engineering, Pune, Maharashtra, India, in 2002, in Mechanical Engineering; Completed the requirements for the Master of Science degree with a major in Mechanical and Aerospace Engineering at Oklahoma State University in May, 2010.

Experience: Research Assistant at Oklahoma State University from January 2008-Present; Teaching Assistant at Oklahoma State University from January 2008-May 2008; Apprentice Engineering Trainee at Mahindra & Mahindra Ltd., Maharashtra, India from June 2002 to August 2003; Assistant Manager at Tata Motors Ltd., Maharashtra, India from December 2003 to June 2007.

Professional Memberships: Phi kappa Phi Honor society; Golden Key Honor society; American Society of Mechanical Engineers.

Name: Pramod Raul Date of Degree: JULY, 2010

Institution: Oklahoma State University Location: Stillwater, Oklahoma

Title of Study: FREQUENCY RESPONSE OF WEB SYSTEMS CONTAINING LOAD CELLS AND DANCERS, DIMENSIONAL ANALYSIS, AND MODEL REFERENCE ADAPTIVE SCHEMES FOR TENSION CONTROL

Pages in Study: 125 Candidate for the Degree of Master of Science

Major Field: Mechanical and Aerospace Engineering

Scope and Method of Study: The focus of this study is on understanding the behavior of web tension using frequency response analysis and design of tension control systems for improved tension regulation. Two key tension sensing elements, load cells and dancers, are studied. Development of a model for the pendulum dancer is considered. Dimensional analysis is used as a tool to obtain reference values for parameters and process variables for a candidate web line by using dimensional equivalence of the candidate web line with a well developed web line with a well tuned controller. Model reference adaptive control techniques are investigated for web tension control. Experiments on a large web platform and computer simulations of models are used throughout to reinforce discussions.

Findings and Conclusions: Comparisons of results from experiments and model simulations shows that the developed model is able to predict the frequency content found in the experimental results. Experimental results also show that the tension control system with dancer feedback attenuates low frequency tension variations better than that with load cell feedback. The minimum resonant frequency with the dancer system is lower than that of the load cell system, which may mean the dancer system may be more susceptible to resonances. Dimensional analysis of various scenarios of web transport system indicates that it can be effectively used to scale process parameters and variables. Results from implementation of various model reference adaptive schemes indicate that adaptive schemes provide better tension regulation than fixed gain PI controllers under changing process parameters.

ADVISOR'S APPROVAL: _____